

January 2015

Deuterium Enrichment and the Kinetic Isotope Effect during Ruthenium Catalyzed Fischer-Tropsch Synthesis

Jennifer Naumovitz
Eastern Kentucky University

Follow this and additional works at: <https://encompass.eku.edu/etd>

 Part of the [Biochemical and Biomolecular Engineering Commons](#)

Recommended Citation

Naumovitz, Jennifer, "Deuterium Enrichment and the Kinetic Isotope Effect during Ruthenium Catalyzed Fischer-Tropsch Synthesis" (2015). *Online Theses and Dissertations*. 408.
<https://encompass.eku.edu/etd/408>

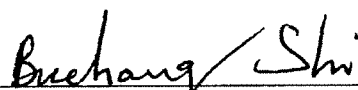
This Open Access Thesis is brought to you for free and open access by the Student Scholarship at Encompass. It has been accepted for inclusion in Online Theses and Dissertations by an authorized administrator of Encompass. For more information, please contact Linda.Sizemore@eku.edu.

**DEUTERIUM ENRICHMENT AND THE KINETIC ISOTOPE EFFECT DURING RUTHENIUM
CATALYZED FISCHER-TROPSCH SYNTHESIS**

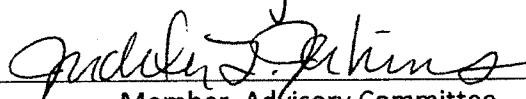
By

JENNIFER NAUMOVITZ

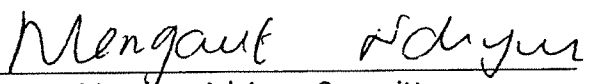
Thesis Approved:



Chair, Advisory Committee



Member, Advisory Committee



Member, Advisory Committee



Dean, Graduate School

STATEMENT OF PERMISSION TO USE

In presenting this thesis in partial fulfillment of the requirements for a Master's degree at Eastern Kentucky University, I agree that the Library shall make it available to borrowers under rules of the Library. Brief quotations from this thesis are allowable without special permission, provided that accurate acknowledgment of the source is made. Permission for extensive quotation from or reproduction of this thesis may be granted by my major professor, or in [his/her] absence, by the Head of Interlibrary Services when, in the opinion of either, the proposed use of the material is for scholarly purposes. Any copying or use of the material in this thesis for financial gain shall not be allowed without my written permission.

Signature 

Date June 19th, 2015

DEUTERIUM ENRICHMENT AND THE KINETIC ISOTOPE EFFECT DURING RUTHENIUM
CATALYZED FISCHER TROPSCH SYNTHESIS

By

JENNIFER NAUMOVITZ

Bachelor of Science
Eastern Kentucky University
Richmond, Kentucky
2015

Submitted to the Faculty of the Graduate School of
Eastern Kentucky University
in partial fulfillment of the requirements
for the degree of
MASTER OF SCIENCE
August, 2015

Copyright © Jennifer Naumovitz, 2015
All rights reserved

DEDICATION

This thesis is dedicated to my parents, Dr. Joseph and Elke Naumovitz who have provided unwavering support and knowledge.

ACKNOWLEDGMENTS

I would like to thank my thesis mentor, Dr. Buchang Shi for provided constant support and answer to all my many varied questions. His guidance has allowed for me to gain a better understanding and appreciation towards research and organic synthesis. I would also like to thank my committee member, Dr. Judy Jenkins and Dr. Margaret Ndinguri for not only serving on my committee but also for their much appreciated feedback. Another integral person who was a great help to this thesis was Yunxin Liao. Yunxin taught me how to work with the specific instrumentation and reactor that was present in the lab. With that being said, I would also like to thank ECU for the space and support. I would like to mention Wilson Shafer at this time and thank him for running the competition and other various samples. He was always very prompt with his results and extremely helpful if I ever had any questions.

I appreciate all of the support and encouragement provided by my friends including Melissa Sterling, Casey Howdieshell, Rachel Ganley, and Todd Green. Of my family I would like to express my thanks to my mother and father who always took an interest and helped me through the rough portions of my thesis, especially when the task seemed to daunting to finish. Lastly, I would like to give a big thanks to my brother, Timothy Naumovitz, for assisting in some mathematical calculations. He helped me to determine and understand the theoretical math and algorithms behind a portion of the theoretical predictions.

ABSTRACT

Fischer Tropsch Synthesis is a highly researched field that is still widely debated today. Research in this field could lead to many different advances, such as alternative fuel sources, explanations of abiogenic hydrocarbons and the formation of organic matter in the solar nebula. Analysis of this synthesis was carried out with a ruthenium catalyst at controlled temperatures and pressures. Two types of experiments were performed: H₂/D₂ switching and competitive methods. The products showed that the hydrocarbon production rate was slightly increased when syngas was switched to D₂/CO. Also, the H/D ratios of the hydrocarbons produced by the FT reaction using equal amount of H₂ and D₂ are always less than 1 indicating deuterium enrichment. We also observed that the ratios of [2-alkene]_H/[2-alkene]_D is about 1.4, indicating a normal isotope effect. However, the ratio of [1-alkene]_H/[1-alkene]_D was around 0.9, indicating a different pathway for production than 2-olefins. We attempt to explain these experimental facts by the modified alkylidene mechanism.

TABLE OF CONTENTS

CHAPTER	PAGE
CHAPTER 1: INTRODUCTION AND BACKGROUND	1
1.1 GAS-TO-LIQUIDS (GTL) PROCESS	1
1.2 FISCHER-TROPSCH SYNTHESIS (FTS)	4
1.3 MECHANISMS OF FTS – AN UNSOLVED MYSTERY	9
1.4 RUTHENIUM CATALYZED FTS.....	16
1.5 PRODUCTS DURING FTS.....	19
1.6 DEUTERIUM TRACER STUDIES OF FTS	23
1.7 INSTRUMENTAL THEORY	25
1.8 DATA ANALYSIS AND CALCULATIONS	29
CHAPTER 2: EXPERIMENTAL	39
2.1 SYNTHESIS OF RUTHENIUM CATALYSTS	39
2.2 SETUP OF FIXED-BED REACTOR FOR FTS	41
2.3 DEUTERIUM/HYDROGEN SWITCHING AND COMPETITION SYNTHETIC PROCEDURES OF FTS	44
2.4 SAMPLE COLLECTION AND ANALYSIS	46
CHAPTER 3: DEUTERIUM TRACER STUDIES OF Ru/SiO ₂ CATALYZED FTS.....	51
3.1 FISCHER-TROPSCH SYNTHESIS USING Ru/SiO ₂ CATALYST	51
3.2 KINETIC ISOTOPE EFFECT DURING Ru/SiO ₂ CATALYZED FTS.....	55
3.3 PRODUCT DISTRIBUTION DURING Ru/SiO ₂ CATALYZED FTS.....	59
3.4 PRIMARY VS. SECONDARY PRODUCT ANALYSIS DURING Ru/SiO ₂ CATALYZED FTS.....	65
3.5 DEUTERIUM ENRICHMENT IN HYDROCARBONS DURING Ru/SiO ₂ CATALYZED FTS.....	70
3.6 Ru/SiO ₂ CONCLUSIONS	75
CHAPTER 4: DEUTERIUM TRACER STUDIES OF Ru/Al ₂ O ₃ CATALYZED FTS.....	77

4.1 FISCHER-TROPSCH SYNTHESIS USING Ru/Al ₂ O ₃ CATALYST	77
4.2 KINETIC ISOTOPE EFFECT DURING Ru/Al ₂ O ₃ CATALYZED FTS.....	79
4.3 PRODUCT DISTRIBUTION DURING Ru/Al ₂ O ₃ CATALYZED FTS.....	82
4.4 PRIMARY VS. SECONDARY PRODUCT ANALYSIS DURING Ru/Al ₂ O ₃ CATALYZED FTS.....	83
4.5 DEUTERIUM ENRICHMENT IN HYDROCARBONS DURING Ru/Al ₂ O ₃ CATALYZED FTS	90
CHAPTER 5: CONCLUSIONS AND FUTURE DIRECTIONS	94
5.1 CONCLUSIONS.....	94
5.2 FUTURE DIRECTIONS.....	98
REFERENCES.....	101
APPENDICES.....	107
A. FIGURES OF % CO CONVERSION.....	107
B. FIGURES OF DEUTERIUM ENRICHMENT: SAMPLE JN19 ISOTOPOMERS AND TRENDS FOR H/D RATIOS.....	111

LIST OF TABLES

TABLE	PAGE
Table 2.1 Column Packing mass data.....	42
Table 2.2 Analyses Performed.....	50
Table 3.1 Ru 1 st Run Mass Data.....	52
Table 3.2 Ru 2 nd Run Mass Data.....	53
Table 3.3 Ru 3 rd Run Mass Data.....	54
Table 3.4 Ru 1 st Run %CO Conversion.....	56
Table 3.5 Ru 3 rd Run %CO Conversion.....	58
Table 3.6 Hydrocarbon Formation.....	58
Table 3.7 Sample C ₁₀ data calculation.....	62
Table 3.8 Silica Catalyst Alpha Values.....	64
Table 3.9 Average alpha data results.....	65
Table 3.10 C ₉ (H ₂ pure).....	66
Table 3.11 Ru 1 st Run: 1-olefin vs. 2-olefin results.....	67
Table 3.12 Ru 2 nd Run: 1-olefin vs. 2-olefin results.....	69
Table 3.13 Sample JN09 H/D competition experiment ratios.....	72
Table 4.1 Ru 5 th Run Mass Data.....	78
Table 4.2 Ru 6 th Run Mass Data.....	79
Table 4.3 %CO Conversion for Ru/Al ₂ O ₃	81
Table 4.4 Ru 5 th Run correction factors.....	85
Table 4.5 Deuterium Correction Sample JN5-5.....	88
Table 4.6 H ₂ pure 1-olefin and 2-olefin results with H/D ratios of 1-olefin and 2-olefin..	89
Table 4.7 Competition H/D Ratios JN6-3.....	92

LIST OF FIGURES

FIGURE	PAGE
Figure 1.1 Nobel Metals in the Periodic Table.....	8
Figure 1.2 Hydroxymethylene Mechanism.....	10
Figure 1.3 CO Insertion Mechanism..	11
Figure 1.4 Alkyl Mechanism.....	12
Figure 1.5 Alkenyl Mechanism.....	13
Figure 1.6 Alkylidene Mechanism.....	14
Figure 1.7 Mechanism variations a. Monomers b. Growing Chains.....	15
Figure 1.8 Overlap of monomers and growing chains of various FT mechanisms.....	16
Figure 1.9 Readsorption and chain growth	22
Figure 1.10 Secondary Isotope (Top) and Inverse Isotope Effect (Bottom)	32
Figure 1.11 Theoretical no favoritism competition experiment	37
Figure 2.1 Reactor Set-Up.....	41
Figure 2.2 In the lab reactor	44
Figure 3.1 Ru 1 st Run mass data vs. time	56
Figure 3.2 Sample GC-FID spectrum	60
Figure 3.3 Observable peaks in one carbon number	61
Figure 3.4 Graph of alpha data points	63
Figure 3.5 Comparison of Ru 1 st Run and Ru 2 nd Run H/D Ratio, 1-olefin vs. 2-olefin	69
Figure 3.6 JN09 H/D ratios graphical representation	73
Figure 4.1 1-olefin vs. 2-olefin H/D ratio	89
Figure 4.2 Competition H/D ratios trend JN6-3.....	93
Figure 5.1 Modified Alkylidene Mechanism	97

Figure 5.2 Theoretical Deuterium Enrichment	100
A.1 Ru 1 st Run (Silica).....	108
A.2 Ru 2 nd Run (Silica).....	108
A.3 Ru 3 rd Run (Silica).....	109
A.4 Ru 5 th Run (Alumina).....	109
A.5 Ru 6 th Run (Alumina).....	110
B.1 JN-19: C8 paraffin.....	112
B.2 JN-19: C9 paraffin.....	113
B.3 JN-19: C10 paraffin.....	113
B.4 JN-19: C11 paraffin.....	114
B.5 JN-19: C12 paraffin.....	114
B.6 JN-19: C13 paraffin.....	115
B.7 JN-19: C14 paraffin.....	115
B.8 JN-19: C15 paraffin.....	116
B.9 JN-19: C16 paraffin.....	116
B.10 JN-19: C17 paraffin.....	117
B.11 JN-19: C18 paraffin.....	117
B.12 JN-19: C19 paraffin.....	118
B.13 JN-19: C20 paraffin.....	118
B.14 JN-19: C21 paraffin.....	119
B.15 JN-19: C22 paraffin.....	119
B.16 JN-19: C23 paraffin.....	120
B.17 Ru 1st Run: JN06.....	120
B.18 Ru 1st Run: JN08.....	121

B.19 Ru 2nd Run: JN2-1.....	121
B.20 Ru 2nd Run: JN2-2.....	122
B.21 Ru 2nd Run: JN2-3.....	122
B.22 Ru 3rd Run: JN3-1.....	123
B.23 Ru 3rd Run: JN3-2.....	123
B.24 Ru 3rd Run: JN3-3.....	124
B.25 Ru 6th Run: JN6-2.....	124

CHAPTER 1

INTRODUCTION AND BACKGROUND

1.1 GAS-TO-LIQUIDS (GTL) PROCESS

The study of hydrocarbons is composed of many different fields and types of production. The more common way used to produce useful hydrocarbons is through the utilization of natural petroleum. Natural petroleum is a very important commodity in today's society as it can produce various fuels, waxes and other useful products.¹⁻³ However, with the human population being consumers, there is a real chance of natural petroleum being depleted. Since, humans rely on products such as naphtha, gasoline, jet fuel and various other products, it is necessary to study synthetic processes of producing hydrocarbons for the time when natural resources are no longer a viable option. Of the processes being researched, gas to liquids (GTL) appears to be one of the more viable alternatives to using natural petroleum.⁴

There are multiple parts of GTL production as well as many companies that pour money into GTL research. These companies include Sasol, Shell, PetroSA, ExxonMobil, BP and Chevron. Most of these are very prominent names and they have recognized the importance of GTL research and production. For the GTL process, typically there are three separate stages. These three stages are syngas generation, Fischer Tropsch (FT) Synthesis and Refining.

The first step of syngas generation requires natural gas, coal or biomass materials as a starting reagent. Natural gas is composed of many different types of gases, most of which are not necessary for the next step of FT synthesis. To obtain the ideal reagent, natural gas can be converted through a couple different processes. Natural gas is composed primarily of methane, somewhere around 90% and a various supply of ethane, propane, butanes, nitrogen, carbon monoxide and other minor contributors.⁵ The two gases necessary for the FT reaction is H₂ and CO, the syngas. There is a fairly low concentration of both these reagents in natural gas; however, methane can be converted to these two starting materials through various processes, such as steam methane reforming or partial oxidation. Chemical equations 1.1 and 1.2 show the conversion that is possible through nickel and cobalt catalysts:^{6,7}



This steam reforming process is the cheapest solution for making syngas.^{6,8} However, in the overall process of GTL production, the creation of the syngas tends to be the most expensive part. Average estimates have listed syngas production as 60% of the total costs for the entire GTL power plant.^{4,6,9} Even though conversion of natural gas appears to be the cheapest, it still utilizes a natural resource. There are other options that do not necessarily require natural gas.

Syngas can also be created through coal or biomass. While coal is a natural resource, biomass sources do not have to be. They can be generated by mostly anything that has a carbon base and is combustible. For example, biodegradable or even non-biodegradable trash can be converted to useful syngas through gasification.¹⁰ Gasification is a process that occurs at high temperatures and produces large amounts of hydrogen, carbon monoxide and carbon dioxide through combustion.¹¹ Carbon dioxide is not a compound desired for FT syngas, so it has to be removed from the mixture before introduction to the FT reactor. This leaves the desired syngas of hydrogen and carbon monoxide to move on to step 2 of the GTL process.

Once in a useful form and ratio, this syngas of H₂/CO can be turned into long-chain straight hydrocarbons (C₁-C₆₀) through the FT process.¹² This synthesis can occur at low or high pressures and typically occurs at high temperatures. The last main ingredient necessary is a catalyst, which could be Fe, Co, Ni or Ru.¹³ The products formed through this process are alkanes (paraffins) and alkenes (olefins). Some other present products are water and alcohols. Water may not be a desirable product, but alcohols can be potentially useful. While the major products of FT synthesized are straight chain hydrocarbons, there is the possibility for a substantial amount of branched hydrocarbon products depending on what type of catalyst is used. Once the products are formed, there is one more major step in the GTL process, which is turning the straight hydrocarbons into more useable substances through refining.

There are multiple processes that can be carried out on the hydrocarbon products to make varying types of useful products. Depending on how long the carbon chain is, different processes can be used to either extend the carbon chain or break it into smaller pieces. For example, products C_4 or less can go through oligomerization to produce gasoline.¹⁴ With hydrocarbons C_{20} or greater, hydrocracking can be performed to make diesel.¹⁵ Some products like C_{13} - C_{19} do not need to undergo a refining process as they are already in a variable form of kerosene, unless other products are desired.¹⁶

1.2 FISCHER-TROPSCH SYNTHESIS (FTS)

Of these three stages of GTL, the main focus for this research has been on the FT synthesis. Fischer-Tropsch is still a highly debated topic despite around 100 years of research. There are multiple applications and reasons to study the FT synthesis. For example, FT can be studied as a reason for practical applications described previously in GTL production. Another reason is for the potential explanation of abiogenesis back in the early days of the earth. The important question is: how did earth come to have organic molecules and compounds from an earth that is inorganic in origin. Somehow, the first hydrocarbon or amino acid must have been formed in order to get more complex molecules. One theory involves the use of electrical current via lightning striking a water source to create some of the first organic molecules. An experiment by Stanley Miller with the help of Harold Urey was performed attempting to recreate the formation in pre-complex organic conditions.¹⁷ While their experiments were successful and formed

methane as well as other small products, it did not create long chain hydrocarbons. This is why some scientists lean more towards the theory of FT rather than Miller's. Fischer-Tropsch can provide another reasonable explanation as to why long chain hydrocarbons formed back before any complex organic molecules existed on earth. While this is a feasible reason to study FT and attempt to understand its complex workings, there is another important reason to study this synthesis. That is to define the mechanism or mechanisms that can apply to this type of reaction.

There have been many discoveries about this type of synthesis, especially for catalyst type and preparation. One of the first discoveries of the produced oils and waxes was through Friedrich Bergius in 1913.¹⁸ These experiments consisted of taking garbage and putting it through various temperatures and pressures. One of his tests happened to also be run in the presence of H₂ gas, which then eventually was able to form minor amounts of hydrocarbons.¹⁹ This conversion became known as the Bergius method. It was not until 1925 that Franz Fischer and Hans Tropsch refined the Bergius method and used a similar process. They modified the method by treating coal with steam, thereby creating a water gas-CO and H₂ concoction.¹² Unlike Bergius, Fischer and Tropsch intentionally used a catalyst to help create the hydrocarbons. At this point, the reaction conditions were still carried out at standard pressure and 180-200°C.

Around the same time, other countries such as the UK and the United States had been researching GTL technology, but in the late 1920's, research in this area mostly stopped. Research was put on hold majorly due to economic reasons and the upcoming

depression. The need to research and produce synthetic fuels was not at the forefront of the U.S.'s problems. Another set-back came from the discovery of a new source of natural petroleum.²⁰ This discovery made the eventual loss of natural petroleum seem much more distant and a less pressing issue. At this time, it was also much more expensive to produce synthetic fuels.²¹ With the market being down and no necessity to produce excess fuels at a higher cost, the natural petroleum process still remained at the forefront.

The research picked back up in the late 1930's for America. Henry H. Storch and coworkers produced fuel from American coal in 1937.²² Research continued to occur in this field in minor amounts. The issue that instigated true interest and much desire to understand these processes was in fact World War II. Major studies began in Germany. The Germans did not have enough natural resources in terms of oil and gasoline to fuel their side of the war. So, Germany started researching into other alternative methods to assist in the production of fuels.⁴ At the start of the war, Germany had the capacity to produce 740,000 metric tons of oil through various Bergius and FT plants.²³ In actuality, 570,000 metric tons were produced, which while is not full capacity, it is still an impressively sizeable number at that time.²⁴ Other countries did not appear to be anywhere near this capacity. Towards the end of the war, other countries started investing more money into the Bergius and FT processes due to Germany's example of success. Before the war ended there was a minor worry on the Allies side of running low on fuels, hence the necessity of interest and investment. In 1944, the Synthetic Liquid Fuels act was passed by the Bureau of Mines in the United States.^{4,25} This act was initiated

because of Germany's self-dependence without the natural resource of petroleum. Thirty million dollars was allocated for the next five years to research and develop methods for coal hydrogenation, FT and oil shale mining/distillation.²⁶

After the war, multiple commercial plants as well as a demonstration plant in Pittsburgh were built to better understand the FT process. This plant in Pittsburgh was eventually declared as a success due to the development of a cobalt catalyst extremely similar to Fischer and Tropsch's original work.²⁶ While it was still more expensive to produce hydrocarbons this way, new research advances were made in the United States. By the early 1950's, large FT reactors were built in Texas with full operation beginning in 1953.⁹ It appeared that the U.S. and other countries were finally determined to understand these processes. Unfortunately, interest waned when the process could not be made cost effective. Also, the methane price, and therefore syngas preparation, increased causing the lab in Texas to shut down. Over the following years, some corporations still believed that they could make the FT process more cost effective and improve the overall process. One of these major contributors was Exxon. One project began in 1981 that led to improved, higher activity catalyst along with a better understanding of the mass transport and surface chemistry during FT synthesis. Improvements were also made to the slurry reactor, leading to a higher octane and cetane number.²⁷

By 2002, a distinction was made between high temperature and low temperature FT reactions. Depending on the temperatures, one could produce varying amounts in

which types of products were formed. Low temperature (200-240°C) was performed with either Fe or Co as the main catalyst, whereas high temperature was typically Fe based catalysts.²⁷ The types of supports were also varied depending on the temperature. Low temperature utilized silica for both iron and Co, but Co could also be supported with alumina or titanium dioxide.⁹ These conditions created high molecular mass linear waxes. For high temperature, iron was supported with alumina or magnesium oxide with the requirement of pre-reduction during the synthesis. High temperature created more low molecular olefins and paraffins.⁹ While the majority of the catalysts were Fe or Co, Exxon also experimented with promoting the catalysts with nobel metals. As shown in Figure 1.1, these metals are all grouped together in the periodic table. Another optional catalyst is ruthenium. The problem with ruthenium is that the cost of the metal is simply too high to use in industry and the worldwide reserves are insufficient for large scale industry.²³

scandium 21 Sc 44.956	titanium 22 Ti 47.867	vanadium 23 V 50.942	chromium 24 Cr 51.996	manganese 25 Mn 54.938	iron 26 Fe 55.845	cobalt 27 Co 58.933	nickel 28 Ni 58.693	copper 29 Cu 63.546	zinc 30 Zn 65.39
yttrium 39 Y 88.906	zirconium 40 Zr 91.224	niobium 41 Nb 92.906	molybdenum 42 Mo 95.94	technetium 43 Tc [98]	ruthenium 44 Ru 101.07	rhodium 45 Rh 102.91	palladium 46 Pd 106.42	silver 47 Ag 107.87	cadmium 48 Cd 112.41
lutetium 71 Lu 174.97	hafnium 72 Hf 178.49	tantalum 73 Ta 180.95	tungsten 74 W 183.84	rhenium 75 Re 186.21	osmium 76 Os 190.23	iridium 77 Ir 192.22	platinum 78 Pt 195.08	gold 79 Au 196.97	mercury 80 Hg 200.59

Figure 1.1 Nobel Metals in the Periodic Table

1.3 MECHANISMS OF FTS – AN UNSOLVED MYSTERY

Ruthenium may not be used as an industrial FT catalyst, but it can still be used as a catalyst to help try to understand the mechanism. The mechanism of FT has not been determined, but there are many theories as to what might be happening inside a FT reactor. Some of the proposed methods are: the carbide mechanism, CO insertion, hydroxymethylene, alkyl, alkenyl, and alkylidene mechanisms.²⁸⁻³⁷ It should be noted that there are other mechanisms besides the ones listed previously. The reason these 6 are mentioned is because all relate to the modified alkylidene mechanism proposed later in this thesis.

The first mechanism, the carbide mechanism, was proposed by Fischer and Tropsch in 1923. While at this point, Fischer and Tropsch were not sure how the metal and carbon monoxide interacted, they believed that some sort of bonding between the two must occur.¹² The hydroxymethylene theory (1951) proposed by Storch et. al, started with the idea that a hydroxyl group was present on the active carbon bonded to the metal catalyst.^{24,38-40} This mechanism proposed that carbon carbon bonds form through the elimination of water. The hydroxymethylene mechanism is shown in Figure 1.2.

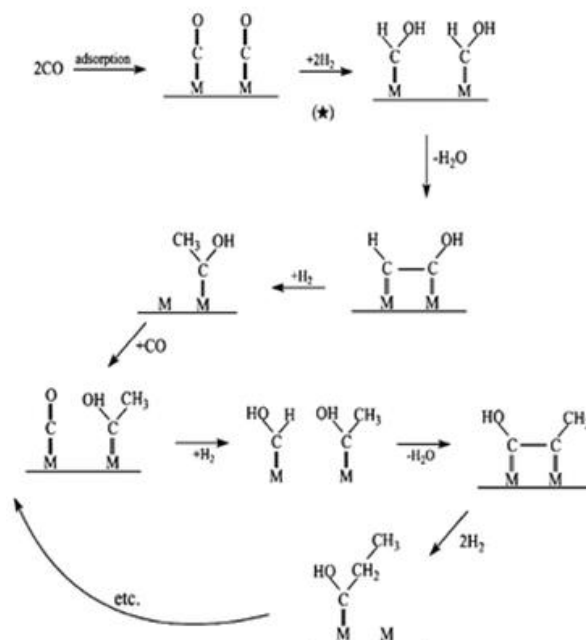


Figure 1.2 Hydroxymethylene Mechanism.

Source: Davis, Burtron H. *Fischer-Tropsch Synthesis: Current Mechanism and Futuristic Needs* CAER, 129-138.

Progressing on, in 1976, Henrici et. al proposed the CO insertion mechanism.⁴¹ This mechanism starts with an activated M – H into which CO is inserted between the M and H. After hydrogenation of the compound and through a hydroxyl intermediate, the carbon is then coordinated to the metal surface. The propagation steps that follow also include the CO insertion process where the CO inserts between the metal and coordinated carbon. This allows for chain growth and an increased carbon number by one. The CO insertion mechanism is shown in Figure 1.3.

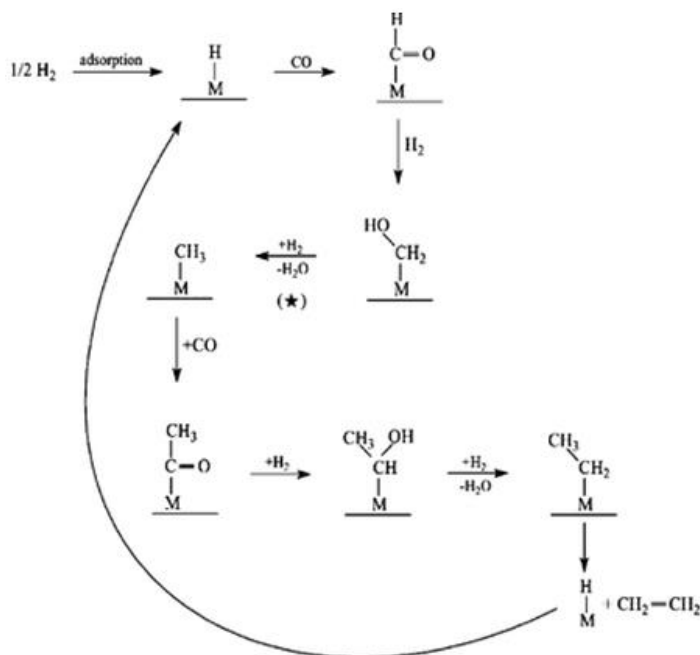


Figure 1.3 CO Insertion Mechanism.

Source: Davis, Burtron H. *Fischer-Tropsch Synthesis: Current Mechanism and Futuristic Needs* CAER, 129-138.

The last three mechanisms are all very similar with minor variations as more data was discovered about the FT synthesis. In 1980, Brady and Pettic proposed the alkyl mechanism,^{30,31} shown in Figure 1.4. The alkyl mechanism used the same growing chain as the CO insertion mechanism, but changed both the monomer and the way propagation occurs. Carbon monoxide insertion involves the monomer of CO whereas the alkyl mechanism uses a monomer of $M = CH_2$. Instead of an insertion mechanism, the alkyl involves the movement of electrons between two adjacent monomers. A pair of electrons between the metal and CH_2 will attack the carbon on the adjacent monomer, forming a bond between the two carbons. After this process, hydrogenation can occur,

fully removing the bonds between one carbon and the metal. This leaves one active carbon bonded to the metal and a carbon group. While this propagation differs from CO insertion, the growing chain is still the same. After hydrogenation, the active carbon is only singly bonded to the metal surface.

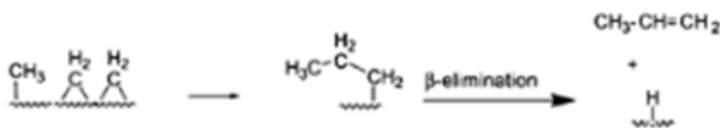


Figure 1.4 Alkyl Mechanism.

Source: Davis, Burtron H. Fischer-Tropsch Synthesis: Current Mechanism and Futuristic Needs CAER, 129-138.

A variation to this growing chain came in the alkenyl mechanism proposed by Turner et. al in 1995,³² as seen in Figure 1.5. The reason for this proposed variation came from research being done with iron catalysts. Iron catalyzed FT produced more branched products, between 20-40%.^{42,43} While the alkyl mechanism explained how straight chain paraffins and olefins were formed, it could not explain the formation of branched products. The alkenyl mechanism could offer a reason as to why so much branched product is formed as a major product. The growing chain, instead of having single bonds throughout, has one double bond between two carbons. The double bond starts between the C₁ and C₂ with C₁ being the carbon directly attached to the metal. As growth occurs on this chain, the new carbon would still attack the C₁. After attack and stabilization, the

double bond would then be between C₂ and C₃. The active hydrocarbon can then proceed through isomerization where the double bond is shifted back between the new C₁ and C₂. This theory also assumed that 1-olefins and 2-olefins are primary products and paraffins are secondary products after readsorption.

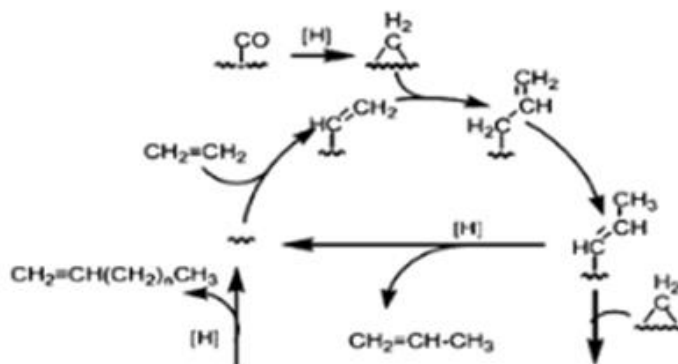


Figure 1.5 Alkenyl Mechanism.

Source: Davis, Burtron H. *Fischer-Tropsch Synthesis: Current Mechanism and Futuristic Needs* CAER, 129-138.

The last past proposed theory mentioned previously is the alkylidene mechanism,³² shown in Figure 1.6. This mechanism also has the same monomer as alkyl and alkenyl mechanism of M = CH₂, but the growing chain again differs. The growing chain contains a double bond not between two carbons, but between the C₁ and the metal. With this type of growing chain, there is no isomerization necessary. With all these mechanisms discussed, as time progressed, various improvements have been added to the overall mechanism as research continued. The suggested primary products of the

alkylidene mechanism are 1-olefins and paraffins, as first suggested by Herrington.⁴⁴ The mechanism proposed later in this thesis is a new addition to this timeline called the modified alkylidene mechanism.

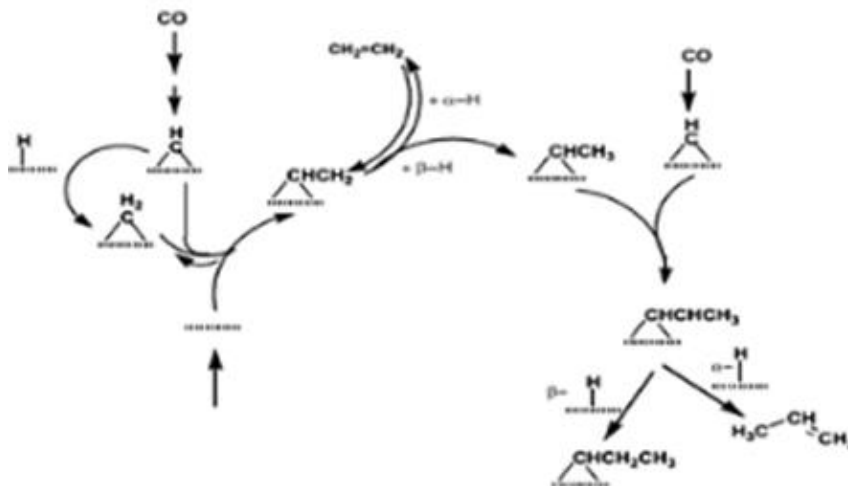


Figure 1.6 Alkylidene Mechanism.

Source: Davis, Burtron H. *Fischer-Tropsch Synthesis: Current Mechanism and Futuristic Needs* CAER, 129-138.

Keeping all of these mechanisms in mind, there are many variables to consider, which is why there are so many various proposed theories. Some such variables are the monomers and growing chains, which can be found in Figure 1.7.

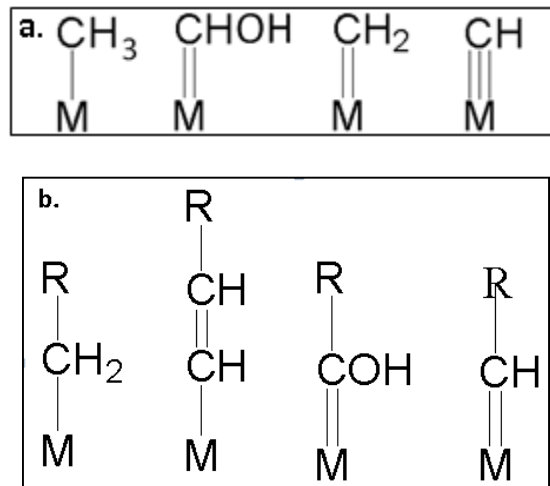


Figure 1.7 Mechanism variations **a.** Monomers **b.** Growing Chains

A comparison and overlap of the various mechanisms previously discussed can be found in Figure 1.8. With this pictorial representation, the major similarities and differences can easily be seen between mechanisms. The alkyl, alkenyl and alkylidene all start with the same monomer, but have various growing chains. Also, the alkyl and CO insertion mechanisms differ in monomer, but not in the growing chain. While the hydroxymethylene does not have the same monomer or growing chain as the other mechanisms, it does have the similar characteristic of the metal being double bonded to the C₁ carbon.

Growing chain \ Monomer	$\begin{array}{c} R \\ \\ CH_2 \\ \\ M \end{array}$	$\begin{array}{c} R \\ \\ CH \\ \\ CH \\ \\ M \end{array}$	$\begin{array}{c} R \\ \\ COH \\ \\ M \end{array}$	$\begin{array}{c} R \\ \\ CH \\ \\ M \end{array}$
CO^*	CO insertion			
$\begin{array}{c} CHOH \\ \\ M \end{array}$			Hydroxy-methylene	
$\begin{array}{c} CH_2 \\ \\ M \end{array}$	Alkyl	Alkenyl		Alkyldene
$\begin{array}{c} CH \\ \\ M \end{array}$				Modified Alkyldene

Figure 1.8 Overlap of monomers and growing chains of various FT mechanisms

1.4 RUTHENIUM CATALYZED FTS

There have been many experiments to attempt to discover the true growing chain in the mechanism, including isotopic tracing. Van Kijk et. al. began by studying the most basic hydrocarbons formed, methane and C_2 .⁴⁵ While this research was done with a cobalt catalyst, it still led to some interesting results regarding FT synthesis. Since it has been suggested that ruthenium appears to act more like a cobalt catalyst than any other catalyst discovered thus far, it would make cobalt a good starting point. Through data collected, it was determined that 1-olefins are the major candidates for readsorption due to their high energy potential.⁴⁵ This was discovered through the monitoring of ethene as the reaction progressed. There was a significantly noticeable difference in how long it took for ethene to begin eluting from the column in comparison to methane and other

products collected. Also, the concentration of eluted ethene was lower than expected, which could be due to the fact that ethene is still active under FT conditions. Ethene was readsorbed onto the catalyst surface and continued with chain growth or subsequently hydrogenated into ethane. Being that terminal olefins are slightly less stable and higher in energy than paraffins, it would make sense that they are better for primary product readsorption. Another discovery made during this experiment concerned C-C bond formation and how it could be controlled to be irreversible.⁴⁶ If low pressure and high temperatures are used, it was determined that the C-C bonds will not break and revert to their previous forms. This makes FT useful since the synthesis will not consume or destroy the products desired.

While much of this in depth study did focus on a cobalt based catalyst, it can still give insight and guidance into Fischer Tropsch. As mentioned before, there are multiple potential catalysts, both industrial and research catalysts. Nickel is one such metal that has the potential for FT, but the majority of the product is CH₄, which is not one of the main desirable products. Since the primary product is methane, the monomer, and not C₂⁺, polymers it is considered a very poor FT catalyst as it does not effectively create polymers. Cobalt does in fact produce the target products leaning more towards paraffin production. On the other hand, iron catalysts produce more olefin and branched products.⁴³ Since iron makes more branched products, this could be potentially more useful as branched products generally have a higher octane number (a measure of efficiency and performance of gasoline/diesel). One less desirable reason for using iron

is the fact that iron catalysts are more affected by water as these two can form inactive iron oxides.⁴⁷⁻⁵⁰ Generally, all three of these types of catalysts are fairly dependent on the reaction conditions. Depending on what condition they are put under can vary the products and activity of the catalysts. This is mostly due to their flexible active sites that are influenced by changes in pressure or temperature. In comparison to ruthenium, the previous mentioned catalysts are all considered less active.^{51,52} Due to this knowledge, it would seem that ruthenium would be the optimal choice for this synthesis. Remember though, ruthenium catalysts are not as appealing to industry even though they offer more production. A big issue with incorporating ruthenium into the industrial world is the pricing. It is simply too expensive to buy or even find ruthenium in mass amounts for eventual production of consumer materials. For research purposes, ruthenium could be a great candidate as it is not necessary to produce enough products to market. The increased product amount allows for greater consistency during analysis and can lead to less outliers. Research also does not require more than a couple of grams to synthesize multiple catalysts leading to much data. Also, while there has been research done on ruthenium catalysts, it is not quite as much as iron or cobalt. So, studying and trying to understand the complexities of FT can be done through the use of ruthenium and can lead to more potential discoveries that cobalt, iron or nickel have not yet yielded.

There are other benefits to ruthenium as a research catalyst; for example, ruthenium is more resistant to oxidation in a water atmosphere.⁵³ The less ruthenium that is oxidized in the reaction column, the more potential there is for increased amount

of active sites. This is important due to the known reaction of the water-gas shift (WGS) that occurs during the FT reaction. If water is constantly present in the reaction, it would benefit more hydrocarbon formation to not have ruthenium oxidize and become inactive.

The WGS has the following reaction:



While this is not considered the main FT reaction, it is still important to hydrocarbon production. Without the WGS, the main product of ruthenium catalyzed FT would be water with minimal concentrations of hydrocarbons.⁵³ Since ruthenium has less of a tendency to react with water, it has even been proposed that the presence of water can increase the probability of chain growth.⁵³ If less water reacts with ruthenium, then there should be less water being produced by the water gas shift to re-achieve equilibrium. Now more of the reagents can be used for FT synthesis instead of maintaining the water equilibrium inside the column.

1.5 PRODUCTS DURING FTS

Mostly, the desired products of FT synthesis are made through Equations 1.4 and 1.5:



Most of the previous mechanisms described have been applied to ruthenium as a FT catalyst. While there are disagreements on how the structures begin and what process they go through in the reaction column, there are still 3 main steps in FT. The first is monomer formation. Whether the carbon has one hydrogen atom, multiple hydrogen atoms or an oxygen atom attached to it, the carbon from carbon monoxide must somehow be coordinated to the metal. Once the monomer is formed the next step can occur, propagation.^{31,54,55} How the polymer is created from the monomer is one of the hotly debated topics about FT. Regardless of how propagation occurs, somehow the monomers have to turn into polymers in this step, otherwise the only product made would be methane. Finally, the last step is termination. There are two main options that the growing hydrocarbon can go through, beta elimination or hydrogenation. Beta elimination produces olefins and depending on which mechanism is being used, this could create terminal olefins or internal olefins. If looking at the alkenyl mechanism, both terminal and internal olefins are primary products, whereas the alkylidene mechanism shows that only 1-olefins are primary products. Also, with certain mechanisms, hydrogenation could be either primary or secondary products. Hydrogenation simply creates paraffins, which are generally inactive in the FT column and do not go through a readsorption process.^{56,57}

The readsorption process requires an active reagent that can reform a bond on the active catalyst surface that has a free site. If a hydrocarbon is readsorbed it can go through secondary reactions making secondary products. The less stable 2-olefins and 1-

olefin can go through this readsorption process over the double bond present in the olefin structure. The re-attached hydrocarbon can now go through propagation or termination again and create secondary products. The main difference here is where the hydrocarbon is now attached to the metal catalyst. In the original polymerization for 1-olefin, the terminal carbon was bonded to the ruthenium metal. Now, after readsorption, the hydrocarbon could be attached either at the terminal carbon, or C2. Due to Markovnikov's rule, the majority of the time, the hydrocarbon will readsorb through the C2 over the terminal carbon. After readsorption, there are four main pathways that the hydrocarbon can now proceed through. The first is simply to reverse and form 1-olefin again. However the other three possibilities are more probable. The second is simply to hydrogenate and create more paraffins, making it difficult to determine the true amount of paraffin produced through the primary reaction pathway. The third option is to eliminate and form 2-olefins. This option is more probable than eliminating to reform the 1-olefin due to 2-olefin having a higher stability than the terminal alkene. This gives two more major products of 2-trans-olefin as well as 2-cis-olefin. The last option that is possible is for propagation to occur. This is how branched products have the potential to be formed. Since the hydrocarbon is most likely readsorbed on C2, the next carbon added onto the chain would bond to C2 instead of C1 as shown in Figure 1.9.

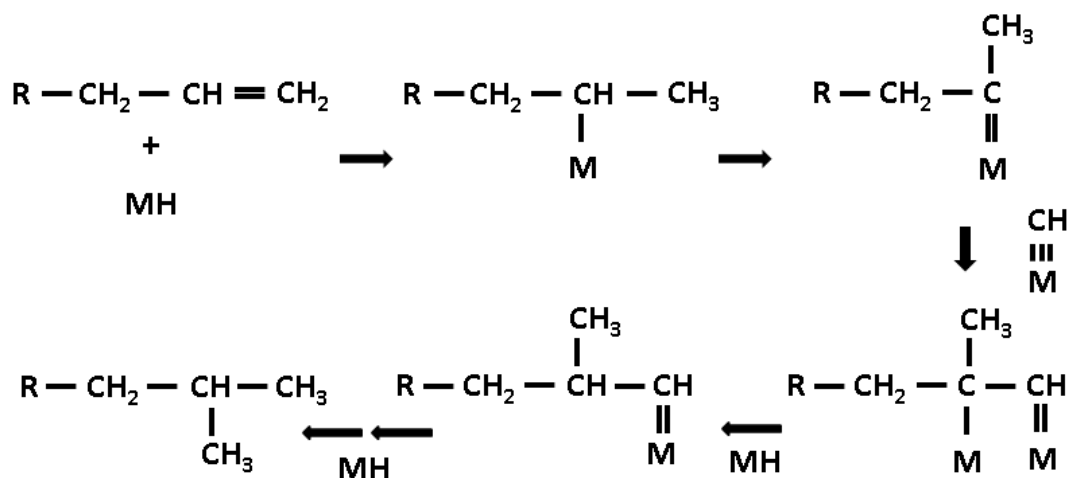


Figure 1.9 Readsorption and chain growth

The chain would then proceed to grow via the extra carbon now added if propagation continues. This creates methyl branched products. The substitution of where the methyl is situated could be anywhere from C2 to C5. Typically not much higher than C5 methyl substituted is observed in the products.⁴³ This creates a plethora of new hydrocarbon products that have simply been put under the umbrella label of branched products. Of all the possible reactions that can occur in a FT reactor, both primary and secondary, there are many products that can form and are often observed. The amount of each product varies based on reaction conditions and primarily what type of catalyst and support is being used.^{58,59}

1.6 DEUTERIUM TRACER STUDIES OF FTS

While there have been multiple publications on ruthenium based FT synthesis, there is still yet more research to be done. This research focuses on a ruthenium based catalyst with two different supports: silica and alumina. Having multiple types of support could give better insight in the FT synthesis. There have been past studies performed to determine the kinetic isotope effect in Ru catalyzed reactions.⁶⁰⁻⁶³ However, for the KIE, there have been multiple reported results that have conflicted. One group observed a normal isotope effect over a ruthenium powder catalyst with the CH₄/CD₄ ratio being 2.2.⁶¹ Another group claimed that no isotope effect could be observed for an alumina supported catalyst.^{62,63} There are still yet other groups who have run FT with ruthenium and found an inverse isotope effect for multiple catalysts.⁶⁰ So, there is a wide spectrum of possible results for ruthenium catalysts. This project will help to see which type of isotope effect is observed if any is observed at all. Both catalysts are synthesized based on the work of Kellner and Bell and will be described further in the experimental section. Since the catalysts will be synthesized in the same way, the results could also show reproducibility for the work done by these previous scientists.

Even though the KIE has been researched extensively for FT synthesis, there are still other tests that can be run with isotopic tracing to help unravel the mechanism. The KIE focuses on switching between hydrogen and deuterium in order to see the difference in hydrocarbon production. Instead of switching between the two, another analysis where hydrogen and deuterium are run at the same time could offer more insight into

the mechanism. This is called a competition experiment as hydrogen and deuterium are directly competing to attach to the hydrocarbon. With this competition, deuterium enrichment, or lack thereof can be observed. Publications including this type of experimentation for cobalt and iron have been researched, but not yet for ruthenium. Observing the presence of deuterium enrichment in C_7^+ hydrocarbons can help support the observations on the KIE. This allows for observations not to be dependent on the gas product collection and analysis. If the observations between the two types of experiments are consistent, it leads to better support of any conclusions that can be drawn about the mechanism.

The main difference between these two experiments has to do with the type of syngas that is utilized. For competition the H_2 and D_2 must compete at the same time. In order for the reaction to not be skewed in either gas's favor, equal starting amounts of the two must be used, along with the complementary and necessary reagent of carbon monoxide. This will show which isotope is more favored to bind and be a part of the final hydrocarbon. If there is no favoritism between the two this could also lead to new information about the mechanism. While getting hydrocarbons with mixed isotopes is the point of the competition experiment, it also makes it difficult for other types of analyses. Hence, the switching experiment is still necessary and should still be performed. Pure hydrogen and deuterium hydrocarbons are also still wanted as these can lead to product analysis on a GC. With the competition, since deuterium and hydrogen are so similar, they elute from GC columns at extremely similar times, which make it difficult to

distinguish. Determining how much 1-olefin, 2-olefin, paraffin and branched products could also help and provide information about ruthenium catalysts. Therefore separation between all of these peaks is necessary, which require purer products or specialized columns.

1.7 INSTRUMENTAL THEORY

There are three main instruments used to analyze the various products acquired. Starting with gas samples that were collected via gas bags, they were analyzed by the Micro-GC. The specific columns used are listed in the experimental section and were used to separate and identify the following compounds: H₂, CO, N₂, ethane, ethylene, propane, propene, n-butane, trans-2-butene, iso-butylene, 1-butene, cis-2-butene, and isobutane. The form of identification used is retention time. Each compound should elute at a different time depending on which column was used. Since this GC has four separate columns, there are four different chromatograms all with varying peak identifications. The identifications of the peaks were provided via the manual and checked with a standard that consisted of all the gas products that could be identified on the four columns. The standard also helped to calibrate the instrument to ensure the best accuracy of analyzed products.

The theory behind chromatography goes back to equilibria. The goal of chromatography is to separate compounds, which can be accomplished by interactions

between the column and the sample injected. Based on how strong the interactions between the sample and the stationary phase of the column are, will allow for varying elution times. The stronger the interaction, the longer the compound will stay in the column. This is due to the compound constantly trying to reach equilibrium between the stationary phase and the mobile phase. So, if at equilibrium the compound likes to be in the stationary phase more, it will take longer to elute. For compounds that find their equilibrium is shifted more towards the mobile phase they will elute faster as the flow rate of the mobile phase will carry them through the column. One of the priorities of this type of separation is to ensure that all compounds separate enough from each other as well as provide a strong peak. The resolution is necessary so that peaks do not mix and one can measure how much of one compound is in the sample. The resolution is based on the number of theoretical plates. The more theoretical plates are present, the better the resolution. The number of theoretical plates is based on three factors: Eddy Diffusion, Longitudinal Diffusion and Mass Transfer.

The first of these three factors, Eddy Diffusion, is based on the number of pathways a molecule can travel down the column. The more pathways there are for the molecule to travel, the higher the number of theoretical plates. Longitudinal Diffusion has to do with a compound spreading out as it travels down the column. This value typically gets smaller with lower pressures. If there is not a lot of pressure from the mobile phase, the compounds will have a tendency to spread out like water does on a table. To prevent this type of diffusion, one needs to ensure that the flow is high enough

so the compounds do not disperse. However, the flow rate cannot simply be increased indefinitely. Too high of a flow rate could push all of the compounds through the column without giving enough time for interaction. The flow must be a happy medium where it is fast enough to prevent longitudinal diffusion, but slow enough to allow the compounds to interact with the stationary phase. Mass Transfer also involves the interactions between the stationary phase, the sample and the mobile phase. This is the key where equilibrium comes into play. As a compound is moving down the column, it may be attracted to the stationary phase. Not every single molecule of this compound will move into the stationary phase at the same time or even the same amount of time. So, the molecules of this compound that are still in the mobile phase will be carried further down the column, separating from the other molecules of the same compound. This widens the amount of time it takes for that compound to elute, leading to lower resolution. The equation for all three of these factors is shown in Equation 1.6 where H is the number of theoretical plates, A is Eddy Diffusion, B is Longitudinal Diffusion, C is Mass Transfer, and μ_x is the flow rate. The larger H is, the better the separation and resolution observed in the chromatogram. So, with chromatography there are many factors to consider in order to have the ideal identification and resolution.

$$H = A + B/\mu_x + C \mu_x \quad (1.6)$$

The gas chromatography described previously for the micro-GC stands for both other GC techniques used in this research. The difference is the micro-GC is how and what it detects. The micro-GC was used to analyze gaseous compounds collected, the

Gas Chromatography-Flame Ionization Detector (GC-FID) is used for oil/wax product analysis. With the GC-FID, the separation of the various compounds works the same way as the micro-GC with a different column. The samples are then detected through the flame ionization detector (FID). Typically this type of instrument is good for analyzing organic compounds as the flame used combusts organic molecules easily for detection. The samples run contain various hydrocarbons ranging from C6 to up to, but not always, C30. All carbon numbers are separated and eluted from the GC column to be detected. The FID starts simply with a flame supported by a glow of hydrogen gas. This flame is kept around 300°C, which makes it easy to volatilize the organic compounds. As the compounds elute and enter this flame, they are turned into ionic compounds. These ions can produce a current which in turn can be a measurable output. The higher the current is, the higher the content of that specific compound in the injected mixture. The GC-FID product spectra give fairly good resolution, enough to tell apart various olefins, paraffins and branched peaks apart. The peak areas produced can then be compared to the whole product in order to collect data.

The last type of detection used was mass spectrometry. This type of analysis was also coupled with gas chromatography. Mass spectrometry can be a very useful technique that helps to identify and quantify compounds. As a compound elutes from the column and enters the mass spectrometer, the very first step is to ionize that compound. This is absolutely essential as the compounds will be measured in the mass spectrometer based on its mass to charge ratio. There are multiple ways to identify the

ions produced based on mass to charge and eventually, once measured, they produce a spectra with massive amounts of results. Each observed peak on the chromatograph can be separated into varying mass to charges found by the mass spectrometer. This is essential when analyzing products that could have varying mass to charges of only 1 unit, such as the mass difference between hydrogen and deuterium.

1.8 DATA ANALYSIS AND CALCULATIONS

There were many various calculations performed on the data collected. The first of which is CO conversion and the kinetic isotope effect (KIE). The CO conversion shows how active a catalyst is and what percentage of CO turns to hydrocarbons or other carbon containing products. This is calculated by monitoring how much CO elutes from the column as well as knowing how much CO is originally put into the reaction. Equation 1.7 shows the CO conversion calculation equation used:

$$\frac{CO_{in} - CO_{out}}{CO_{in}} \times 100 = \%CO \text{ Converted} \quad (1.7)$$

The calculations involve taking into account the flow rate in order to determine moles, which are the numbers then used in the equation. From this conversion, other calculations can be made, like hydrocarbon formation. This involves the removal of CO₂ from the percent of CO converted. The usefulness of these calculations comes in handy

during the switching experiment. Switching between hydrogen and its isotope allows for a kinetic study that can yield information about the mechanism.

There are multiple effects that have the possibility to be observed; they are: normal (primary) isotope effect, secondary isotope effect, the inverse isotope effect and no isotope effect. The normal isotope effect starts with understanding the rate of conversion in secondary readsorption reactions for hydrogen and deuterium. Looking at elimination, it is understood that there must be some form of transition state between conversion. This transition state moving from C-H to C⁻+H and C-D to C⁻+D are very similar in energy. The activation energy for C-D to C⁻+D is larger than C-H to C⁻+H. When comparing the (rate of hydrogen)/(rate of deuterium), it should be observed that $k_H/k_D > 1$ due to this energy difference. Generally when a normal isotope effect is present, a k_H/k_D ratio of 3-6 is observed.

The secondary and inverse isotope effects are related in the sense that they are the opposite process of one another. The secondary isotope effect has to do with changing from sp^3 to sp^2 hybridized. The inverse isotope effect involves changing from sp^2 to sp^3 hybridization. To determine which effect is observed, the energy levels are taken into account. When looking at their respective energies, the C-D bond is more stable and lower in energy than the C-H bond. The gap between these two energy levels can vary depending on the hybridization of the bond. The sp^3 hybridization has a larger energy gap between C-H and C-D than the sp^2 hybridization. So, when looking at the secondary isotope effect, moving from sp^3 to sp^2 hybridization, the activation energy

required to go through the intermediate is smaller for C-H than C-D. With less activation energy, shown in Figure 1.10, C-H is more kinetically favored and is the faster reaction. Therefore when looking for this observation in terms of %CO conversion, more CO would be converted with hydrogen than deuterium. With the inverse isotope effect, the opposite should be observed. More CO should be converted with deuterium than hydrogen. This is due to the activation energy being lower for deuterium than hydrogen when shifting from sp^2 to sp^3 hybridized, also shown in Figure 1.10. The effect observed indicates which change in hybridization occurred in the reaction.

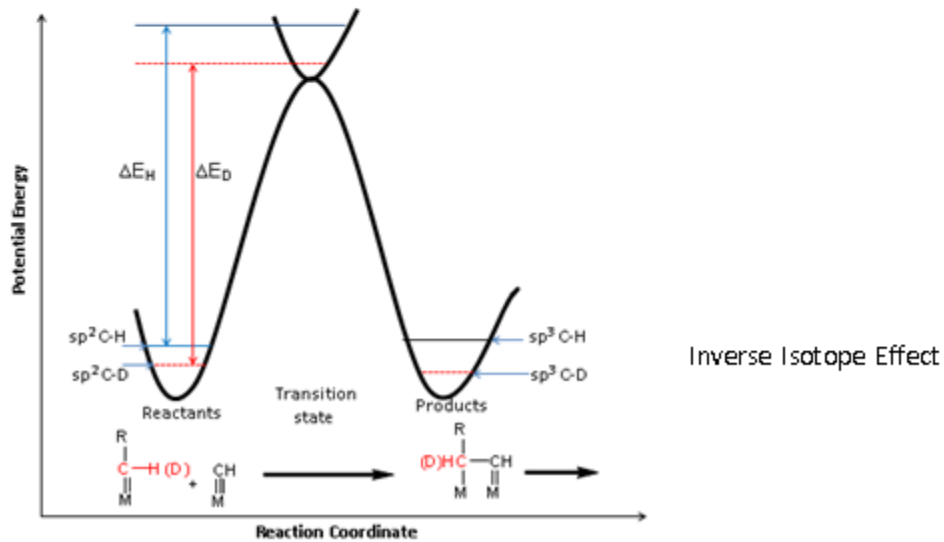
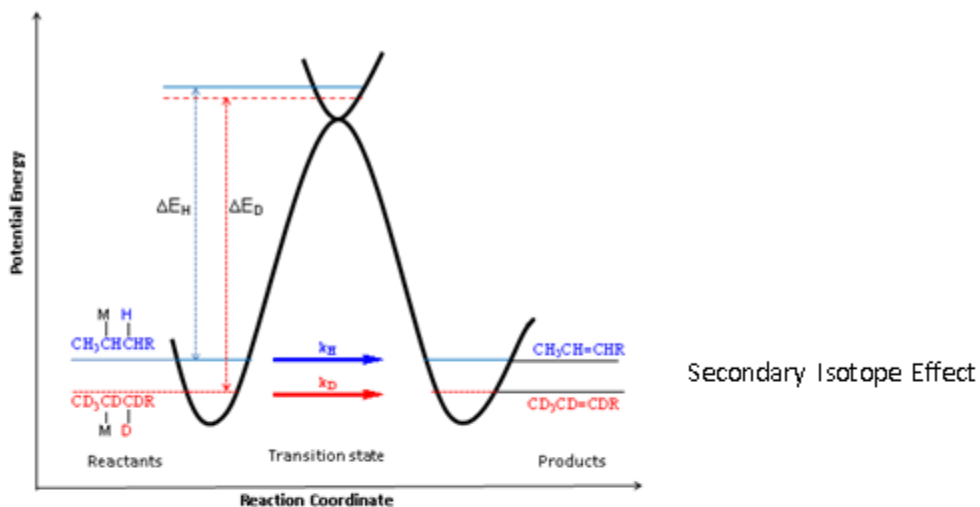


Figure 1.10 Secondary Isotope (Top) and Inverse Isotope Effect (Bottom)

The last optional observation for KIE is no isotope effect. When looking at the rate equations of a reaction, if the slow step is a step that does not involve hydrogen, then the rate cannot depend on hydrogen. If the rate does not depend on hydrogen, switching

between hydrogen and deuterium should give no trend in results when comparing the isotopes.

Another helpful type of analysis with switching experiment products comes from the Anderson-Shultz-Flory (ASF) equation,^{64,65} shown in Equation 1.8, where n represents the carbon number, r_n is the rate of formation of carbon #n, and r_1 is the rate of formation of the monomer.

$$r_n = r_1 \alpha^{n-1} \quad (1.8)$$

If $n = 1$, r_n would be the rate of formation of methane. The alpha variable represents the growth probability of hydrocarbons. This alpha can be calculated from experimental results. To do these calculations, some manipulation of the ASF equation is required. First there are a few things that must be known. If the rate of the formation of hydrocarbon n is divided by the rate of formation of the total hydrocarbons, the mole percent of C_n is the yield ($r_n/r_T = \text{mol\% of } C_n$). Likewise, the r_1/r_T should be the mol% of methane. Using this knowledge the ASF equation can be manipulated as shown in Equations 1.9 through 1.13, where r_T represents the rate of the total reaction.

$$\frac{r_n = r_1 \alpha^{n-1}}{r_T} \Rightarrow \frac{r_n}{r_T} = \frac{r_1}{r_T} \alpha^{n-1} \quad (1.9)$$

Substitute in the known mol % to Equation 1.9.

$$\text{mol\% of } C_n = \text{mol\% of } CH_4 \times \alpha^{n-1} \quad (1.10)$$

Equation 1.10 can be linearized through the natural log, which yields Equation 1.11.

$$\ln(\text{mol\% of } C_n) = \ln(\text{mol\% of } CH_4 \times \alpha^{n-1}) \quad (1.11)$$

Manipulate Equation 1.11 through multiple steps to reach Equation 1.13.

$$\ln(\text{mol\% of } C_n) = \ln(\text{mol\% of } CH_4) + \ln(\alpha^{n-1}) \quad (1.12)$$

$$\ln(\text{mol\% of } C_n) = \ln(\text{mol\% of } CH_4) + (n-1) \times \ln(\alpha) \quad (1.13)$$

Equation 1.13 has the format of a linear ($y = mx + b$) equation, where $y = \ln(\text{mol\% of } C_n)$, $m = \ln(\alpha)$, $x = (n-1)$, and $b = \ln(\text{mol\% of } CH_4)$. Since $m = \ln(\alpha)$, $\alpha = e^m$. The mol% of C_n can be calculated for each carbon number analyzed by GC-FID and plotted against carbon number. The slope of the line can then be found and manipulated through the use of natural logs to find α for one sample. This can be done for any pure hydrogen or pure deuterium sample collected. These calculations yield information about chain growth. The higher the alpha is, the higher the probability of longer chain growth.

The previous alpha calculations come from analysis of the products through GC-FID. There are other useful calculations that can also be done with these results. One of which can be the determination of primary and secondary reaction pathways. Generally, the mechanisms propose that 1-olefins and paraffins are primary products with 1-olefin being the major candidate for readsorption. It is also generally accepted that branched products are secondary products formed after readsorption. The 2-olefins have been proposed as both primary and secondary products from various research groups. With the product spectra acquired, the 1-olefin and 2-olefin peaks can be compared in order to attempt to determine if these products are formed through the same reaction pathway or not. This type of analysis utilizes hydrogen and its isotope. It is necessary to have pure

hydrocarbon and pure deuteriocarbon as the calculations are based on Equations 1.14 and 1.15.

$$\frac{[1\text{-olefin}]_H}{[2\text{-olefin}]_H} = a \quad (1.14)$$

$$\frac{[1\text{-olefin}]_D}{[2\text{-olefin}]_D} = b \quad (1.15)$$

If 1-olefins and 2-olefins are created through the same reaction pathway, then a should equal b. Assuming this, Equations 1.14 and 1.15 can be set equal to each other to yield Equation 1.16.

$$\frac{[1\text{-olefin}]_H}{[2\text{-olefin}]_H} = \frac{[1\text{-olefin}]_D}{[2\text{-olefin}]_D} \quad (1.16)$$

Equation 1.16 can then be rearranged to yield Equation 1.17 in order to yield a comparison of 1-olefins vs. 2-olefins. These concentrations and subsequently ratios can be calculated through peak areas given by the GC-FID. If the ratios of hydrogen to deuterium are the same, then the formation of 2-olefins and 1-olefins must be through the same reaction pathway. If the values differ significantly, then 2-olefins are produced through a different pathway than 1-olefins. Since 1-olefins are considered primary products, this could indicate whether 2-olefins are primary or secondary products.

$$\frac{[2\text{-olefin}]_H}{[2\text{-olefin}]_D} = \frac{[1\text{-olefin}]_H}{[1\text{-olefin}]_D} \quad (1.17)$$

The last type of analysis comes from the competition experiment. The chromatogram obtained is similar to the GC-FID chromatogram in terms of elution of peaks. The difference is in the type of analysis. Using mass spectrometry, each peak can be analyzed for mass to charge units. Since the products are hydrocarbons, the ions formed are not pieces of the original product. This allows for easier analysis of exactly what hydro/deuterio carbons are formed.

There are hundreds of various products formed through the competition experiment. This is due to the fact that any number of hydrogen or deuterium can bind to the hydrocarbon with the mixed syngas. Take for example, a C₈ paraffin. The number of products could vary from C₈H₁₈ to C₈D₁₈ with any variation on number of hydrogen and number of deuterium in between. Therefore, the possible range of C₈ paraffin isotopomers is from 114-132 g/mol. Taking into account any hydrocarbons that are olefins, the entire possible product range for just C₈ molecules is 112-132 g/mol. The most probable theoretical formation if no favoritism between hydrogen and deuterium is expected is for number of hydrogen to equal the number of deuterium. For the C₈ paraffin, this would be C₈H₉D₉. As the number of deuterium increase or decrease from this C₈H₉D₉, the probability of their formation decreases. By the time the pure hydrogen (C₈H₁₈) or deuterium (C₈D₁₈) is reached, the amount of theoretical product is so small that it is negligible. The expected curve of the various isotopomers should follow a Gaussian trend with the centroid being placed at C₈H₈D₈ for any given olefin. A theoretical C₈ paraffin with no isotopic favoritism is shown in Figure 1.11.

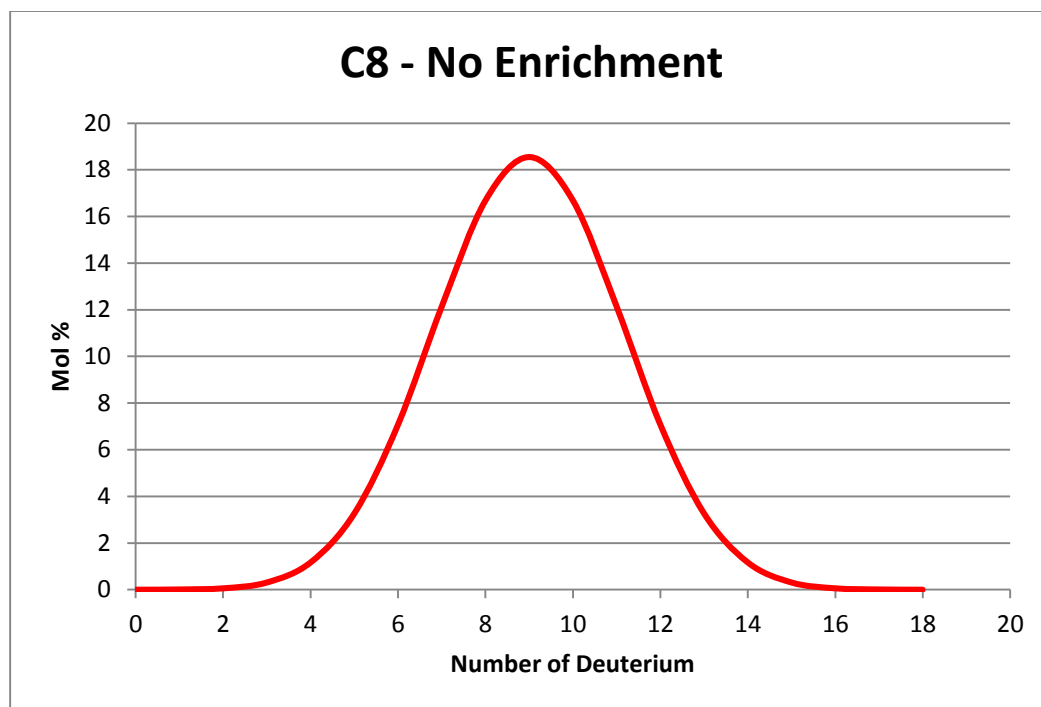


Figure 1.11 Theoretical no favoritism competition experiment

To determine whether or not the data follows this curve, each isotopomer is identified for each carbon number and the peak area recorded. These peak areas can be plotted in a Gaussian curve just as the theoretical was calculated. If the data overlaps the theoretical peak (Figure 1.11), then there is no favoritism and no deuterium enrichment. If the number of hydrogen in the average hydrocarbon is more than deuterium, this would cause a shift in the Gaussian curve to the left. This is the opposite of deuterium enrichment. Deuterium enrichment is where deuterium is more favored to bind and would therefore have and increases presence in the hydrocarbon product. The results of this experiment are listed as H/D ratios. If the ratio is less than one, there is more deuterium than hydrogen present in that carbon number. The ratios for each carbon

number can then be plotted to observe any trends as well as if deuterium enrichment is present in the products.

CHAPTER 2

EXPERIMENTAL

2.1 SYNTHESIS OF RUTHENIUM CATALYSTS

Two different ruthenium catalysts were synthesized, both originating from the compound RuCl_3 . The RuCl_3 was acquired from both Sigma Aldrich Chemistry and Acros Organics. The RuCl_3 from Aldrich had a 45-55% purity and the RuCl_3 from Acros had a 35-45% purity. The purity is the only relevant difference found between the content of the bottle. The RuCl_3 from Sigma Aldrich was used to synthesize the silica supported catalyst. The silica gel used was obtained from Fischer Scientific and had a 70-230 mesh. The catalyst created with silica was approximately 4.8% Ru. The process began in a round bottom flask by dissolving 0.98 grams of RuCl_3 in 100 mL of water. Next, the silica (9.8 grams) was added slowly to the solution with thorough mixing. The solvent was evaporated via a Buchi Switzerland Rotovapor R11 and subsequently placed in an oven at 105-110°C for 24 hours. Unfortunately, the dried catalyst had to be re-dissolved into solution as it was not buffered to the correct acidity. Once the pH was close to 2, the solvent was again evaporated and the catalyst placed in the oven. To ensure the removal of all unwanted contaminants, like other organics, the catalyst was placed in a micro furnace at 400°C for 3-4 hours. The reaction of the support to ruthenium yielded approximately 10.6 grams of catalyst.

The second catalyst was supported with alumina instead of silica. The alumina utilized has high surface area of 219 m²/g and was acquired from Alfa Aesar. The alumina was crushed with a mortar and pestle to obtain a powdery support ready for bonding. The alumina catalysts were synthesized through similar steps as the silica catalyst. While all the steps were completed for the first alumina catalyst synthesized, there was an issue with the activity of this first alumina catalyst. Since the catalyst was not active enough and contradicted what past literature had reported, something must have gone wrong during the experiment. The reason the alumina catalyst was not active was due to the overuse of water in the initial steps. The Ru could not properly bind to the alumina even though it was buffered to the proper pH. After this mistake was realized, it was reconciled with a second alumina catalyst starting with minimal amounts of water. This second alumina synthesis still mimicked the synthesis of the silica supported catalyst. The mass of RuCl₃ used from Acros Organics was 0.49 grams bonded to 5.96 grams of alumina. For this catalyst generation, the solution was buffered before the solvent was evaporated the first time. The alumina catalyst was heated in two separate ovens, one at 105°C for 24 hours and then at 400°C for 4 hours. The final catalyst after the various ovens was a 3% Ru catalyst. The synthesis yielded approximately 6.5 grams of catalyst prepared for FT synthesis.

2.2 SETUP OF FIXED-BED REACTOR FOR FTS

Over the course of this thesis, 6 runs using a fixed-bed reactor were completed; three runs with the silica support and three runs with the alumina support. Runs 1-3 all used the catalyst synthesized with silica. Run 4 was the run that determined the first alumina catalyst was inactive and an unsuccessful synthesis. Runs 5 and 6 utilized the more active and productive alumina catalyst. All runs were prepped and loaded in the reaction column through the same process each time. Figure 2.1 shows how the column was packed.

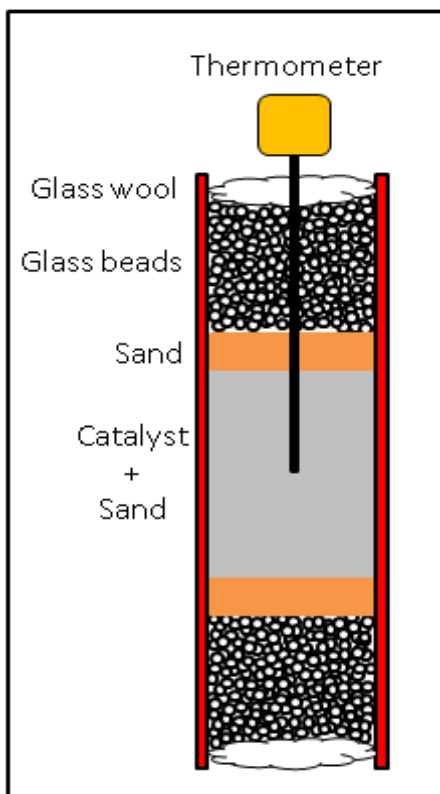


Figure 2.1 Reactor Set-Up

Starting at the ends of the column was glass wool, which served as plugs to hold all of the essentials inside. Next was the largest section, which consisted of inert borosilicate glass balls obtained from Sigma Aldrich. The last layer on each side before the catalyst bed was approximately 2 grams of white quartz sand that had a 50+70 mesh from Sigma Aldrich. See Table 2.1 for specific amounts for each run. The catalyst bed is found at the center of the column and is in fact a mixture of sand and catalyst. The ratio between the two was 4:1, sand:catalyst. Specific amounts can also be found in Table 2.1. This mixture was combined and ground with a mortar and pestle to obtain a uniform mixture as well as particle size. Once loaded inside the column, the catalyst bed was approximately two inches in length. At the center of the catalyst bed was a temperature probe in order to monitor the temperature during the reaction.

Table 2.1 Column Packing mass data

Run	Support	Sand (g)	Sand+Catalyst (g)	Sand (g)
1 st	SiO ₂	2.46	8.12+1.97	2.41
2 nd	SiO ₂	2.27	7.95+1.96	2.16
3 rd	SiO ₂	2.06	8.16+1.92	2.16
5 th	Al ₂ O ₃	2.01	8.04+1.93	1.91
6 th	Al ₂ O ₃	2.00	8.09+1.93	1.99

The column, after being packed, was then wrapped with the heating wire. This heating wire was covered with a mesh insulator. Over this insulated wire was two more layers of insulation as the goal was to keep heat in the system and not lose it to the

atmosphere. These layers allowed for more stability in reaction temperature and less fluctuation. The last step before mounting the column into the reactor was to apply heating tape where necessary to minimize leaks along the column. The final mounted column is an enclosed system with the ability to control and maintain temperature, pressure and flow rate.

With the column mounted, there are multiple other parts to the overall reactor. An image of the reactor used in this experiment is shown in Figure 2.2. The synthetic gas (syngas) feed is linked to the column at the top, allowing for the products being formed to simply move down the column and elute after termination. The flow rate and high pressure also help the products to elute in a timely manner. Now as the products elute from the column, it is not ideal to collect every product in the same vessel. If all products were collected in a hot trap, the high carbon numbers would be in liquid form and easy to collect. But, the lower carbon numbers would still be in gaseous form, making it difficult to collect from the hot trap. So, after the high molecular hydrocarbons are collecting in the hot trap, the gas flow proceeds to the cold trap. This cold trap is cooled by a Thermo Scientific Haake SC 100 and A 10. Ethylene glycol obtained from Sigma Aldrich is used as solution in this contraption. The ethylene glycol is fed through a tube that is wrapped around the cold trap, keeping the collection vessel at approximately 0 degrees C. The cold trap will cool the hot gases and turn some hydrocarbons from the gaseous form back into liquid form. Typically, C6 and above hydrocarbons are collected in this vessel. All the carbon numbers below C6 remain in the gas phase and are collected

as such. Majority of the gases are released, but at certain intervals they are collected and analyzed to observe the production of C1-C4. This gas collection also includes CO and hydrogen that elute from the column and were not used in the synthesis.

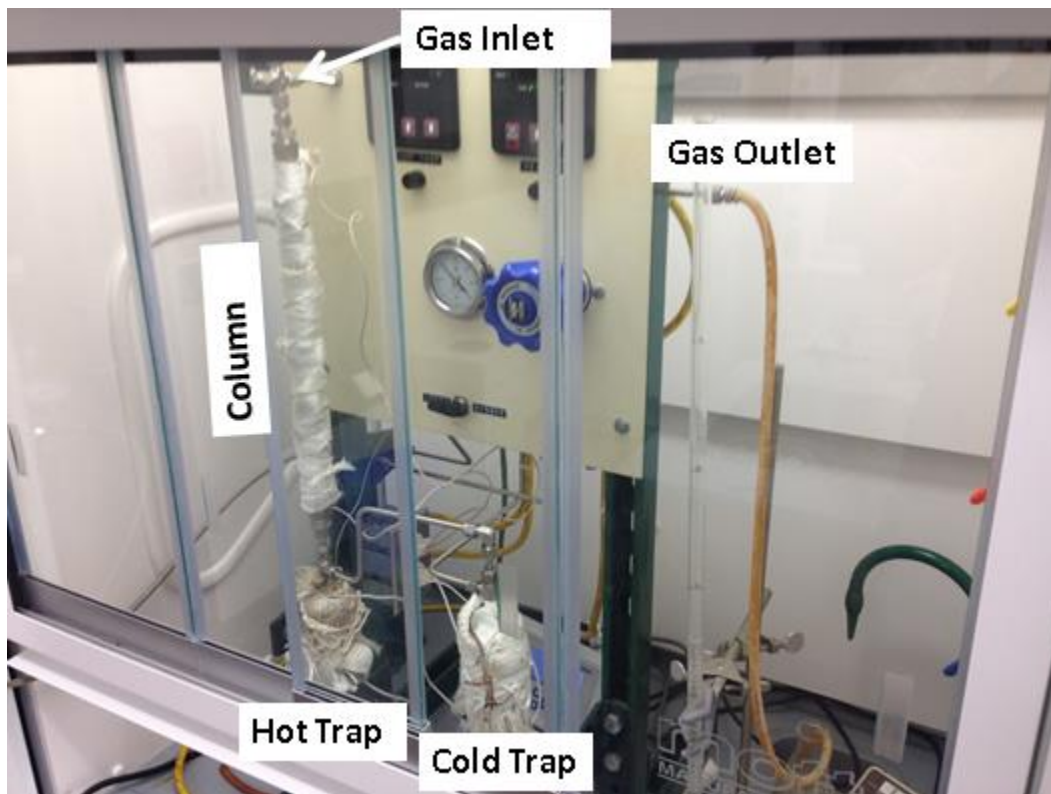


Figure 2.2 In the lab reactor

2.3 DEUTERIUM/HYDROGEN SWITCHING AND COMPETITION SYNTHETIC PROCEDURES OF FTS

The reaction conditions are maintained via the front panel of the reactor. The hot trap is typically set at 100°C and the cold trap at about 0°C. The pressure is maintained

typically at 200 psi although there are some lower pressures used during the various runs. The temperature was maintained between 240°C and 270°C depending on the run and which stage the run was in. A run always begins with the activation of the catalyst. Activation is simply protonating the catalyst surface via hydrogen gas. Pure hydrogen was run through each column for at least 24 hours prior to actual synthesis. All activation took place under low pressure (50 psi) and high temperature (270°C). The low pressure was utilized at this point since it created more active surfaces overall on the catalyst. After activation, the temperature was lowered and the pressure increased. This part is necessary in order to determine the blank flow rate of the gases without any synthesis occurring. This flow rate is a factor that must be included in any gas production calculations, therefore an initial blank flow rate is necessary as a comparison during actual synthesis. The next step is to increase the temperature to whatever reaction condition is desired. Before increasing the temperature, the gas tanks should be switched to the proper syngas as FT synthesis cannot occur without carbon monoxide. Depending on which type of analysis was preferred indicated which syngas was the best to use.

Besides the activation (pure H₂) gas tank, there are three other types of syngases. The first syngas typically used is the H₂/D₂/CO/N₂ mixture tank. All of the tanks contained nitrogen filler, but since N₂ is inert, it will not affect the reaction. The H₂/D₂/CO tank is 30% hydrogen, 30% deuterium and 30% carbon monoxide with a ratio of 1:1:1 respectively. This allows for the competition experiment between hydrogen and its isotope. Typically, competition experiments are run at the beginning of the experiment

since this is the time the catalyst is the most active and more products are formed. The more products produced, the easier it is to see consistency in the varying mass number during product analysis. If there is no competition between the isotopes, then there should be no preference between which isotope binds. The other two tanks are both utilized for the switching experiment. One tank contains H₂/CO/N₂ and the other contains D₂/CO/N₂, again N₂ is a filler. The hydrogen and deuterium in their respective tanks are both 60% while CO is 30%. This gives a 2:1 ratio of H₂ or D₂ to CO. Whichever type of syngas used can give various data depending on types of analysis. The gas tanks were acquired from various places such as Purity Plus Specialty Gases and the American Gas Group, Specialty Gases of America Inc.

2.4 SAMPLE COLLECTION AND ANALYSIS

Products from the hot trap and cold trap were collected daily when possible with at least one if not multiple gas samples collected throughout the day. Gas samples were collected via a gas bag. The bag was then attached to a micro-GC for analysis. After useable data was collected, the sample was discarded. The liquid/wax products were collected in 20 mL liquid scintillation vials. The products from the hot and cold trap were placed in separate labeled vials. Since these samples were collected on the same day at the same time, they are technically considered 1 sample and given the same lab number. These products are stored in a fridge for later analysis either by GC-FID or GC-MS.

The micro-GC used was made by Agilent Technologies model 3000A. This GC has four separate columns into which the gas sample is injected. There are no preparatory steps necessary for the sample before injection, the gas bag was simply connected to the injection port and the sample injected with pressure applied to the bag. The sample was flushed through the pre-injection system to insure no residuals from previous samples would affect the concentration. The inlet for the entire micro-GC is maintained at 80°C. The run conditions for each of the four columns varies as they are intended to analyze different gaseous compounds. Each column has its own injector that can be set to a specific temperature. The first column has an injector temperature of 90°C with a pressure of 30 psi. It is a molecular sieve column and the oven is held at a constant 90°C. The products analyzed on this column in order of elution are: H₂, N₂, CH₄ and CO. This first column is very important as it contains the analysis of the original reagents. The purpose of monitoring the reagents can help to determine how much CO and H₂ reacted inside the reaction column. The other three GC columns monitor mostly hydrocarbon products with the exception of CO₂. The second column analyzes, in order of elution, CO₂, ethylene and ethane. Monitoring the amount of CO₂ can help to determine if a catalyst is effective and also shows how much unwanted byproduct is created from the WGS reaction. Column 2 is a Plot U column with an injector temp of 85°C at 32 psi and the column is maintained at a temperature of 85°C. Column 3 is the highest temperature of all four columns. The injector is kept at 100°C, 32 psi and the column is at a temperature of 120°C. This alumina column determines if any C₃ is present as well as some C₄ products. The hydrocarbons that interact with this column are: propane, propene, n-

butane, trans-2-butene, iso-butene, iso-butylene, 1-butene and cis-2-butene. Determining the amount of these products can help in the overall product distribution analysis. The last, fourth, column is an OV-1 column and is only used to determine a single product, iso-butane. The injector temperature is 90°C at 30 psi and a column temperature of 90°C. The combined use of all four of these columns allow for detailed product analysis of the C1-C4 as well as carbon monoxide, carbon dioxide and hydrogen gas. The note that should be made for the micro-GC is its inability to distinguish deuterium, from hydrogen. Plus this peak elutes slightly later, enough so that it could potentially start mixing with the nitrogen peak. While the hydrogen peak might not be useful for either tank that contains deuterium, the CO peak should still be useful. There might be a difference in how much is converted, which could alter the CO peak, but the deuterium will not conflict with the CO analysis on the micro-GC.

The liquid/wax samples collected were analyzed depending on which experiment was being performed. For the competition experiment, the samples were diluted in carbon disulfide (from Fischer Scientific) and sent to Wilson Shafer at CAER. These products are analyzed by GC-MS in order to determine the concentration of each mass number. Depending on how many deuterium vs. hydrogen are in a single hydrocarbon can vary the mass number. These variations can only be differentiated in and analyzed through MS. The other liquid/wax products were collected during the switching experiment and were analyzed by a Thermo Scientific Focus GC with a Flame Ionization Detector. While there were typically three samples, and therefore three days, collected

between each tank before switching from H₂ to D₂ or vice versa, some of the samples still had impurities (in relation to hydrogen and its isotope). Three days was necessary to give any deuterium containing products time to elute from the column, giving pure hydrogen containing samples. The same wait time was necessary if desiring a deuterium pure hydrocarbon for analysis. These pure samples were also diluted with carbon disulfide with one microliter of the diluted sample mixture injected into the column. The temperature ramp began at 35°C and reached a maximum of 285°C over the course of two hours. This program yielded separation of C₇/C₈ to C₂₀'s if present. Each carbon number had a grouping of the various types of products formed. When looked at closer, the peaks could be identified as 1-olefin, paraffin, 2-trans-olefin, 2-cis-olefin and even minor peaks for branched products or oxygenates. The peak areas of these data allow for product analysis and help to determine how much of each carbon number is created in relation to the other products formed. The results acquired through GC-FID could also be used for alpha analysis through the ASF equation as well as comparative analysis between certain products.

The types of analyses performed on the various runs are summarized in Table 2.2.

Table 2.2 Analyses Performed

Run	Support	Competition	Switching Experiment			
		Deuterium Enrichment	KIE	α_H	α_D	2-olefin vs. 1-olefin
1 st	SiO ₂	X	X	X	X	X
2 nd	SiO ₂	X	X	X	X	X
3 rd	SiO ₂	X	X	X		
5 th	Al ₂ O ₃		X	X		X
6 th	Al ₂ O ₃	X	X	X		

CHAPTER 3

DEUTERIUM TRACER STUDIES OF Ru/SiO₂ CATALYZED FTS

3.1 FISCHER-TROPSCH SYNTHESIS USING Ru/SiO₂ CATALYST

The first catalyst was synthesized with a silica support. The amount of ruthenium bonded was based on previous work by A.T. Bell. The process is described in the experimental chapter. The mass of RuCl₃ used was 0.98 grams with 9.79 grams of silica. The yield of this process gave approximately 10.6 grams of catalyst of a 4.8 Ru/SiO₂. This is plenty of catalyst that can be used for multiple runs. Each run used about 2 grams of catalyst. Refer to Table 2.1 for specific values for each run.

The first run carried out with the silica supported catalyst was run under the conditions of 200 psi and 250°C. For this run, one gas sample, one sample from the cold trap and one sample for the hot trap were collected daily. The mass produced by the oil, wax and water products is shown in Table 3.1.

Table 3.1 Ru 1st Run Mass Data

Hours	Sample	Syngas	Hot Trap (g)	Cold Trap (g)	Total (g)
24	JN06	H ₂ /D ₂	8.18	2.21	10.40
48	JN08	H ₂ /D ₂	4.80	2.86	7.66
60	JN09	H ₂ /D ₂	3.39	2.25	5.64
83	JN10	H ₂	1.41	1.72	3.14
109	JN11	H ₂	1.34	1.76	3.11
132	JN12	H ₂	1.13	1.35	2.48
156	JN13	H ₂	1.11	1.34	2.45
179	JN14	H ₂	1.06	1.48	2.54
203	JN15	H ₂	1.10	0.95	2.11
227	JN16	D ₂	1.33	2.24	3.57
252	JN17	D ₂	2.09	2.22	4.31
277	JN18	D ₂	1.72	3.10	4.82
303	JN19	H ₂	1.13	1.11	2.24
323	JN20	H ₂	1.09	.65	1.74
347	JN21	H ₂	1.09	.82	1.91
371	JN22	H ₂	0.87	1.03	1.90

For the gas samples, the bags were collected and stored for later analysis as at this point the necessary instrumental analysis had to be completed off-site. This is the reason why collection of gas samples was limited to one per day as there were not enough gas bags to allow for multiple collected samples. After each gas sample was collected, a flow rate was taken via a buret and timer. An average of 10 different readings was taken to get an accurate flow rate. The run lasted 16 days and both the competition and switching experiment were performed.

The second run with the silica catalyst varied slightly in reaction conditions. The pressure was still set to 200 psi, but the temperature was lowered to 240°C instead of 250°C. Still for the first half of the run, only one gas sample per day was collected. By the

end of the run, the micro-GC was returned and fully functional, which allowed for more gas samples per day to be collected. The collection of liquid and wax products remained constant at 1 sample per day. The various masses for the 2nd run are shown in Table 3.2

Table 3.2 Ru 2nd Run Mass Data

Hours	Sample	Syngas	Hot Trap (g)	Cold Trap (g)	Total (g)
24	JN2-1	H ₂ /D ₂	5.49	0.07	5.56
54	JN2-2	H ₂ /D ₂	5.04	2.12	7.16
77	JN2-3	H ₂ /D ₂	3.84	0.07	3.90
95	JN2-4	H ₂	1.99	0.02	2.01
119	JN2-5	H ₂	0.90	1.25	2.15
144	JN2-6	H ₂	0.14	1.55	1.69
168	JN2-7	H ₂	0.11	1.32	1.42
194	JN2-8	D ₂	0.40	2.50	2.90
219	JN2-9	D ₂	0.47	2.39	2.86
247	JN2-10	D ₂	0.31	2.35	2.66
265	JN2-11	H ₂	0.22	0.86	1.08
289	JN2-12	H ₂	0.10	0.91	1.01
314	JN2-13	H ₂	0.31	0.79	1.09

While the second run yielded slightly less product at 240°C vs. 250°C, there were still plenty of products formed for analysis. Both the competition and switching experiments were run on this column, which cumulatively lasted 13 days. For the second run, there were some issues with the gas samples collected, and so a third run was performed.

The third run varied slightly from the 2nd run in that its primary purpose was to study specifically the switching experiments for the CO conversion. The reaction

conditions were the same as run 2 (200 psi, 240°C). With this column, many gas samples were taken as they could be analyzed daily. Both the competition and switching experiments were run, however, the length of time between switching tanks was shorter. The competition experiment was still run for the typical three days, but the H₂/CO and D₂/CO tanks were only run for approximately one day each. This allowed for switching to deuterium to occur not once, but twice. While this benefitted the study of the kinetic isotope effect in relation to gas products, it severely hampered any liquid/wax product analysis from the switching experiment. Typically, it takes 2-3 days to obtain a pure enough liquid/wax sample from either H₂/CO or D₂/CO. Since the tanks were switched daily, the products are not pure enough to see the proper peaks on any chromatograms. This negates any alpha analysis and secondary/branched product analysis. The masses were still recorded of liquid and wax products collect and are listed in

Table 3.3.

Table 3.3 Ru 3rd Run Mass Data

Day	Syngas	Hot Trap (g)	Cold Trap (g)	Total (g)
1	H ₂ /D ₂	5.94	.81	6.76
2	H ₂ /D ₂	3.58	.72	4.30
3	H ₂ /D ₂	2.66	1.15	3.81
4	H ₂	.62	1.04	1.66
5	D ₂ & H ₂	-	-	-
6	H ₂ & D ₂	.92	2.57	3.49
7	H ₂	.43	1.60	2.03
8	H ₂	.40	.81	1.20

3.2 KINETIC ISOTOPE EFFECT DURING Ru/SiO₂ CATALYZED FTS

Starting with the kinetic isotope effect analysis, qualitatively, it is helpful to look at the mass of the product formed. For this, only the first and second run will be helpful. As shown in Figure 3.1, it is observed that more mass is made during the portions of the run that utilize deuterium. Deuterium is the heavier isotope and would therefore cause more mass to be observed. However, the mass is increased too much to be accounted for by the extra neutron in each deuterium atom. The amount of product produced is approximately two times as much mass. The point is to remember that the majority of the mass comes from carbon and not hydrogen or deuterium. So, a significant increase in mass indicates an increase in product formation. With the data collected, the deuterium masses increased significantly with both the first and second run. Since the third run did not stay on either H₂/CO or D₂/CO syngas very long, this data is unreliable for this preliminary type of analysis.

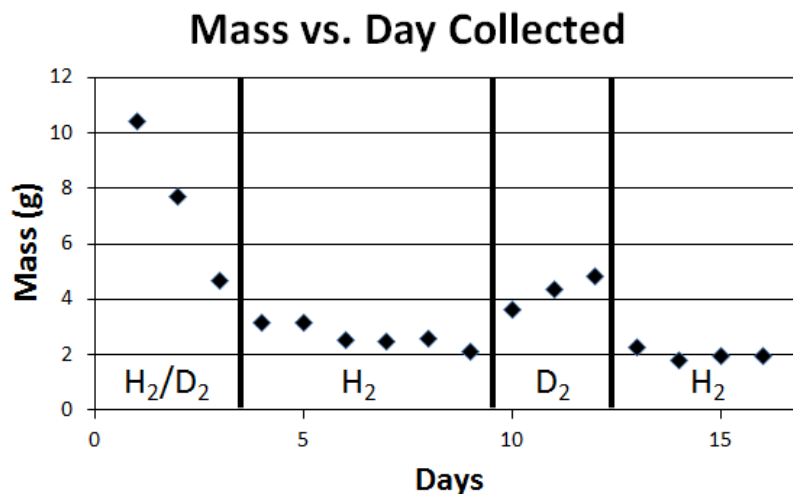


Figure 3.1 Ru 1st Run mass data vs. time

To confirm what the results of the preliminary mass data give about the kinetic isotope effect, the gas data will suffice. With the gas samples, the CO conversion can be taken into account. For the CO conversion, multiple gas samples were taken with flow rates. The samples for each syngas were averaged for each time switched between gas tanks. The results for the 1st run are shown in Table 3.4. Graphical representations for %CO Conversion of the silica catalyst are listed in Appendix A.

Table 3.4 Ru 1st Run %CO Conversion

Syngas	H ₂ /D ₂	H ₂	D ₂	H ₂
%CO Conversion	24.90	10.97	25.57	2.48

The first run confirmed what was seen with the preliminary mass data. The percent CO conversion increased when the deuterium syngas was applied. This would indicate an inverse isotope effect. For the second run, there were some issues with some of the gas samples collected. The gas samples toward the end of the run were analyzed on the micro-GC recently fixed and brought back to the lab. While the GC was calibrated, the results of the samples run appeared skewed. The CO output seemed to increase after the reaction took place for a few samples. Since FT does not form CO, this does not seem possible. Also, since liquid and wax products were both collected, some of the CO must have been used to synthesize these products. Due to the conservation of mass, carbons simply cannot be created out of thin air. Therefore, the liquid and wax products must have come from CO. Since the % CO collected was not good data, the other gas data from those samples are also untrustworthy. This is why the % CO conversion is wonky and it appears to have no isotope effect from the second run data. Since the second run did not yield useable information about the kinetic isotope effect, the third run was performed. After the competition experiment, to ensure the catalyst was still active enough to switch multiple times between H₂/CO and D₂/CO, less time overall was spent on each tank. Each tank was run for approximately a day with multiple gas samples collected and run throughout that day. The spectra results for this run did not have any issues observed in the second run. The averages for these gas sample % CO conversions were calculated and are shown in Table 3.5.

Table 3.5 Ru 3rd Run %CO Conversion

Syngas	H ₂ /D ₂	H ₂	D ₂	H ₂	D ₂	H ₂
% CO Conversion	25.70	15.84	16.59	12.99	13.27	12.45

When graphed it is observed that % CO converted increases when tanks are switched from H₂/CO to D₂/CO and subsequently, % CO converted decreases when switching from D₂/CO to H₂/CO. This third run supports the first run in that both show the observation of the inverse isotope effect is observed.

Observations on the hydrocarbon formation can also be observed. This is simply the % CO converted minus the % CO₂ formed. The observations for the first and third run are listed in Table 3.6.

Table 3.6 Hydrocarbon Formation

Syngas	H ₂ /D ₂	H ₂	D ₂	H ₂	D ₂	H ₂
Ru 1 st Run	24.84	10.92	25.49	2.47	-	-
Ru 3 rd Run	25.68	15.82	16.56	12.79	13.23	12.43

Looking at hydrocarbon formation also indicates an inverse isotope effect. More evidence of the inverse isotope effect can be seen in C₁ (methane). When calculating this % CH₄ formation, it is not a percentage of overall % CH₄ formation. The percent refers to how much of the hydrocarbon formation is methane. Knowing this, calculations can also be performed to see how much C₂⁺ is formed out of the % CO converted. These numbers

indicate how much polymer has been formed without any byproducts or monomers. The higher the % C_2^+ formation is, the more polymers formed via the Fischer Tropsch reaction.

3.3 PRODUCT DISTRIBUTION DURING Ru_4/SiO_2 CATALYZED FTS

Now while the C_2^+ formation is a good indicator of what percent of polymers are formed, it does not give any specificity on how much of each carbon number there is. For FT catalysts, it is a priority to know whether the catalyst will synthesize long chain waxes or short chain oils. To do this, product analysis based on content through the GC-FID is helpful. The samples were all prepared in the same fashion. A few drops of oil and wax were added to about 1 mL of carbon disulfide in order to dilute the sample. If the sample was directly injected, it would overload the column and cause the peaks to be flat at the top. This is due to the FID only being able to detect so much current; once that limit is reached, the detector cannot accurately measure the data. Once diluted, 1 μ L of the sample was injected and each run took 2 hours to complete. A sample GC-FID spectrum from the silica catalyst is shown in Figure 3.2.

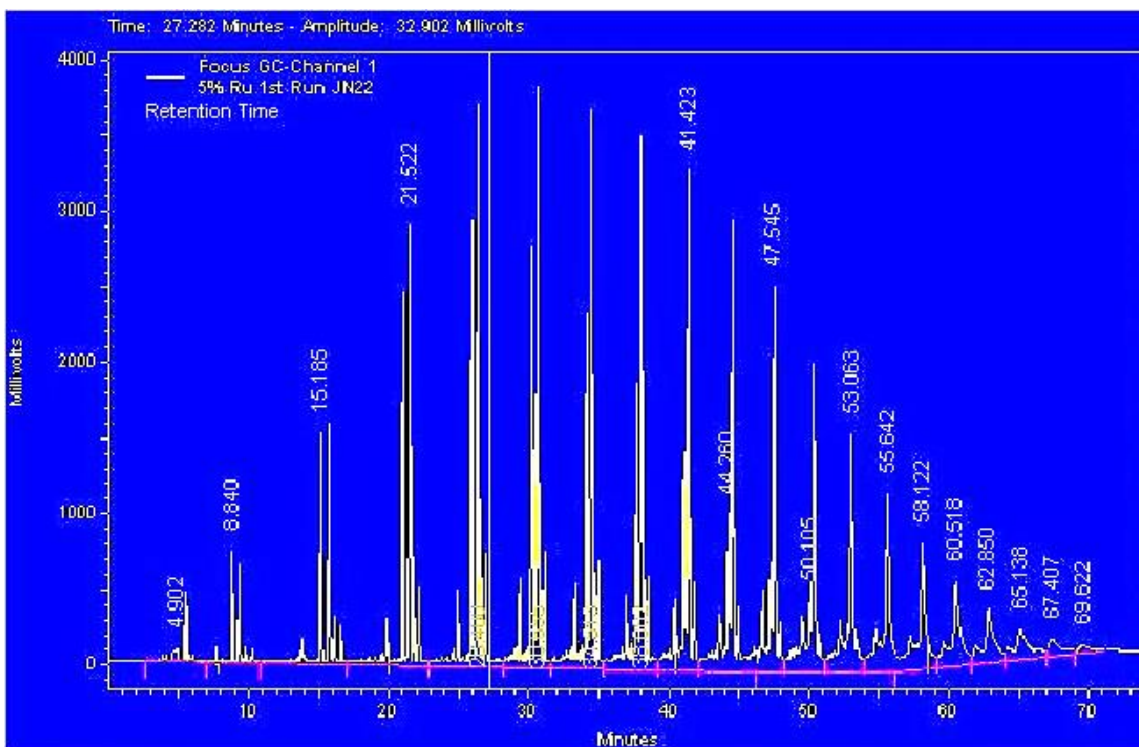


Figure 3.2 Sample GC-FID spectrum

Each grouping eluted is a new carbon number. To determine which carbon number, a standard of octane was run to determine the retention time of C8. At this time the RT of C8 was around 8 minutes. Now all of the peaks can be labeled. It is known that the major peaks elute in the order of: 1-olefin, paraffin, 2-trans-olefin and 2-cis-olefin with the branched products for that carbon number eluting before 1-olefin. The observed peaks for a single carbon number are shown in Figure 3.3.

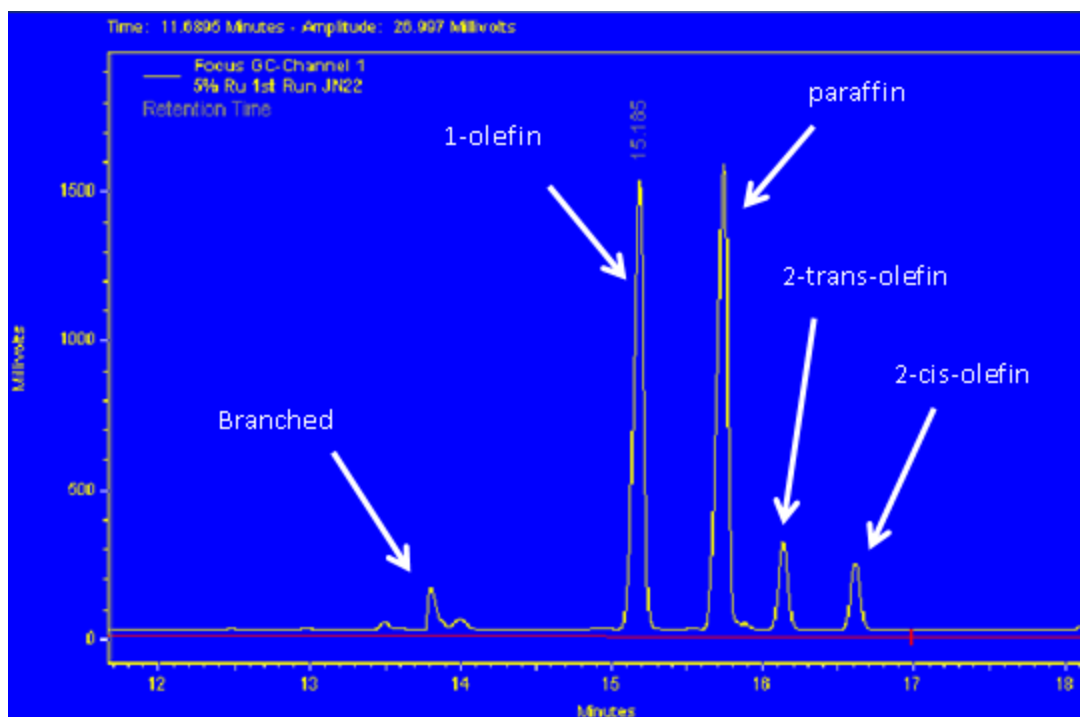


Figure 3.3 Observable peaks in one carbon number

All of these peaks can be analyzed to give a peak area, indicating content of that carbon number in the overall sample. With this data calculations of these products all occurred with the mol % of carbon number and type (1 or 2-olefin, paraffin). The sum of all the peak areas of the major products (not including branched) was found first. Then a calculation for each individual peak for area percent was found in the whole sample. This was considered the weight percent for the sample in relation to one peak. Next, the molecular weight was taken into account to determine moles. Finally the mole percent could be determined by dividing the moles by the total moles in the whole sample. A sample calculation for C_{10} is shown below using the data in Table 3.7 and Equations 3.1 through 3.3. Keep in mind that the totals used include all carbon numbers observed in

the GC-FID. With these mole percents, multiple observations and subsequent calculations can be performed.

Table 3.7 Sample C₁₀ data calculation

	Peak Area	Weight %	MW	Mole	Mole %
1-olefin	170789334	3.47	140	.025	4.33
Paraffin	23226433	4.69	142	.033	5.77
2-trans-olefin	55660227	1.13	140	.008	1.41
2-cis-olefin	41410444	.84	140	.006	1.05
Sample Total	4910784314			.572	
C ₁₀ Total					12.56

$$\text{Weight \%: } \frac{170789334}{4910784314} \times 100 = 3.47 \quad (3.1)$$

$$\text{Mole: } \frac{3.47}{140} = .025 \quad (3.2)$$

$$\text{Mole \%: } \frac{.025}{.572} \times 100 = 4.33 \quad (3.3)$$

Firstly, the alpha from the ASF equation can be determined. The mole percents for each carbon number can be calculated and linearized through natural logarithms. This requires the summation of the mole percents for each carbon number. The data for sample JN22 is graphically represented in Figure 3.4.

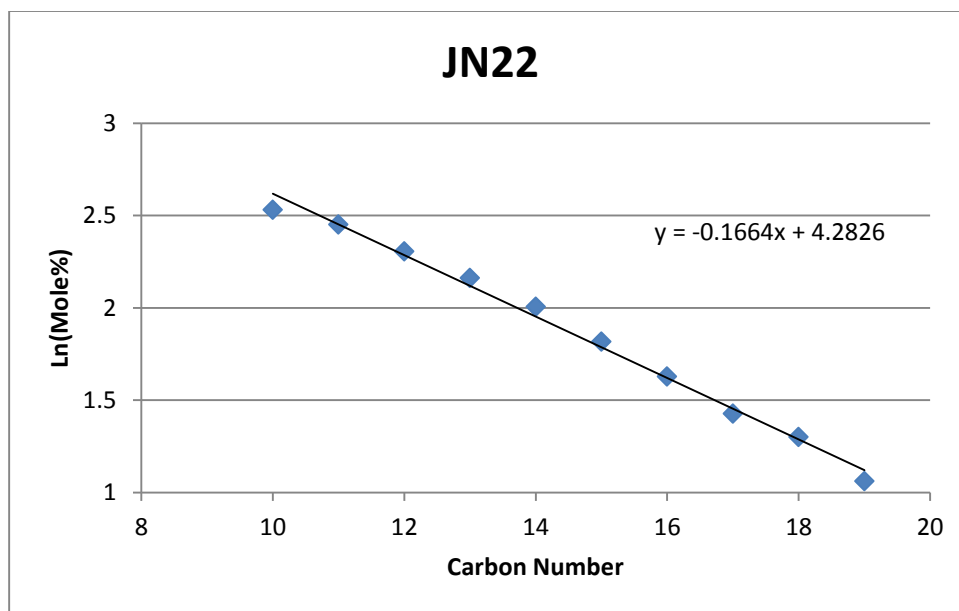


Figure 3.4 Graph of alpha data points

Equation 1.12 shows that $m = \ln(\alpha)$. Using a linear fit, a linear regression can be obtained. For sample JN22, the linear regression is: $y = -0.1664x + 4.28$. The value of .1664 is m and is therefore equal to the $\ln(\alpha)$. To solve for α , simply take $e^{-.1664}$, which gives a value of .847.

These alpha values can be calculated for any sample pure enough of hydrogen or deuterium. With the GC-FID, if there was too much of a mixture, the hydrogen and deuterium peaks could not be distinguished. There was not enough resolution, which led to peak mixing. Theoretically the most pure samples should be the ones collected right before the syngas tanks are switched. While other products might be pure enough to see only hydrogen or deuterium peaks, the most reliable data should come from the samples collected before switching. All samples with pure enough products for the silica catalyst

were calculated. The most pure products with their alpha values are listed in Table 3.8 for the first and second run (third run not pure enough).

Table 3.8 Silica Catalyst Alpha Values

Run	Sample #	Syngas	Alpha Value
1 st	JN15	H2/CO	0.847
1 st	JN18	D2/CO	0.902
1 st	JN22	H2/CO	0.846
2 nd	JN2-7	H2/CO	0.856
2 nd	JN2-10	D2/CO	0.892
2 nd	JN2-13	H2/CO	0.834

Once the alpha value is known, it can be used to determine the average molecular weight of the products. This involved plugging the determined alpha back into the ASF equation ($C_n = C_1 * \alpha^{n-1}$). To start, assume that C_1 is 100% as every polymer has to start with the monomer. So, a value of 1 is used for C_n . As carbon number increases (and therefore n), the overall value of C_n decreases. How fast it decreases depends on the alpha value. Since carbon numbers have been observed up to C40 for FT, this is the limit of the values included. The summation of these numbers can yield a mole percent for each carbon number, and taking into account the molecular weight of each subsequent carbon number can yield the weight percent. To determine the average molecular weight for the entire sample, simply divide the mole percent (which would always be 100) by the total weight percent. This yields an average molecular weight for the pure sample.

Average molecular weights for the 1st and 2nd run are listed in Table 3.9 along with the corresponding K value.

Table 3.9 Average alpha data results

	Syngas	Average Alpha	Avg MW	K value
Ru 1st Run	H ₂ /CO	0.847	92.70	6.6
	D ₂ /CO	0.902	135.66	9.7
Ru 2nd Run	H ₂ /CO	0.845	91.57	6.5
	D ₂ /CO	0.892	125.59	9.0

The K value represents what the average carbon number is for the entire sample. To find this, the average molecular weight was simply divided by 14, a CH₂ unit. So, for the silica catalyst, it appears the most common carbon number formed was between 5 and 6. This would indicate that Ru/SiO₂ catalyzed FT under high temperature and pressure creates more oils than waxes.

3.4 PRIMARY VS. SECONDARY PRODUCT ANALYSIS DURING Ru/SiO₂ CATALYZED FTS

While understanding which products have been produced is important, there are other analyses performed on the GC-FID results. Again the peak areas will be utilized in relation to one another and eventually converted to the mole %'s. With these next calculations, they should lead to information on the formation of 2-olefins being primary or secondary products. If it is assumed that 1-olefins and 2-olefins are produced through

the same reaction mechanism, then Equation 1.16 stands true. To find these ratios, the mole %'s calculated can be used to find the values in equation 1.16. These values will be percentages calculated for each carbon number. For example, take sample JN22 data for C₉ shown in Table 3.10.

Table 3.10 C₉ (H₂ pure)

Product	Mole %
1-olefin	3.74
Paraffin	4.62
2-trans-olefin	1.22
2-cis-olefin	.99
Total	10.57

With these values, the ratios of 1-olefin and 2-olefin divided by the total can be calculated for each carbon number. For 1-olefin, there are no geometric isomers, so the mole % of 1-olefin is the only value used. For 2-olefin, the E and Z isomers both contribute to this value and both have to be taken into consideration for 2-olefin. With this knowledge, calculations in Equations 3.4 and 3.5 can be completed.

$$\frac{1\text{-olefin}}{\text{total}} = \frac{3.74}{10.57} = .35 \quad (3.4)$$

$$\frac{2\text{-olefin}}{\text{total}} = \frac{1.22+.99}{10.57} = .2 \quad (3.5)$$

These two values can now be used as $[1\text{-olefin}]_H$ and $[2\text{-olefin}]_H$. To find the other two values of $[1\text{-olefin}]_D$ and $[2\text{-olefin}]_D$, a pure run of deuterium is used. This means that D_2/CO syngas was run for two to three days to obtain a pure enough sample for the peak areas to be integrated properly. There was one sample from the 1st run pure enough for this analysis and two samples from the 2nd run. The same calculations as the hydrogen run shown previously are used to calculate $[1\text{-olefin}]_D$ and $[2\text{-olefin}]_D$.

For the 1st run, there were multiple hydrogen sample viable for the $[1\text{-olefin}]_H$ and $[2\text{-olefin}]_H$ calculations. In total, six samples were used to calculate the hydrogen half of the calculations. These samples are: JN11, JN12, JN13, JN14, JN15, and JN22. The averages of these results were taken for each carbon number. Since there was only one viable deuterium sample, no extra calculations or averages was necessary. The last step is simply division of the hydrogen products and deuterium products by matching the 1-olefin vs. 2-olefin for each carbon number. All values are also shown in Table 3.11.

Table 3.11 Ru 1st Run: 1-olefin vs. 2-olefin results

Carbon #	$[1\text{-olefin}]_H$	$[2\text{-olefin}]_H$	$[1\text{-olefin}]_D$	$[2\text{-olefin}]_D$	$[1\text{-olefin}]_{H/D}$	$[2\text{-olefin}]_{H/D}$
6	0.408	0.262	0.461	0.126	0.886	2.08
7	0.370	0.252	0.442	0.149	0.837	1.69
8	0.364	0.204	0.439	0.157	0.829	1.30
9	0.327	0.215	0.376	0.156	0.871	1.38
10	0.312	0.206	0.341	0.183	0.916	1.13
11	0.290	0.210	0.305	0.191	0.951	1.09
12	0.269	0.200	0.277	0.181	0.970	1.10

The results of these calculations show that the ratios of $[1\text{-olefin}]_{\text{H/D}}$ do not equal $[2\text{-olefin}]_{\text{H/D}}$. In fact what is found is the ratio of the 2-olefin products are consistently above 1, whereas the ratios of 1-olefins are consistently below 1. This first of all indicates that 1-olefins and 2-olefins are not through the same reaction pathway. 1-olefins and 2-olefins cannot both be primary products. With this knowledge there is now a potential explanation as to why $[2\text{-olefin}]_{\text{H/D}} > 1$ while $[1\text{-olefin}]_{\text{H/D}} < 1$. This comes back to the stability of the C-H vs. C-D. With the 1-olefins being the primary candidates for readsorption, it would make sense that 1-olefins are converted to 2-olefins. Since C-D is more stable than C-H, it is slightly harder to break. With that being said, it would indicate that more $[1\text{-olefin}]_{\text{H}}$ would be converted than $[1\text{-olefin}]_{\text{D}}$. So, when comparing the two H/D ratios, the numerator of $[1\text{-olefin}]_{\text{H}}$ should decrease at a greater rate than $[1\text{-olefin}]_{\text{D}}$, making this number smaller. Likewise, more $[2\text{-olefin}]_{\text{H}}$ is being formed than $[2\text{-olefin}]_{\text{D}}$ making the overall ratio larger. This is supported by the experimental results represented in Equations 3.6 and 3.7.

$$\frac{[2\text{-olefin}]_{\text{H}}}{[2\text{-olefin}]_{\text{D}}} > 1 \quad (3.6)$$

$$\frac{[1\text{-olefin}]_{\text{H}}}{[1\text{-olefin}]_{\text{D}}} < 1 \quad (3.7)$$

The data for the 2nd run was slightly different than the 1st run. This run was also shorter than the 1st, and had 3 pure hydrogen samples and 2 pure deuterium samples. The averages and ratios are shown in Table 3.12.

Table 3.12 Ru 2nd Run: 1-olefin vs. 2-olefin results

Carbon #	[1-olefin] _H	[2-olefin] _H	[1-olefin] _D	[2-olefin] _D	[1-olefin] _{H/D}	[2-olefin] _{H/D}
6	.419	.194	.407	.176	1.02	1.10
7	.378	.201	.407	.183	.93	1.09
8	.332	.212	.377	.194	.88	1.09
9	.320	.228	.328	.212	.97	1.07
10	.259	.272	.283	.246	.91	1.10
11	.240	.285	.250	.260	.96	1.09

The values observed still are not equal indicating different reaction pathways, but the 1-olefin data seems less stable than the first run. See Figure 3.5 for a comparison of the 1st and 2nd run.

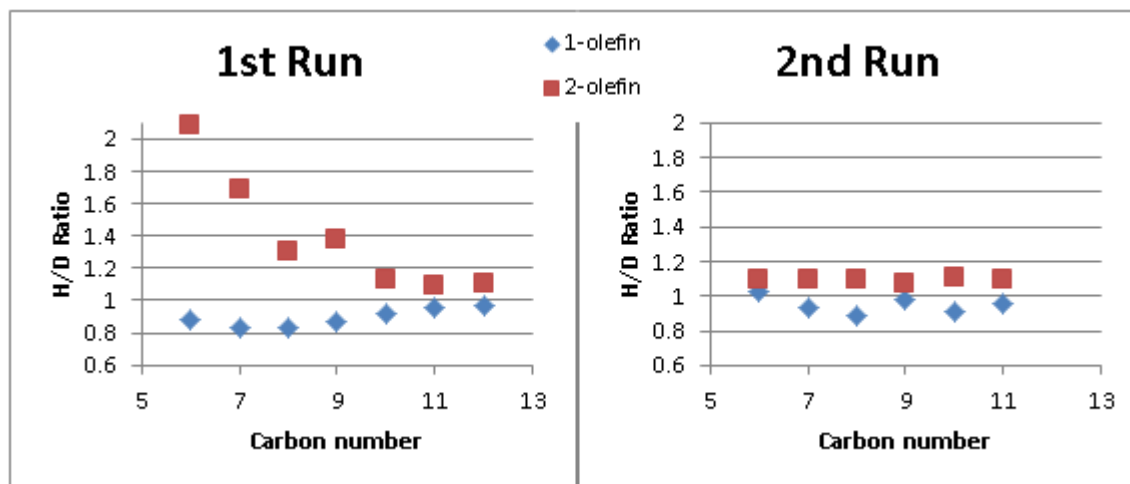


Figure 3.5 Comparison of Ru 1st Run and Ru 2nd Run H/D Ratio, 1-olefin vs. 2-olefin

With the first run, there is a trend observed in both 2-olefin and 1-olefin, which are both eventually lead to a steady consistent value. For the ratio of 2-olefin, the value levels out at 1.1 and for 1-olefin at .9. With the 2nd run, the 2-olefin is fairly constant at a ratio of 1.1, but 1-olefin appears to have no consistent ratio. The 1-olefins range from 1.02 to .88. While the data points (with the exception of 1.02) are below a ratio of 1, they appear more staggered. If perhaps the calculations could have been taken past C11 or C12, a more stable trend might have appeared. Unfortunately it was difficult to consider the peak areas for larger carbon numbers due to the low concentration and peak broadening. While a value cannot be successfully assigned to the 1-olein ratio for run 2, the data still gives viable support for secondary vs. primary products. Also the ratios for both runs still follow the trend of $[2\text{-olefin}]_{\text{H/D}} > [1\text{-olefin}]_{\text{H/D}}$.

This test was not completed for the third run due to impure products from frequent switching of the syngas tanks.

3.5 DEUTERIUM ENRICHMENT IN HYDROCARBONS DURING Ru/SiO₂ CATALYZED FTS

The last major type of analysis to be completed is deuterium enrichment. This type of data collection required GC-MS analysis as the calculations require the differentiation between 1 m/z unit (1 hydrogen vs. 1 deuterium). The samples were sent out and the data returned for analysis. Special old software was required for this type of data analysis. The graph of produced looked like the GC-FID spectra previously collected

as they are both gas chromatographs. The difference is with the mass spectrometry data, more detailed analysis can occur. Looking at a single peak, differentiation of all m/z found in that peak is possible. This can lead to finding the peak area for each hydrogen and deuterium isotopomer for every carbon number formed and detected. With this type of analysis comes much manual labor as every m/z for each carbon number had to be typed in and the peak area manually recorded. For every run there were three samples that had to be analyzed. The data was typically collected from C_8 to C_{20} for 1-olefin, paraffin, 2-trans-olefin and 2-cis-olefin. With the peak areas, calculations of H/D ratios on each carbon number can be calculated. A big factor that must be taken into consideration with mass spectrometry are the naturally occurring isotopes of ^{13}C and ^{14}C . If there is one ^{13}C in a hydrocarbon chain, this will cause the m/z to change by 1 unit. The problem is, this interferes with the next peak that contains 1 more deuterium than the previous peak. A correction must be made based on the abundance of each carbon number as they can contribute in a minor way to other peak areas. Once this corrected value is found, the number of hydrogen and deuterium can be determined and compared to the expected no favoritism values. With the H/D ratio, the amount of deuterium in each isotopomer of that carbon number can be calculated and plotted. Figures for each carbon number of one sample (JN09) for paraffin can be found in Appendix B.

Whenever the H/D values are less than 1, the experimental curve shifts to the right of the no favoritism curve. With this knowledge, the H/D ratios for 1-olefin, paraffin, 2-trans-olefin and 2-cis-olefin can be compared for trends. While the H/D ratios are

observed for both olefins and paraffins, the amount of olefin decreases drastically as carbon number increases, especially in 1-olefins. Good values of olefin ranged from C₉ to C₁₃₋₁₅ depending on which olefin was being analyzed. These numbers were calculated and observed to be less than one, but it was difficult to determine a trend in some cases. Paraffin offers the best choice to observe a trend as its values are stable at least to C₁₈, if not the low C₂₀'s. The values for all H/D ratios from the third sample of the 1st run can be found in Table 3.13. The results of the other competition samples from the first run can be found in Appendix B.

Table 3.13 Sample JN09 H/D competition experiment ratios

Carbon #	1-olefin	paraffin	2-trans-olefin	2-cis-olefin
8	.688	.794	.683	.684
9	.692	.700	.677	.675
10	.691	.687	.677	.680
11	.694	.674	.687	.679
12	.681	.675	.692	.674
13	.676	.670	.700	.672
14	.678	.672	.703	.673
15	.671	.672	.710	.679
16		.674	.715	
17		.677	.728	
18				
19		.699		
20		.694		
21		.694		
22		.688		
23		.707		

The spaces left blank above either had poor peak shape in the mass spec program or the curve of the isotopomers no longer fit a Gaussian shape. The data usually lost Gaussian shape when the peak areas were low and close to the limit of quantitation. Therefore, these data points should not be used in observing trends. A graph of sample JN09 with the H/D ratios is shown in Figure 3.6.

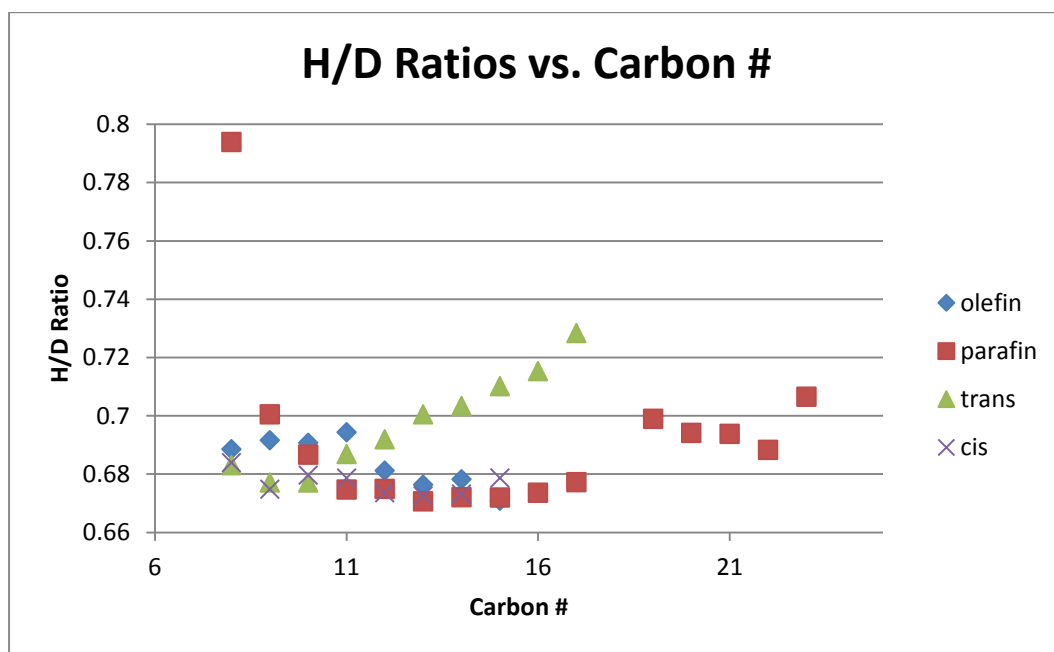


Figure 3.6 JN09 H/D ratios graphical representation

For the products in this sample, there are multiple trends depending on which product is observed. 1-olefin and 2-cis-olefin appear to have no consistent trend, but contain minor variations in the H/D ratio. An increasing trend is observed for 2-trans-olefin. For paraffin, the trend is decreasing with a light increase around the range of C₁₅-

c₁₇. While there are many various trends observed, all of the H/D ratios are still less than 1 indicating deuterium enrichment. This less than 1 H/D ratio stood true for all three samples analyzed in the 1st run as well as the trends shown previously.

The competition experiment was also performed on the 2nd and 3rd run. This data was collected in the same fashion as the 1st run. A summary of these 6 samples (3 from the 2nd and 3 from the 3rd) can be found in Appendix B. All of the H/D ratios indicate that deuterium enrichment is present for the silica based catalyst. This was consistent over all 3 silica runs completed as observed by the H/D ratio being less than 1. Another important observation to make is that the H/D ratio varies as carbon number changes. In this case, the H/D ratio generally decreases as carbon number increases. This indicates that the H/D ratio is a function of carbon number. If the H/D ratio is a function of carbon number, then deuterium is favored in the steps of propagation. Propagation includes both a growing chain and a monomer, which means both are involved with deuterium favoritism. If deuterium enrichment was found in any other step, the H/D ratio could not be a function of carbon number as no other step involves increasing the polymer chain. Since, it is a function of carbon number, it means that deuterium favoritism, and therefore the inverse isotope effect, is present in both monomer and growing chain. Therefore, if a mechanism does not contain an inverse isotope effect in both monomer and growing chain, it no longer fits the experimental data collected.

3.6 Ru/SiO₂ CONCLUSIONS

After all the experiments and analyses were complete, there are multiple conclusions that can be drawn from the data collected. First, the 4.8% Ru/SiO₂ is a successful and fairly active catalyst with a % CO conversion ranging from 10-30%. Using the ASF equation for polymerization reactions, it is determined that the most common molecular weight for H₂/CO syngas is between 91-93 g/mol. Also, the most common molecular weight with D₂/CO syngas is between 125-136 g/mol. This shows that synthesis with deuterium induces more chain growth before termination. Third with respect to the KIE, and inverse isotope effect is observed from many various sources. This was determined preliminarily through liquid/wax product mass formation. More substantially, the inverse isotope effect is supported by the CO Conversion gas samples from the switching experiment. Also supporting the mass and CO conversion data is the competition experiment in which deuterium enrichment is present. An H/D ratio of less than 1 indicates that deuterium is more favored to bind during propagation. Since deuterium enrichment is seen during this step, this shows that the inverse isotope effect must come from both the monomer and the growing chain. What can be drawn from this is that the growing chain and the monomer must exhibit an inverse isotope effect and change from either sp² to sp³ or sp to sp². This hybridization change must be in the rate determining step and occur on a carbon that has a hydrogen bound to it. Lastly, with respect to primary and secondary products, it is shown that 1-olefins and 2-olefins are not through the same reaction pathway. If it is assumed that 1-olefins are the primary products of the reaction, then 2-olefins must be secondary products formed after

readsorption of 1-olefin. Due to the higher stability of the C-D bond than C-H bond, it is expected that the 2-olefins should have an H/D ratio of greater than 1 whereas the 1-olefins should have an H/D ratio of less than 1, as observed with the 4.8% Ru/SiO₂ catalyst.

CHAPTER 4

DEUTERIUM TRACER STUDIES OF Ru/Al₂O₃ CATALYZED FTS

4.1 FISCHER-TROPSCH SYNTHESIS USING Ru/Al₂O₃ CATALYST

The second catalyst was synthesized in mostly the same manner as the silica catalyst. The variation came in the amount of water used to dissolve the initial amount of ruthenium trichloride. For details, refer to the experimental chapter. The support utilized was alumina. Approximately 0.49 grams of ruthenium trichloride and 5.96 grams of alumina was used leading to a 3% catalyst. The yield of this catalyst was 6.5 grams, giving enough catalyst to try multiple runs. Two runs total were completed with this catalyst (overall the 5th and 6th run with ruthenium).

The fifth run was under the conditions of 250°C and 200 psi in the beginning. The pressure was changed mid-run to 180 psi during the switching experiment. This was due to the low pressure remaining in the D₂/CO syngas tank. The deuterium tank was also only run for half a day to ensure that the pressure in the gas tank did not drop below the set reaction pressure of the reactor. When the tanks were switched back to H₂/CO, samples at both 200 psi and 180 psi were taken. This variation in pressure should only minorly affect synthesis and will change the flow rate. Since the flow rate is used in the calculations for the gas products collected, it was necessary to collect two blank flow rates for the respective samples. Only the switching experiment was performed on this run, no

competition data was collected. The mass data for the 5th run is shown below in Table 4.1 along with the syngas.

Table 4.1 Ru 5th Run Mass Data

Hours	Sample	Syngas	Hot Trap (g)	Cold Trap (g)	Total (g)
24	JN5-1	H ₂	7.13	.97	8.10
46	JN5-2	H ₂	2.96	1.02	3.98
69	JN5-3	H ₂	1.89	1.13	3.02
110	JN5-4	H ₂ , followed by D ₂ and H ₂	2.51	2.59	5.10
140	JN5-5	H ₂	1.93	1.00	2.93
163	JN5-6	H ₂	0.77	0.82	1.59
188	JN5-7	H ₂	0.77	0.10	0.87

Note that for day 5, the D₂/CO syngas tank was switched mid-day and run for approximately 8 hours. Multiple gas samples were taken during these 8 hours for more consistent results. All the gas samples were run shortly after collection. Analysis for KIE, alphas for hydrogen and 2-olefins vs. 1-olefins was completed for this run.

After it was apparent that this alumina catalyst was successful, another run was ordered. This would be the second run with this alumina catalyst, but the 6th run overall. For this run, both the competition and switching experiments were performed. Competition was again run first to get the most product and accurate results. As with the fifth run, the pressure had to be lowered for the deuterium syngas tank. Instead of just decreasing the pressure for D₂/CO and part of H₂/CO, the pressure was reduced for the entire switching experiment. So, the reaction conditions are 250°C at 200 psi and 250°C

at 180 psi for the competition and switching experiment respectively. The mass of the liquid and wax products collected for the 6th run can be found in Table 4.2.

Table 4.2 Ru 6th Run Mass Data

Hours	Sample	Syngas	Hot Trap (g)	Cold Trap (g)	Total (g)
24	JN6-1	H ₂ /D ₂	8.56	1.01	9.57
47	JN6-2	H ₂ /D ₂	5.93	1.25	7.18
80	JN6-3	H ₂ /D ₂	6.37	2.19	8.56
119	JN6-4	H ₂	1.88	0.87	2.75
144	JN6-5	H ₂	1.27	1.83	3.10
168	JN6-6	H ₂	2.17	2.67	4.84
192	JN6-7	H ₂ , followed by D ₂ and H ₂	1.69	0.04	1.73
215	JN6-8	H ₂	2.06	1.74	3.80
235	JN6-9	H ₂	0.82	1.16	1.98
260	JN6-10	H ₂	0.65	2.00	2.65
286	JN6-11	H ₂	.73	1.72	2.45

The D₂/CO tank again was run for less than one day. Analysis of deuterium enrichment, KIE, alphas for hydrogen and 2-olefins vs. 1-olefins were all carried on this second alumina run.

4.2 KINETIC ISOTOPE EFFECT DURING Ru/Al₂O₃ CATALYZED FTS

For the 5th run a total of 15 gas samples were collected at the varying pressures of 180 psi and 200 psi. The difference seen here between the alumina and silica catalyst is the overall increase in %CO conversion. There was an increase from 20-30% (silica) to 50-

70% (alumina). While this is logical when comparing the lower temperature conditions of the 2nd and 3rd run, it is also true for the 1st run, which was at the same reaction conditions as the alumina runs. This indicates that the alumina catalyst synthesized is more active than the silica catalyst. The 6th run also showed higher conversion, but there were more outliers when looking at all of the data points. The samples collected and analyzed in the 5th run were much more consistent.

In relation to the kinetic isotope effect, it was difficult to use the liquid/wax data for a preliminary analysis. This is due to the switching between collecting H₂/CO and D₂/CO fairly quick. While the one sample that contains the most deuterium should have an increased mass output, it is only a single data point. Collecting only one deuterium sample is then more dependent on time. For the 5th run, at least 24 hours was between the previous sample and the partial deuterium sample collected. There was a slight increase, but it was no longer large enough to successfully say that it was not simply due to the heavier isotope. The 6th run also did not have enough data for this preliminary analysis. The deuterium sample collected was less than 24 hours between the previous hydrogen samples. The sample collected had very little liquid product from the cold trap. Most of the mass came from the wax products. The only indication that might be useful is that more long chain hydrocarbons were formed, but overall it could not be determined that the mass showed an inverse isotope effect. The next step was to look at the %CO conversion for the switching experiment.

The 5th run had very consistent data in terms of CO output. The calculations to figure out %CO conversion were calculated the same as the silica catalyst using Equation 1.7. Also, the correct blank flow rates were taken into account for the samples with the two different pressures. The results yielded average %CO conversions shown in Table 4.3. Again, graphical representations are listed in Appendix A for %CO Conversion. Clearly, in the 5th run, the switching experiment exhibited an inverse isotope effect. There is also a similar trend seen in the 6th run. Data for the 6th run is also shown in Table 4.3.

Table 4.3 %CO Conversion for Ru/Al₂O₃

Syngas	H ₂ /D ₂	H ₂	D ₂	H ₂
Ru 5 th Run	-	56.85	67.02	60.17
Ru 6 th Run	37.65	8.72	21.04	1.73

There is some concern for the Ru 6th run data as the calculations for the H₂/CO conversions were terribly low. While a decrease is expected since the inverse isotope effect was previously observed in the 5th run, this is quite a drastic drop from 20% to 2%. Since there was no drastic decrease in the other products (liquid and wax), some part of collecting the samples or GC analysis must have caused some experimental error. However, based on the 5th run, an inverse isotope is present, supporting the change in hybridization from sp² to sp³.

4.3 PRODUCT DISTRIBUTION DURING Ru/Al₂O₃ CATALYZED FTS

In relation to alphas for the alumina catalyst, it was difficult to obtain a pure deuterium product. All alphas calculated came from hydrogen samples for both alumina runs. The calculations still proceeded through the identification of the correct peaks and peak areas, finding the mole percents, and finally linearizing the data points for each carbon number through the use of natural logs. For an example calculation, see section 3.3. For the 5th run, since no competition experiments were performed at the beginning, all of the samples collected are H₂ (pure). Also, since the deuterium syngas feed was run for less than a day it made re-purification of the samples much quicker when switched back to hydrogen. The samples with good spectra for hydrogen alphas are: JN5-1, JN5-2, JN5-3, JN5-4, JN5-6 and JN5-7. Since there were so many pure product results, the average of all the alphas was calculated for further calculations. These calculations would be determining the average molecular weight and the corresponding K value. The average alpha for all six samples was 0.829, which led to an average molecular weight of 83.79g/mol. The corresponding K value is 6.0. Remember K is on average, the most common number of CH₂ groups found in the entire product spectrum.

With the 6th run, the competition experiment was performed, which led to less pure H₂/CO samples overall. A couple of days of H₂/CO syngas had to be run before obtaining products viable for alpha analysis. Again, since D₂/CO syngas feed was run for less than 1 day, it was not possible to obtain a pure enough product for GC-FID and eventually alpha analysis. The pure enough H₂/CO samples are: JN6-5, JN6-6, JN6-9, JN6-

10 and JN6-11. The average alpha of these five samples is 0.842. The average molecular weight for the 6th run is 90.04 g/mol with a corresponding K value of 6.4. This data is generally consistent with the 5th run for the alumina catalyst. These values also seem to be reasonably similar to the silica catalyst for H₂ pure samples. While the alphas do not indicate what types of polymers are formed, it does yield information about chain growth. With both the silica and alumina catalyst having similar values at the same reaction temperatures shows that these two supports have similar growth probabilities with ruthenium as the metal catalyst.

4.4 PRIMARY VS. SECONDARY PRODUCT ANALYSIS DURING Ru/Al₂O₃ CATALYZED FTS

With the same GC-FID results used to calculate alphas, typically the secondary product analysis of 1-olefin vs. 2-olefin would be performed. However, there is no pure enough sample for deuterium that will yield viable GC-FID data. While this does make these calculations improbable through GC-FID data, it is not impossible to figure out through other means. More data analysis of the deuterium, hydrogen mixture sample is necessary. (This sample would be the one collected during the switching experiments, not the competition experiment.) If the mixed sample is run through GC-MS, the deuterium pure products can be isolated through the molecular weight. The samples run were JN5-5 for the fifth run and JN6-7. Before the products of these samples are isolated and used for calculation, there are other steps that must be done first. Since only the mixed samples were run on GC-MS, this means that the data from the hydrogen pure

samples will come from the GC-FID. Since these are two different instruments and detectors, a correction factor must be utilized in order to compare the data to each other. The goal of going through this process is to yield percent amounts of 1-olefin, paraffin and 2-olefin for deuterium products in the one sample.

To determine the correction factor, a standard of pure deuterium products had to be used first. The only pure samples obtained came from the Ru/SiO₂ runs previously described. The sample chosen was JN18 from the 1st run. Once the GC-MS data was acquired for the standard, the necessary correction factors could be calculated as GC-FID data for JN18 was already collected and analyzed. The peak areas for each carbon number of 1-olefins, paraffins and 2-olefins (trans and cis) were identified. Even though paraffins are not part of the secondary 2-olefin vs. 1-olefin product analysis, it is still a major product and therefore necessary to calculate the percent amounts of each major product. Since these are the four major products, minor products like branched products can be neglected due to their low concentration. So, the first step is to determine the constants for GC-FID and GC-MS are necessary from the standard. The constants determined are in fact ratios of the major products for each carbon number. The two ratios chosen are [1-olefin]/[2-olefin] = a and [1-olefin]/[paraffin] = b. In order to differentiate between the GC-FID and GC-MS constants, the subscripts of _{cor} and _m were given respectively. The a_{cor} value is already known from the peak areas acquired from the GC-FID analysis of the standard. The a_m values were trickier to determine. The m/z's could be isolated via the same program utilized by deuterium enrichment analysis. There were multiple m/z's

taken into account ranging from $C_nD_{(2n+2)}$ to $C_nD_{(2n+2)-4}$ for paraffin, and $C_nD_{(2n)}$ to $C_nD_{(2n)-4}$ for olefin. This is due to the exchange principle, which states that up to 5 deuterium atoms can be switched with hydrogen atoms or vice versa while the growing chain is still active. So, the peak areas for all 5 isotopomers must be added together as they are also possible since there is still active hydrogen in the reactor while the deuterium syngas was running. It was discovered that there was in fact very little of these other isotopomers, but it was still a factor. After correcting the peak areas for m+1 and m+2, the necessary values for a_m calculations were finally determined. Both these constants are needed as $a_m * (\text{correction factor}) = a_{cor}$. The same is necessary for b_m and b_{cor} . To find the correction factor, a_{cor} was simply divided by a_m . The correction factor was also found for b, or $[1-\text{olefin}]/[\text{paraffin}]$ for each carbon number. A list of correction factors is shown in Table 4.4 for both a and b in the 5th run.

Table 4.4 Ru 5th Run correction factors

Carbon Number	Correction Factor	
	a	b
8	2.94	1.05
9	3.99	1.20
10	3.92	1.48
11	3.74	1.49
12	3.55	1.41
13	3.23	1.38
14	3.52	1.76

Now that the correction factors for GC-MS analysis have been determined, analysis of the mixed sample can commence. Calculations begin with determining the peak areas for 1-olefin, paraffin, and 2-olefin correcting for naturally occurring isotopes. With the peak areas for the sample, a_m for the sample can be calculated. In order to convert these values to useable GC-FID values, the correction factor must now be taken into account. By multiplying the correction factor for an individual carbon number with the sample a_m value should yield a_{cor} , all while taking into account each respective carbon number. This would be the expected GC-FID [1-olefin]/[2-olefin] or [1-olefin]/[paraffin] value if a pure deuterium sample was collected and run for the alumina catalyst. With these two ratios, the percent amounts of 1-olefin, paraffin and 2-olefins can be determined.

First, [1-olefin] is given the arbitrary value of 1. Once this is done, the following is now true: [2-olefin] = $1/a_{cor}$ and [p] = $1/b_{cor}$. This is necessary to determine the percent amount in the sample for each carbon number. Now the percent of 1-olefin is shown in Equation 4.1.

$$\frac{\text{1-olefin}}{\text{Total}} = \frac{1}{1 + \frac{1}{a_{cor}} + \frac{1}{b_{cor}}} \quad (4.1)$$

Likewise, it is also known Equation 4.2-4.3 is now true.

$$\frac{\text{2-olefin}}{\text{Total}} = \frac{\frac{1}{a_{\text{cor}}}}{1 + \frac{1}{a_{\text{cor}}} + \frac{1}{b_{\text{cor}}}} \quad (4.2)$$

$$\frac{\text{Paraffin}}{\text{Total}} = \frac{\frac{1}{b_{\text{cor}}}}{1 + \frac{1}{a_{\text{cor}}} + \frac{1}{b_{\text{cor}}}} \quad (4.3)$$

For example, JN5-5 was the sample utilized in the fifth run to calculate deuterium production. The first step for determining these values for a sample is to find the a_{cor} and b_{cor} values. Using C_{12} as an example the following calculations shown in Equations 4.4-4.5 were performed.

$$\frac{\text{1-olefin peak area}}{\text{2-olefin peak area}} = \frac{13868}{68087} = .204 = a_m \quad (4.4)$$

$$\frac{\text{1-olefin peak area}}{\text{paraffin peak area}} = \frac{13868}{209691} = .067 = b_m \quad (4.5)$$

Next a_m and b_m must be corrected, and converted to GC-FID value using the standard that was previously calculated. The correction value for $a = 3.55$ and $b = 1.41$. The calculations are shown in Equations 4.6-4.7.

$$a_m * (\text{correction factor}) = .204 * 3.55 = .723 = a_{\text{cor}} \quad (4.6)$$

$$b_m * (\text{correction factor}) = .067 * 1.41 = .093 = b_{\text{cor}} \quad (4.7)$$

Now all the values have been determined for Equations 4.1-4.3. The values determined are the percent of 1-olefin, paraffin and 2-olefin for deuterium in the products collected. The corrected values for all carbon numbers calculated are shown in Table 4.5.

Table 4.5 Deuterium Correction Sample JN5-5

Carbon Number	[1-olefin] _D	[2-olefin] _D	Paraffin
9	.084	.155	.761
10	.080	.162	.757
11	.069	.138	.793
12	.076	.106	.818
13	.063	.093	.844
14	.052	.088	.860

The values discovered above are now the values that can be used in secondary product analysis. The 1-olefin and 2-olefin are the values for deuterium calculations which fills in all variables in equation 1.7.

Due to the low concentration of deuterium products, especially in comparison to the hydrogen products, there were only so many values present. For the 6th run (JN6-7 and JN6-8), there were too few 1-olefin peaks that were above the limit of integration. This made it still impossible to calculate the amount of major products present. Perhaps a reason for this is that the switch to deuterium was made too late in the run and also for too short of a time. This could lead to less active sites and not enough time to form

enough deuterium products. The 5th run was more beneficial through this type of analysis. Peaks ranging from C₉ to C₁₄ were observed in the GC-MS program, allowing for the determination of percent products. The corrected deuterium values, GC-FID H₂ pure values and the [1-o]_{H/D} and [2-o]_{H/D} (reference Table 4.5 for deuterium values) are listed in Table 4.6. A graphical interpretation is shown in Figure 4.1.

Table 4.6 H₂ pure 1-olefin and 2-olefin results with H/D ratios of 1-olefin and 2-olefin

Carbon Number	[1-olefin] _H	[2-olefin] _H	[1-o] _{H/D}	[2-o] _{H/D}
9	.167	.201	.789	1.30
10	.157	.188	.938	1.16
11	.141	.160	.937	1.16
12	.133	.141	1.02	1.33
13	.107	.112	.960	1.20
14	.092	.099	.976	1.12

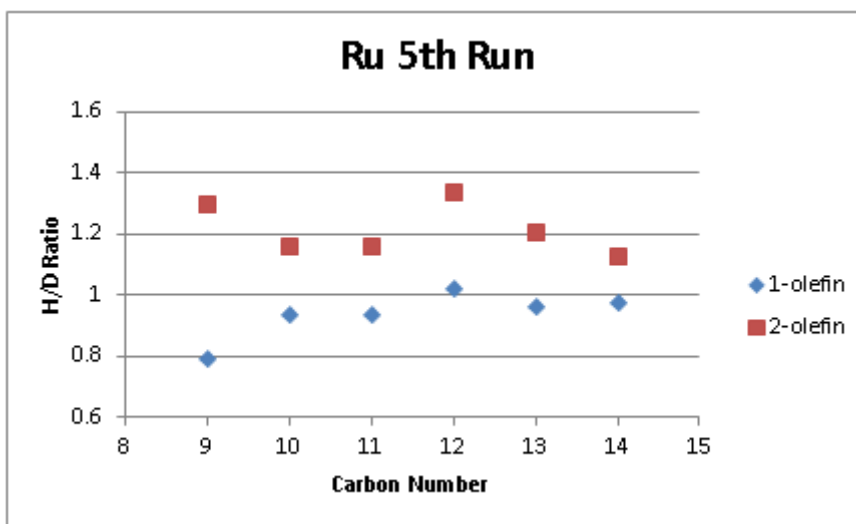


Figure 4.1 1-olefin vs. 2-olefin H/D ratio

The data for the alumina catalyst is more varied than that of the silica catalyst. The H/D ratios seem less stable and fluctuate more readily. However, from this data, it can be concluded that 1-olefins and 2-olefins are not through the same reaction pathway. All of the 2-olefin ratios for each carbon number are higher than that of 1-olefin. Also, all $[1\text{-olefin}]_{\text{H/D}}$ are less than 1 with one exception and all $[2\text{-olefin}]_{\text{H/D}}$ values are greater than 1. The one exception as well as the fluctuating data from the 5th run could be due to the low peak areas in the mass spectrometry data. 1-olefin is typically less in amount due to less stability. Therefore, on a run where the deuterium syngas feed is utilized for more than one day, the peaks should be more stable and offer more consistent data. From the data collected between the alumina and silica catalyst, the conclusions about 1-olefins vs. 2-olefins are consistent. The H/D ratios indicate that firstly, they are not produced through the same reaction pathway and secondly suggests that 1-olefins are converted to 2-olefins due to $[2\text{-olefins}]_{\text{H/D}} > [1\text{-olefins}]_{\text{H/D}}$.

4.5 DEUTERIUM ENRICHMENT IN HYDROCARBONS DURING Ru/Al₂O₃ CATALYZED FTS

Of the conclusions drawn so far about the alumina catalyst, they have all come from the switching experiment and subsequent data analysis. Moving on to the other experiment performed on alumina, the discovery or lack thereof, of deuterium enrichment can be performed. The competition experiment was only performed on the 6th run. The reason the competition experiment was not performed on the 5th run was due to the failed 4th run. The 4th run was a previous alumina catalyst synthesized that

showed minor activity. Since the H₂/D₂/CO/N₂ gas is fairly expensive, it was logical to use a much cheaper gas to determine the activity of the catalyst. Since the competition experiment works a lot better when the catalyst is fully active, the syngas was not switched to the competition experiment mid to late run. It was already determined that a 6th run would be performed if the second alumina catalyst was active enough.

The competition experiment was run the same for the alumina catalyst as the silica catalyst. After activation, the syngas tank was switched from pure H₂ to H₂/D₂/CO/N₂ competition tank. The experiment was run for three days with three total liquid/wax samples collected. The sample with the most data and consistently Gaussian peaks was the third sample (JN6-3). A table of the H/D ratios calculated can be found in Table 4.7.

Table 4.7 Competition H/D Ratios JN6-3

Carbon Number	1-olefin	paraffin	2-trans-olefin	2-cis-olefin
7	.714	.813	.732	.725
8	.699	.827	.719	.721
9	.705	.749	.716	.714
10	.688	.743	.713	.709
11	.686	.740	.713	.714
12		.732	.716	.710
13		.728	.723	.711
14		.724	.728	.707
15		.725	.733	.707
16		.725	.743	
17		.723		
18		.739		
19		.733		
20		.731		
21		.722		
22		.722		

This set of data was the most stable and showed some interesting trends as shown in Figure 4.2. While little 1-olefin was produced for the competition experiment, there was still enough data through C₁₁ to see a small trend. 1-olefin appears to be decreasing as carbon number increases. The same is true for 2-cis-olefin with more data points. For 2-trans-olefin, the H/D ratio decreases until C₁₂ where the trend begins to increase. Finally, with respect to paraffin the trend is decreasing in relation to increasing carbon number. There is however a slight jump in the data for C₁₈. It is still unknown as to why there is a change so high in carbon number. The trends for the other two samples were less consistent as the sample data fluctuated more. In general all the samples H/D ratios

were less than one, and the H/D ratio changed as carbon number increased. Data for samples JN6-2 and JN6-1 can be found in Appendix B.

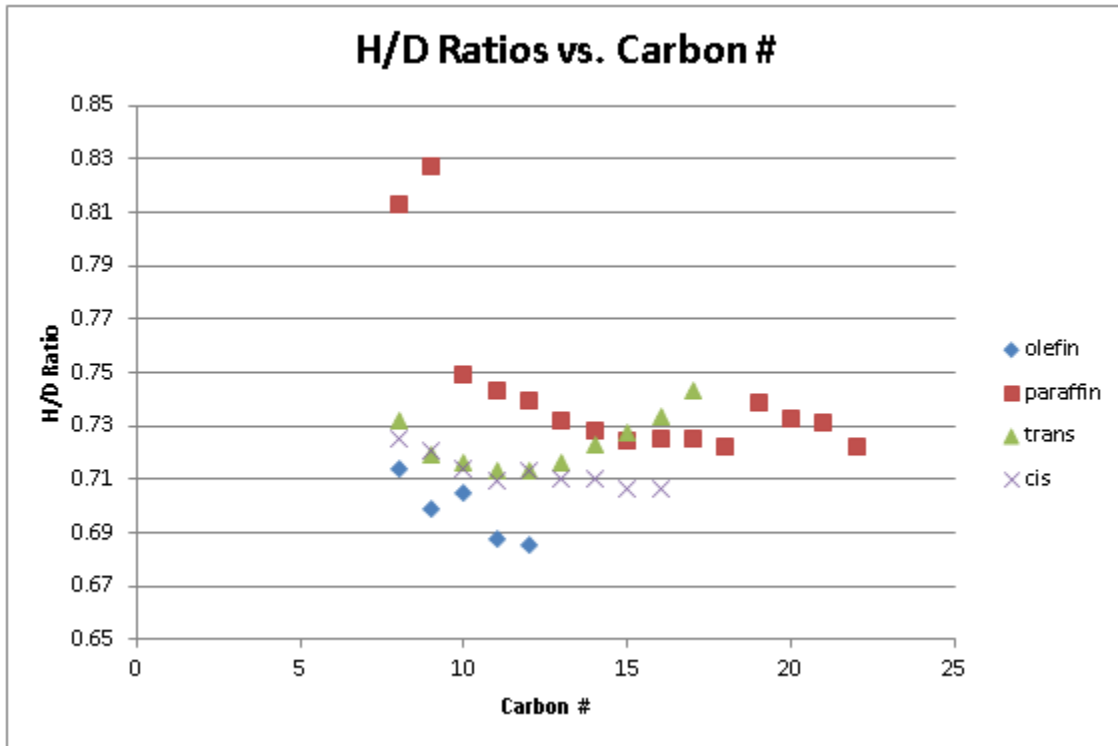


Figure 4.2 Competition H/D ratios trend JN6-3

CHAPTER 5

CONCLUSIONS AND FUTURE DIRECTIONS

5.1 CONCLUSIONS

Looking at all of the data and conclusions that have been collected, certain mechanisms can be ruled out. First, beginning with a result from the switching experiment, the inverse isotope effect indicates that there must be a change in the mechanism from $sp^2 \rightarrow sp^3$ or $sp \rightarrow sp^2$ hybridized carbon. This carbon also has to be attached to a hydrogen atom in order to study the secondary isotope effect. First, with CO insertion, the monomer is CO and the growing chain is M-CH₂-R. During the rate determining steps of propagation, there is no theoretical change from $sp^2 \rightarrow sp^3$ or $sp \rightarrow sp^2$. This means CO insertion is not a viable candidate for Ru catalyzed FT. Since the alkyl mechanism has the same growing chain as CO insertion, this indicates that an inverse isotope effect would not be observed. However, the monomer is different in this mechanism (M=CH₂). The monomer starts with a sp^2 hybridized carbon and changes to an sp^3 hybridized carbon. This could show an overall inverse isotope effect in the products formed. With this being said, this indicated that the alkenyl and alkylidene mechanism will also have an observable inverse isotope effect through the monomer. With the alkylidene mechanism, both the growing chain and the monomer will display an inverse isotope effect. Therefore this mechanism cannot be discarded yet. The alkenyl mechanism is a different story.

The alkenyl mechanism has a growing chain of $M-CH=CH_2-R$. Since the inverse isotope effect is observed in the monomer, another type of analysis is necessary to reinforce or discard this mechanism. This mechanism goes through propagation steps which lead to the double bond moving on the growing chain. Termination can then occur before or after isomerization of the double bond. This would indicate that 2-olefins could be primary products and produced through the same reaction mechanism as 1-olefins. Based on the isotopic studies data, it was discovered that 1-olefins and 2-olefins are not produced through the same reaction pathways. This allows for the alkenyl mechanism to be set aside. The alkylidene mechanism does however follow all of the rules laid forward thus far based upon results. The mechanism even follows the rules found via deuterium enrichment. Since the H/D ratios changed as a function of carbon number, this indicates that both the monomer and growing chain must have an inverse isotope effect. This further supports that CO insertion, alkyl, alkenyl and hydroxymethylene mechanism are not quite accurate. The alkylidene and the modified alkylidene mechanism are the two mechanisms that are still valid after all the data is applied. Seeing as how the only difference between the alkylidene ($M=CH_2$) and the modified alkylidene ($M\equiv CH$) mechanisms is the monomer, it would make sense that both follow all of the data trends observed. Now, the debate becomes which monomer is more likely to occur in the catalyst bed. It is possible to have many different types of coordinated carbons to the metal surface; the question is, which among them is the most stable. After studying the theoretical mathematically more stable coordination, the conclusion of $M\equiv CH$ being the most stable was reached. While there is no experimental data to suggest which monomer

is more stable, the density function theory (DFT) study indicates that it is $M\equiv CH$.⁶⁶ This leads to the conclusion that the modified alkylidene mechanism is slightly more accurate than the alkylidene mechanism.

The modified alkylidene mechanism is shown in Figure 5.1. The first step of propagation involves the electrons in one bond of $M\equiv CH$ attacking the carbon in another monomer to form a bond between the two carbons. Once this occurs the stable carbon-carbon bond has been formed and the hybridization of the monomer has changed from sp to sp^2 . At this stage the growing chain is attached to the metal surface through both carbon atoms. Through the addition of absorbed hydrogen, one of the carbons can become detached from the metal surface. At this point, either propagation or termination could occur. Another propagation would lead to C_3 or eventually C_3^+ . Termination could lead to ethane or ethene, through hydrogenation or beta-elimination respectively. Of the other viable processes that are proposed in the modified alkylidene mechanism, all are proposed after readsorption. Readsorption would generally be through 1-olefins due to their active double bond. After readsorption, this opens many new avenues and possible products to be formed. Since readsorption is on the inner carbon, this could lead to either more paraffin or 2-olefins through termination. If propagation occurs, this would lead to methyl branched products. Depending on how many propagation steps occur determines where the methyl substituted group is at. Previously observed are 1, 2, 3, 4 and sometimes even 5-methyl substituted carbons. This concludes the main reaction schemes of the modified alkylidene mechanism.

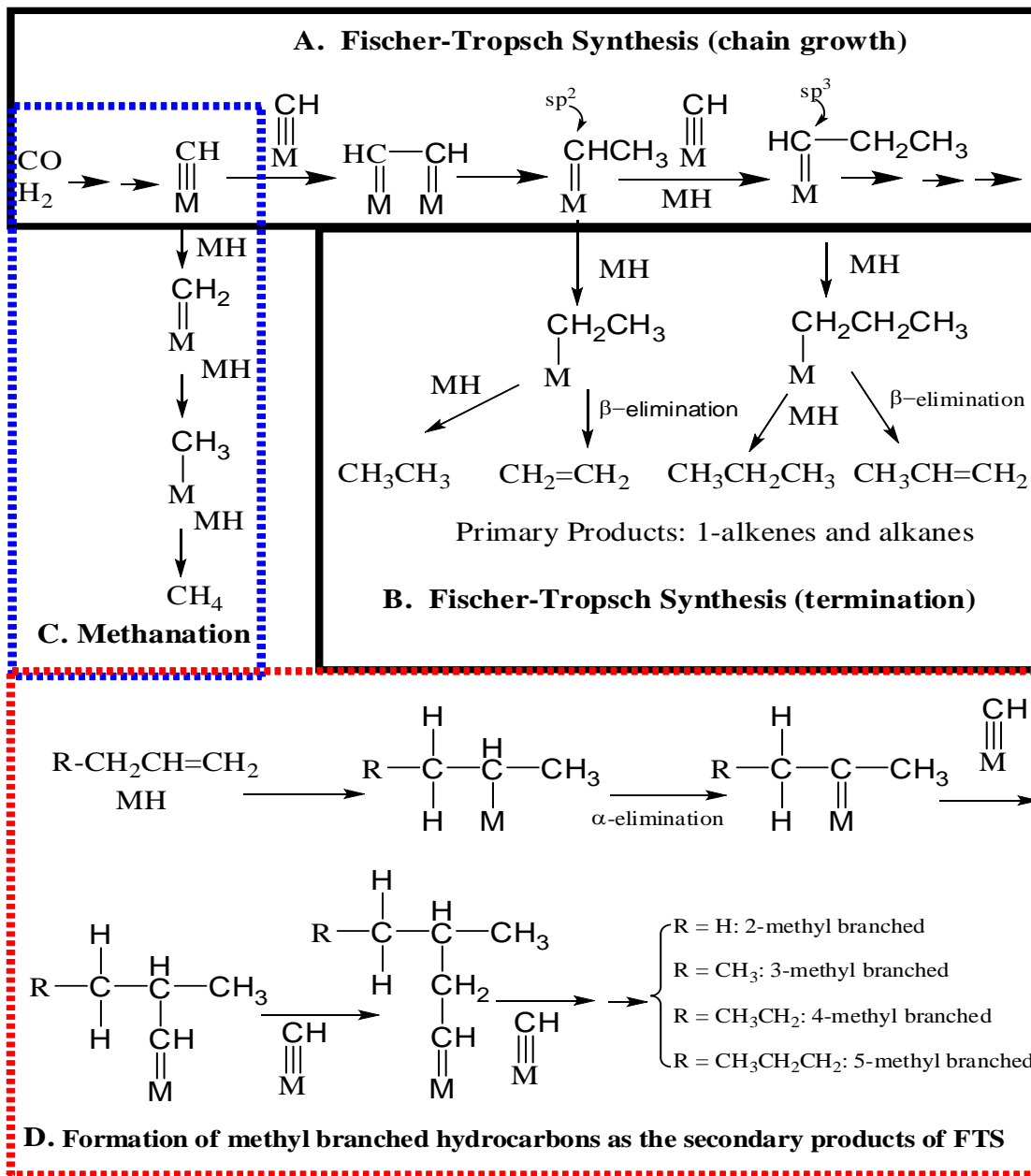


Figure 5.1 Modified Alkylidene Mechanism

All of the data from both the silica and alumina catalyst do not contradict this mechanism. The inverse isotope effect was observed in multiple ways. First evidence began with the liquid and wax products formed. The mass of the deuterium samples

formed was significantly higher than the mass of the hydrogen samples present (only data is through silica catalyst). This indicated that production had increased with the D₂/CO syngas. Support through the % CO conversion also indicated an inverse isotope effect. With the D₂/CO syngas feed, the % CO converted increased in relation to H₂/CO % CO converted. Since the % CO conversion increased from H₂ to D₂ and subsequently decreased from D₂ to H₂, this ensures it is not simply a matter of delayed activity on the part of the catalyst. This data clearly supports the inverse isotope effect.

Furthermore, deuterium enrichment not only supports the observed inverse isotope effect, but also yields more information. The presence of deuterium enrichment indicates at least two pieces of information. Since all the H/D ratios were less than 1, there is favoritism to deuterium binding and therefore an inverse isotope effect. Also, since this H/D ratio changes as a function of carbon number, this suggests that the inverse isotope effect occurs not only in the monomer, but also in the growing chain. While the H/D ratios varied greater in the silica catalyst, there was also enough variation in the alumina catalyst to successfully say deuterium enrichment as a function of carbon number is present.

5.2 FUTURE DIRECTIONS

While much research on ruthenium catalyzed FT has been completed, there are still other experiments and analyses that can be performed. For example, perhaps

running these syntheses at a lower temperature could lead to more insight. There was very little manipulation of the reaction conditions, which could lead to different amounts of the various products. An attempt was made to do a pressure changing experiment on a ruthenium alumina catalyst, however, this was the 4th run. The 4th run displayed little activity and therefore no conclusions could be drawn from the data. There is also the option for varying the support. Cobalt and iron have shown activity for other supports like TiO₂; perhaps studying ruthenium bonded to a different support could lead to more insight.

As for deuterium enrichment future goals, research for this project could benefit from the theoretical side of the mechanism. The theoretical deuterium enrichment curve was only created up to C₈ as shown in Figure 5.2. The values chosen for α_D and α_H are arbitrarily chosen, with the knowledge that $\alpha_D > \alpha_H$. The ideal situation would be to carry the calculations out to C₂₀, however, this is very time consuming even with the algorithm program utilized. An attempt by Timothy Naumovitz was made to write an algorithm for deuterium enrichment, but the programming available was not able to go past C₈. When the program was asked to calculate for C₉, it simply froze. Perhaps with better collaboration and more effective commands in the algorithm programming could lead to more theoretical deuterium enrichment numbers.

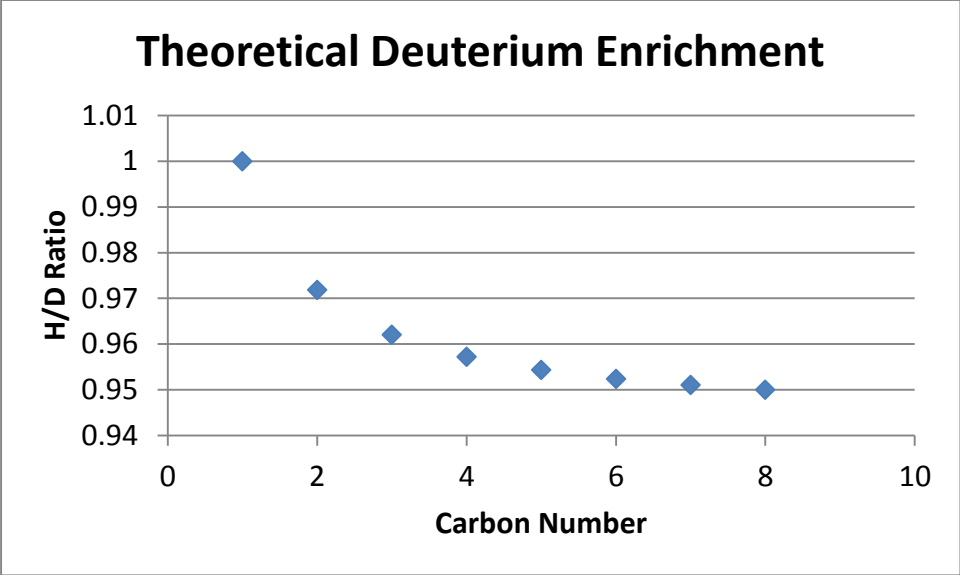


Figure 5.2 Theoretical Deuterium Enrichment

Note: $\alpha_D = 0.9$, $\alpha_H = 0.8$

REFERENCES

1. Gary, James H.; Handwerk, Glenn E.; Kaiser, Mark J. *Petroleum Refining Technology and Economics, Fifth Edition*; CRC: Boca Raton, FL, 2007.
2. Fischer, F.; Tropsch, H. *Ges. Abh. Kennt. Kohle* **1928**, *10*, 313.
3. Pichler, H. *Adv. Catal*, 1952, *4*, 271.
4. Stranges, Anthony N. *The US Bureau of Mines' Synthetic Fuel Programme, 1920-1950s: German Connections and American Advances*, *Ann. Of Sci.* **1997**, *54*, 29-68.
5. <https://www.uniongas.com/about-us/about-natural-gas/Chemical-Composition-of-Natural-Gas> (accessed April 28, 2015).
6. Rostrup-Nielsen, Jens R. *Syngas in Perspective*, *Catal. Today* **2002**, *71*, 243-247.
7. <http://www.thyssenkrupp-industrial-solutions.com/de/produkte-loesungen/chemieindustrie/wasserstoff/steam-reforming/overview.html> (accessed March 15, 2015)
8. Olsson, Henrick; Winter-Madsen, Sandra *Steam Reforming Solutions* Haldor Topsoe A/S, Denmark, July 2007
9. Dry, Mark E. *The Fischer-Tropsch process: 1950 – 2000*, *Catal. Today* **2002**, *71*, 227-241.
10. Basu, Prabir *Biomass Gasification and Pyrolysis: Practical Design and Theory* Academic Press: Oxford, 2010; pp 342-344.
11. Smoot, L.D.; Smith, P.J. *Coal combustion and gasification*; Plenum Press: New York, 1985.

12. Fischer, Franz; Tropsch, Hans *Über die Herstellung synthetischer olgemische (Synthol) durch Aufbau aus Kohlenoxyd und Wasserstoff* Brennst Chem 4, **1923**, 276-285.
13. Iglesi, A. *Selectivity control and Catalyst design in the Fischer-Tropsch synthesis: sites, pellet and reactors* Adv. In Cat. **1993**, 39, 221-302.
14. <https://www.ihs.com/products/chemical-technology-pep-reviews-oligomerization-for-gasoline-2009.html> (accessed March 30, 2015)
15. <http://www.refiningnz.com/visitors--learning/classroom--learning-resources/learning-centre/how-it-works---the-refining-process/hydrocracker.aspx> (accessed March 30, 2015).
16. Al-Shalci, Wisam Gas to Liquids (GTL) Technology
<http://www.scribd.com/doc/3825160/Gas-to-Liquids-GTL-Technology>
(accessed April 28, 2015).
17. Fredrich Bergius – Biographical
http://www.nobelprize.org/nobel_prizes/chemistry/laureates/1931/bergius-bio.html (accessed March 1, 2015)
18. Miller, Stanley L. *A Production of Amino Acids Under Possible Primitive Earth Conditions*, Science **1952**, 117, 528-529.
19. Baum, Arthur W. What can we use oil for? *Saturday Evening Post* November 27, 1943, p 18.
20. <http://petroleumhistory.ca/history/globalHistory.pdf> (accessed April 28, 2015).
21. <http://www.airpower.maxwell.af.mil/airchronicles/aureview/1981/jul-aug/becker.htm> (accessed February 15, 2015)
22. Storch, H. H.; Anderson, R.B.; Hofer, L.J.E.; Hawk, C.O.; Anderson, H.C.; Golumbic, N. *Synthetic liquid fuels from hydrogenation of carbon monoxide* U.S. Bur. Mines, **1948**, 709, n. pag. Print.

23. Khodakov, Andrei Y.; Chu, Wei; Fongarland, Pascal *Advances in the Development of Novel Cobalt Fischer-Tropsch Catalyst Synthesis of Long Chain Hydrocarbons and Clean Fuels* Chem. Rev. **2007**, *107*, 1692-1744.
24. <http://www.netl.doe.gov/about/netl-history> (accessed February 15, 2015).
25. Baird, Michael J.; Schehl, Richard R.; Haynes, William P.; Cobb Jr., James T. *Fischer-Tropsch Processes Investigated at the Pittsburgh Energy Technology Center since 1944* Ind. Eng. Chem. Prod. Res. Dev., **1980**, *19* (2), 175-191.
26. Eisenberg, Benjamin; Fiato, Rocco A. *The Evolution of Advanced gas-to-liquids technology* Chemtech. **1999** *29* (10), 32.
27. Storch, H.H.; Golumbic, N.; Anderson, R.A., *The Fischer-Tropsch and Related Synthesis* Wiley **1951**.
28. Teng, B.; Zhang, C.; Yang, J.; Cao, D.; Chang, J.; Xiang, H.; Li, Y. *Oxygenate Kinetics in Fischer-Tropsch synthesis over an industrial Fe-Me catalyst* Fuel **2005**, *84* (7-8), 791-800.
29. Brady III, R. C.; Petic, R. *Reactions of diazomethane on transition-metal surfaces and their relationship to the mechanism of the Fischer-Tropsch reaction* J. Am. Chem. Soc. **1981**, *102*, 1287-1289.
30. Brady III, R.C.; Petic, R. *On the mechanism of the Fischer-Tropsch reaction – the chain propagation step* J. Am. Chem. Soc. **1981**, *103*, (5), 1287-1289.
31. Turner, M.L.; Long, H.C.; Shenton, A.; Byers, P.K.; Maitlis, P.M. *The Alkenyl Mechanism for Fischer-Tropsch Surface Methylene Polymerization – the Reactions of Vinyllic Probes with Co/H-2 over Rhodium Catalysts* Chem-Eur. J. **1995**, *1*, (8), 549-556.
32. Akita, <. Musashi, H.; Akanishi, N.S.; Moro-oka, Y. *Photochemical C-H bond activation of diruthenium bridging alkylidene complexes: Interligand H-exchange on $Cp_2Ru_2(\mu-CH_2)(\mu-CHR)(CO)_2(R=H, Me)$* J. Organomet. Chem. **2001**, *617*, (1), 254-260.

33. Ekstrom, A.; Lapszewicz, J. A. *Reactions of cobalt surface carbides with water and their implications for the mechanism of the Fischer-Tropsch reaction* J. Phys. Chem. **1987**, *91*, (17), 4514-4519.
34. Akin, A.N.; Onsan, Z.I. *Kinetics of CO hydrogenation over coprecipitated cobalt-alumina* J. Chem. Technol. Biotechnol. **1997**, *7*, (3), 304-310.
35. Wang, Y.D.; Bavis, B.H. *Fischer Tropsch Synthesis. Conversion of alcohols over iron oxide and iron carbide catalysts* Appl. Catal. A-Gen. **1999**, *180*, (1-2), 277-285.
36. Deng, B.L.; Campbell, T.J.; Burris, D.R. *Hydrocarbon formation in metallic iron/water systems* Environ. Sci. Technol. **1997**, *3*, (4), 1185-1190.
37. "US Consumption of Alternative Road Fuels Growing", Oil & Gas Journal, July 12, 1999, pg 37-39
38. "Emission Comparison of Alternative Fuels in an Advanced Automotive Diesel Engine", SAE 981357
39. "Nissank super-ultra-low emissions vehicle", Automotive Engineering International, Nov99, pg 64- 65.
40. Davis, Burtron H. *Fischer-Tropsch Synthesis: Current Mechanism and Futuristic Needs* CAER, 129-138.
41. Henrici-Olive, G.; Olive, S. *The Fischer-Tropsch Synthesis: Molecular Weight Distribution of Primary Products and Reaction Mechanism* Angew. Chem. Int. Ed. Engl. **1976**, *15* (3), 136-141.
42. Shi, B.; Keogh, R. A.; Davis, B. H., *Fischer-Tropsch synthesis: The formation of branched hydrocarbons in the Fe and Co catalyzed reaction*. J. Mol. Catal. A: Chem, **2005**, *234*, 85-97.
43. Shi, B.; Lin, W.; Liao, Y.; Jin, C.; Montavon, A. *Explanations of the Formation of Branched Hydrocarbons During Fischer-Tropsch Synthesis by Alkylidene Mechanism* Top. Catal **2013**, *57*, 451-459.

44. Herrington, E.F.G. *Chem. Ind.* **1946**, 347.
45. Van Kijk, H.A.J.; Hoebink, J.H.B.J.; Schouten, J.C. *A mechanistic study of the Fischer-Tropsch synthesis using transient isotopic tracing. Part-1: Model identification and discrimination* *Top. Catal.* **2003**, *26*, 111-119.
46. Van Kijk, H.A.J.; Hoebink, J.H.B.J.; Schouten, J.C. *A mechanistic study of the Fischer-Tropsch synthesis using transient isotopic tracing. Part-2: Model quantification* *Top. Catal.* **2003**, *26*, 163-171.
47. Newsome, D.S. *The Water-Gas Shift Reaction* *Cat. Rev. – Sci. Eng.* **1980**, *21*, (2) 275-318.
48. R.B. Anderson, *Hydrocarbon synthesis, hydrogenation and cyclisation*, in: P. Emmett (Ed.), *Catalysis*, Vol. IV, Reinhold, New York, 1956, p. 1.
49. Dry, M.E., *Fischer-Tropsch synthesis*, in: J.R. Anderson, M. Boudart (Eds.), *Catalysis Science Technology*, Vol. I, Springer, Berlin, 1981, p. 159.
50. B. Jager, R. Espinoza, *Catal. Today* **23** (1995) 17.
51. M.A. Vannice, *Catal. Rev.* **14** (2) (1976) 153.
52. Vannice, M.A., *J. Catal.* **1975**, *37*, 449.
53. Claeys, M.; van Steen, E. *On the effect of water during Fischer-Tropsch synthesis with a ruthenium catalyst* *Catal. Tod.* **2002**, *71*, 419-427.
54. Biloen, P.; Helle, J.N.; Sachtler, W.M.H. *J. Catal.* **1979**, *58*, 95.
55. Brady, R.C.; Pettit, R.J. *Am. Chem. Soc.* **1980**, *102*, 6181.
56. Burwell, R.L. *Acc. Chem. Res.* **1969**, *2*, 289.
57. Miyahara, K.; Terantani, S.; Tsumura, A. *J. Res. Inst. Catal., Hokkaido Univ.* **1966**, *14*, 144.
58. Vannice, M.A. *J. Catal.* **1975** *40*, 129.

59. Vannice, M.A. *J. Catal.* **1976** *44*, 152.
60. Kellner, S.C.; Bell, A.T. *Evidence for H₂/D₂ Isotope Effects on Fischer-Tropsch Synthesis over Supported Ruthenium Catalysts* *J. Catal.* **1981**, *67*, 175-185.
61. McKee, D.W.; *J. Catal* **1967**, *8*, 240.
62. Dalla Betta, R.A.; Shelef, M. *J. Catal.* **1980**, *65*, 374.
63. Shelef, M.; Dalla Betta, R.A. *J. Catal.* **1979**, *60*, 169.
64. ASF equation - R.A. Friedel, R.B. Anderson, *J. Am. Chem. Soc.* **72** (1950) 1212.
65. Flory, P.J. *J. Am. Chem. Soc.* **1936**, *58*, 1877.
66. Liu, Ahi-Pan; Hu, P. *J. Am. Chem. Soc.* **2002**, *124*, 11568-11569.

APPENDIX A:
Figures of %CO Conversion

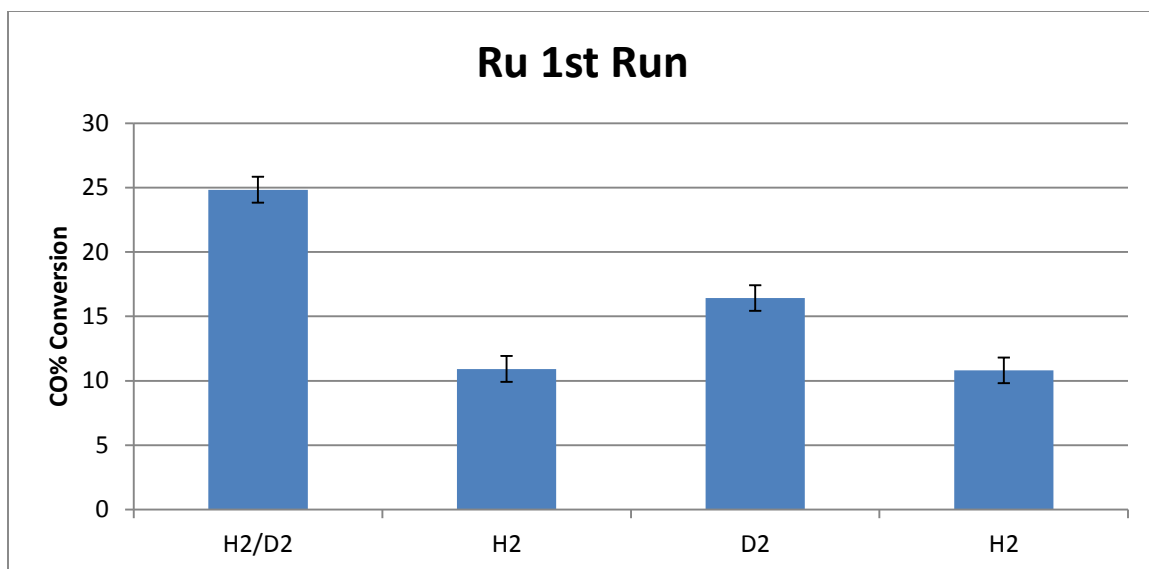


Figure A.1 Ru 1st Run (Silica)

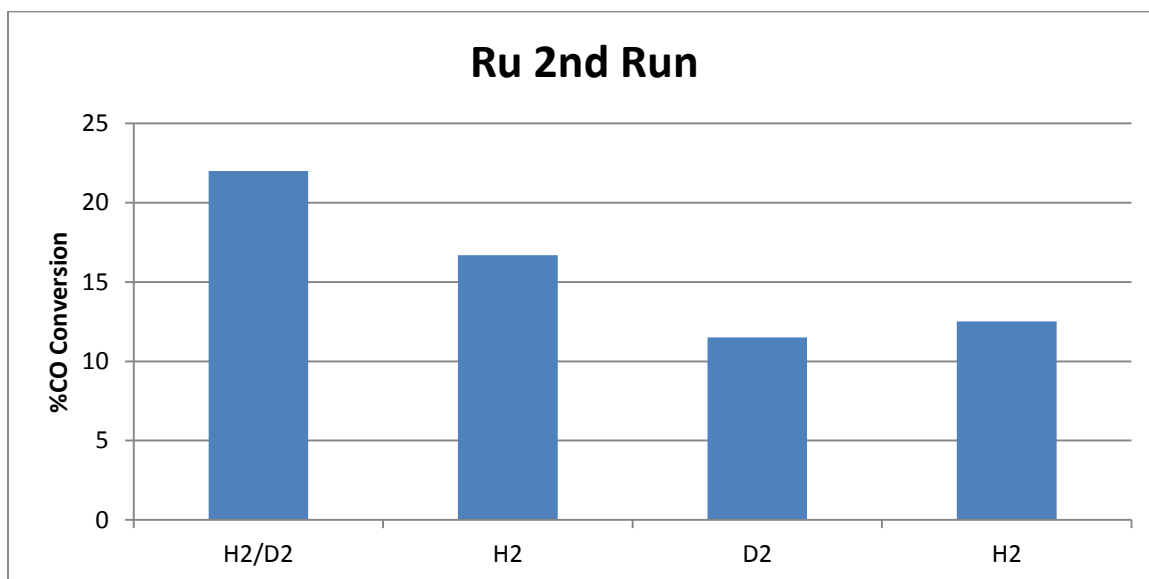


Figure A.2 Ru 2nd Run (Silica)

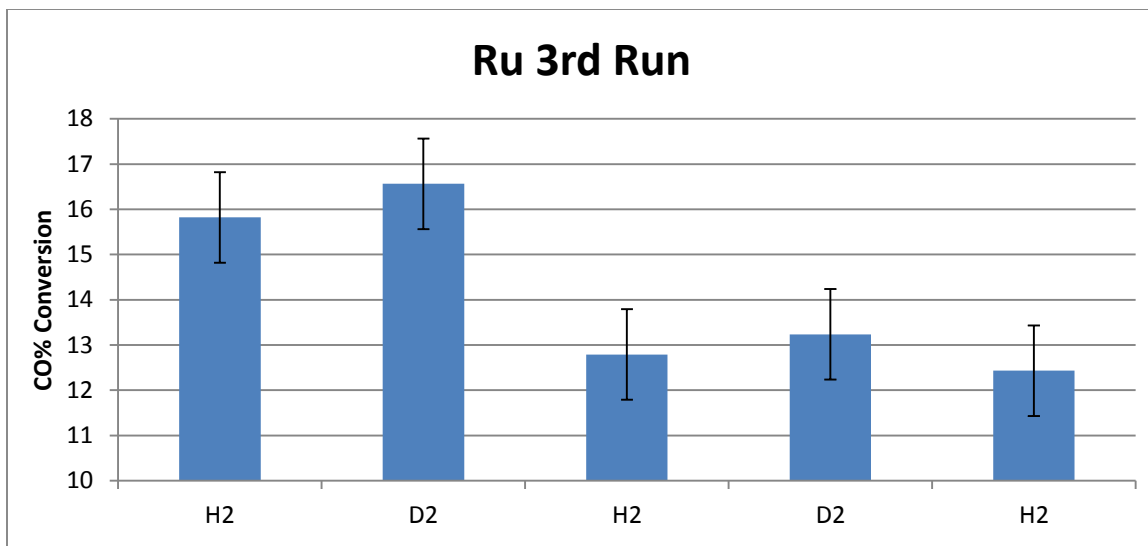


Figure A.3 Ru 3rd Run (Silica)

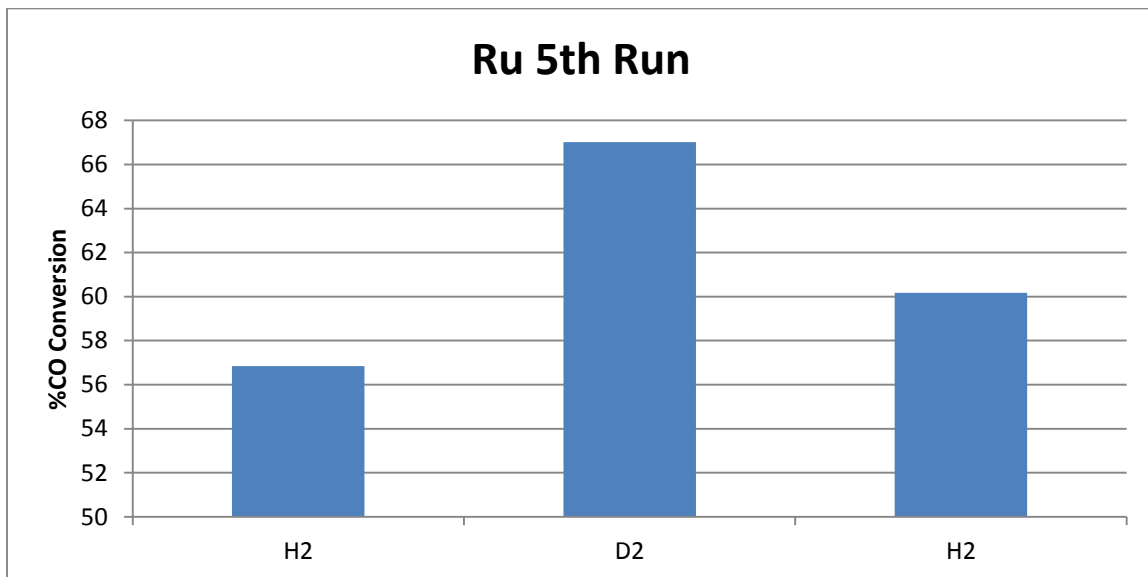


Figure A.4 Ru 5th Run (Alumina)

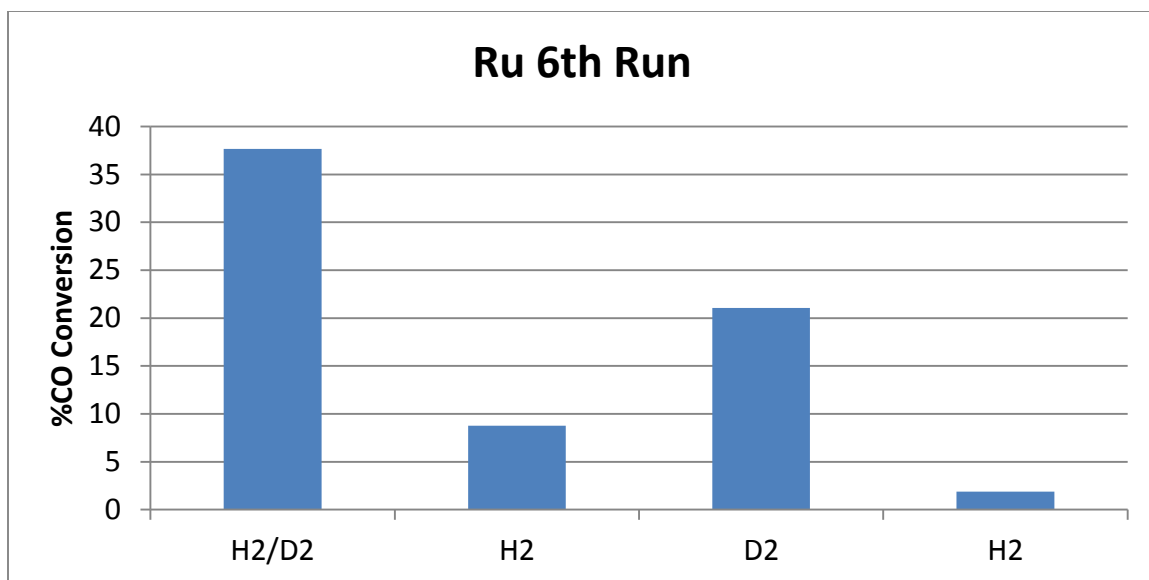


Figure A.5 Ru 6th Run (Alumina)

APPENDIX B:

Figures of Deuterium Enrichment: Sample JN19 isotopomers and trends for H/D ratios

The following spectra are the comparisons of theoretical competition experiment results with that of the experimental results. The red peak indicates the theoretical whereas the connected blue dots are the experimental points recorded and plotted. All the samples shown here are paraffins in varying carbon number. A shift of the blue line to the right indicates deuterium enrichment is present.

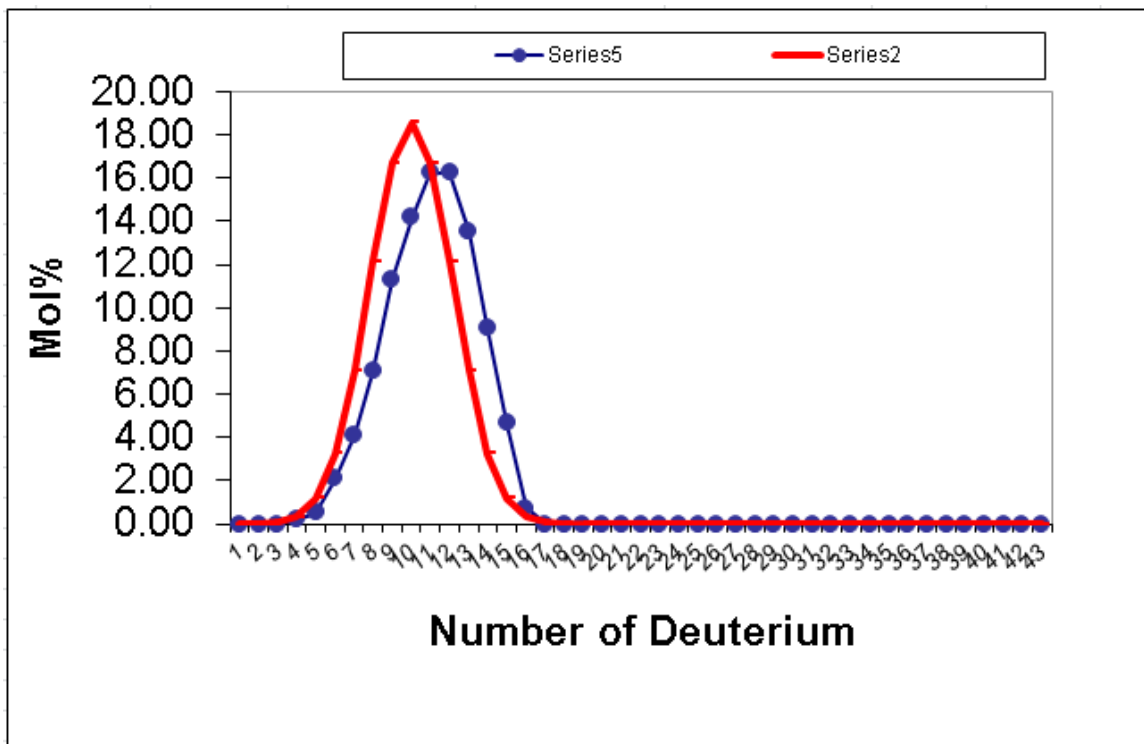


Figure B.1 JN-19: C₈ paraffin

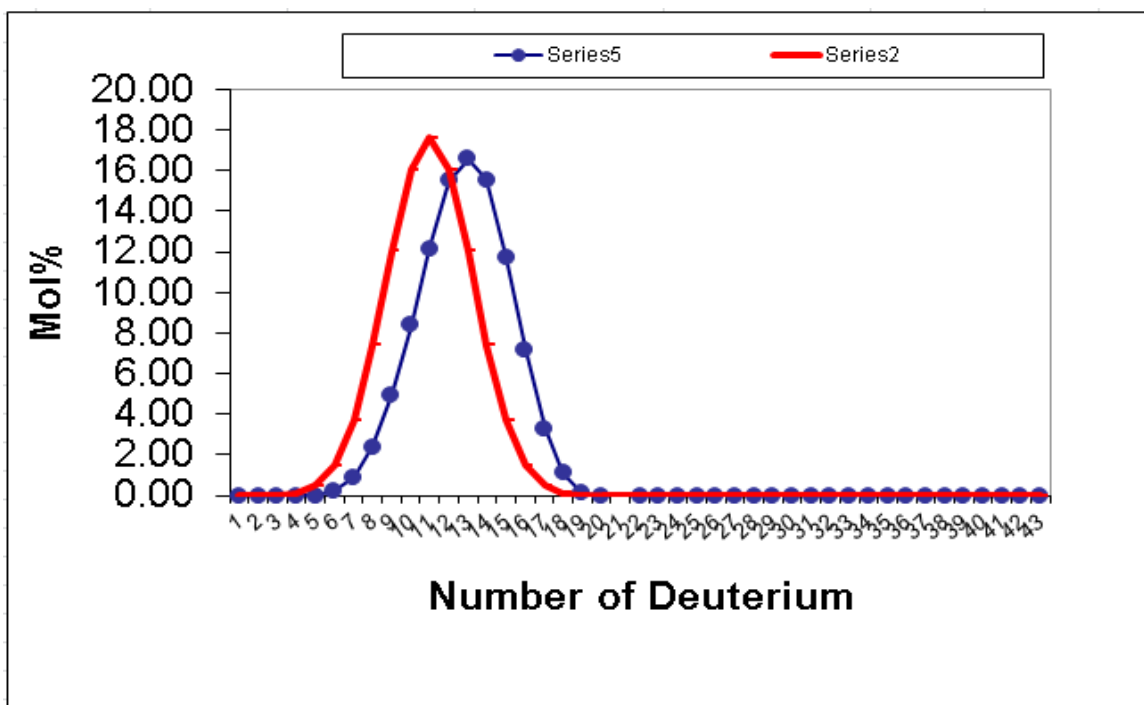


Figure B.2 JN-19: C₉ paraffin

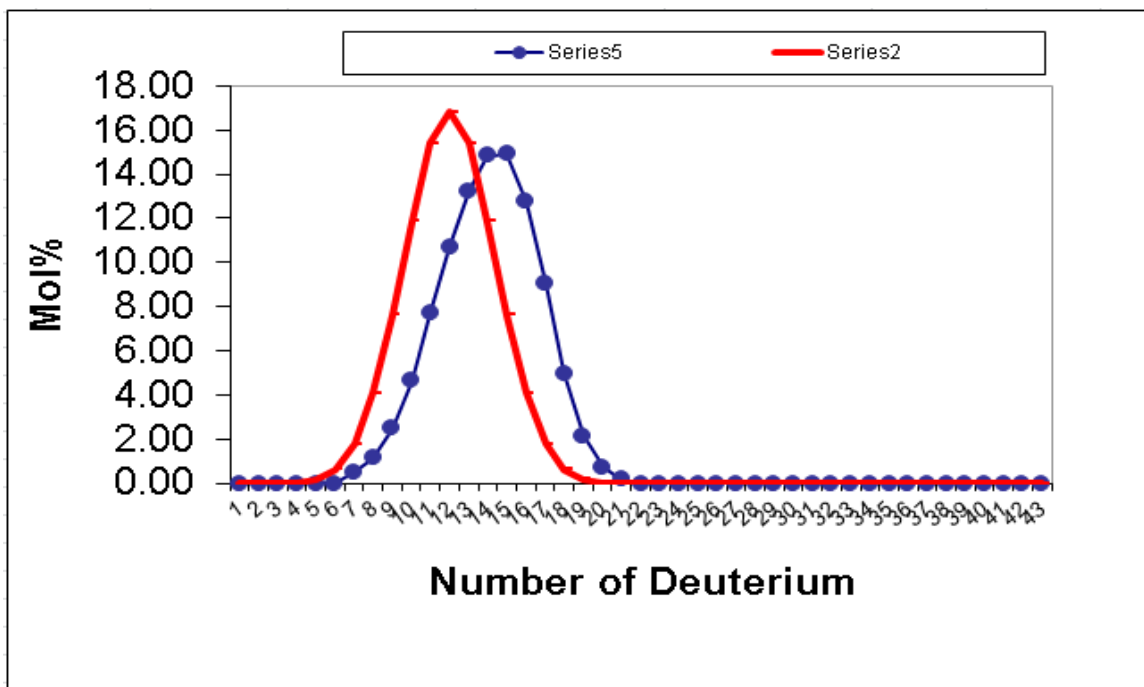


Figure B.3 JN-19: C₁₀ paraffin

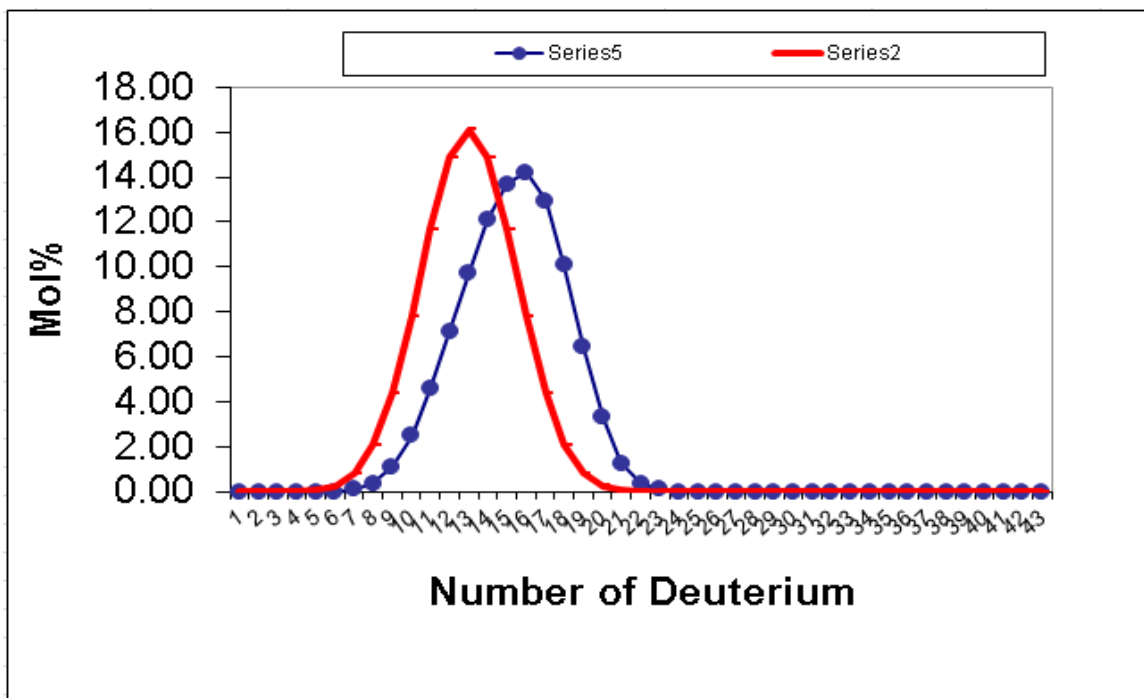


Figure B.4 JN-19: C₁₁ paraffin

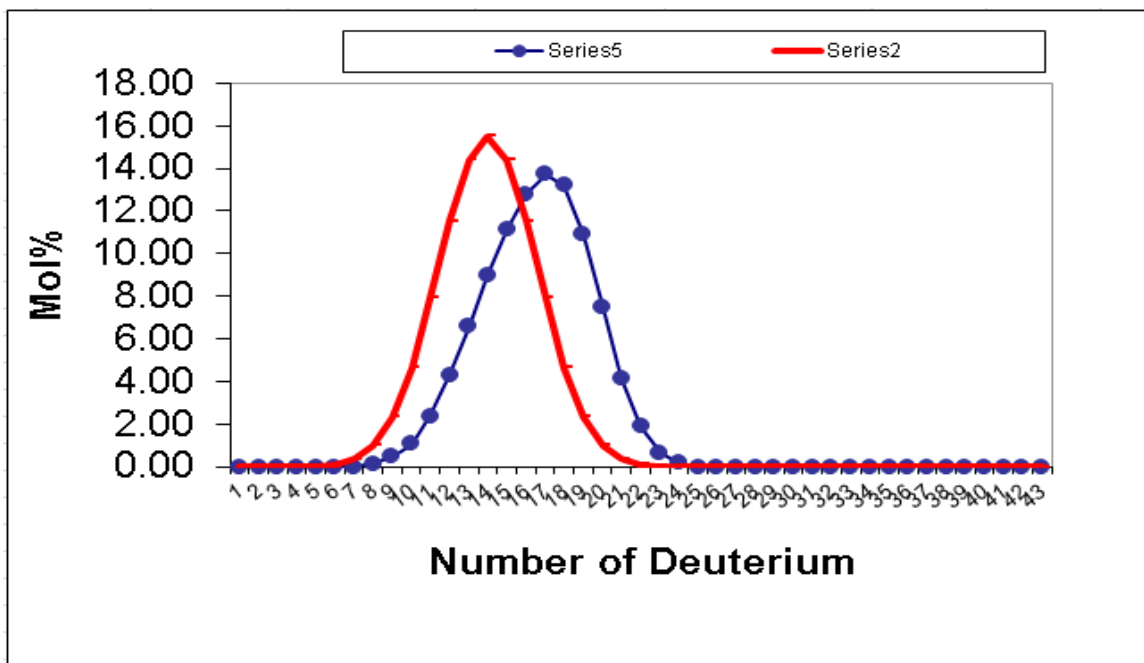


Figure B.5 JN-19: C₁₂ paraffin

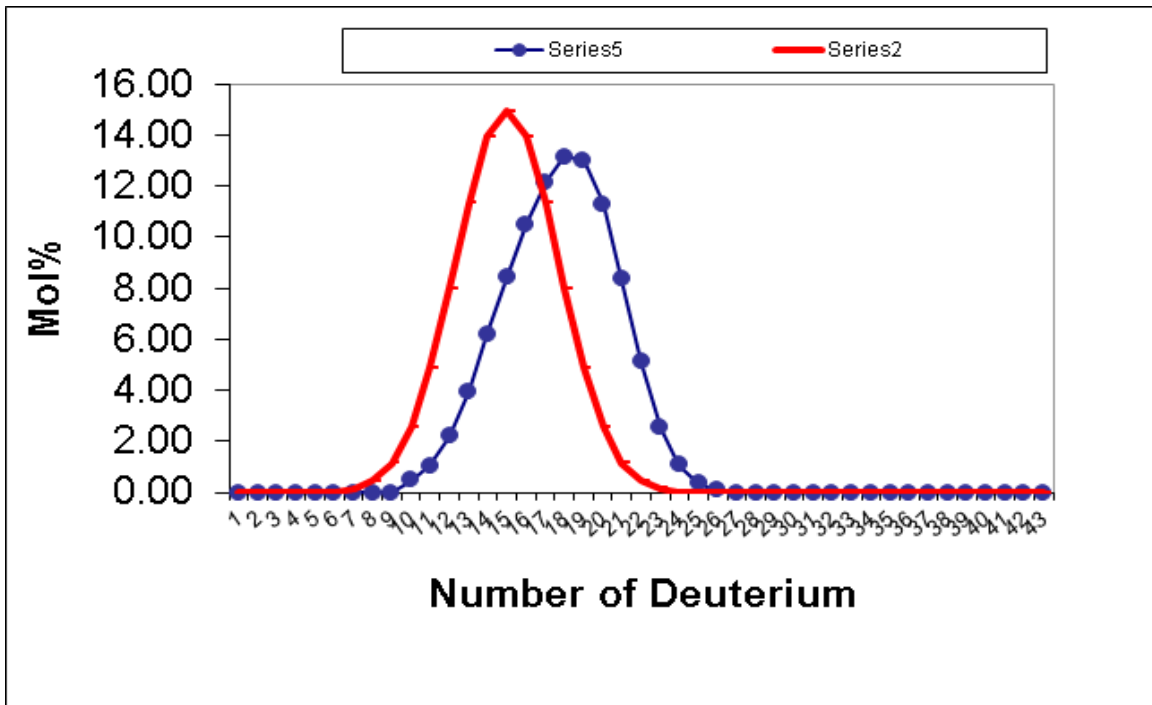


Figure B.6 JN-19: C₁₃ paraffin

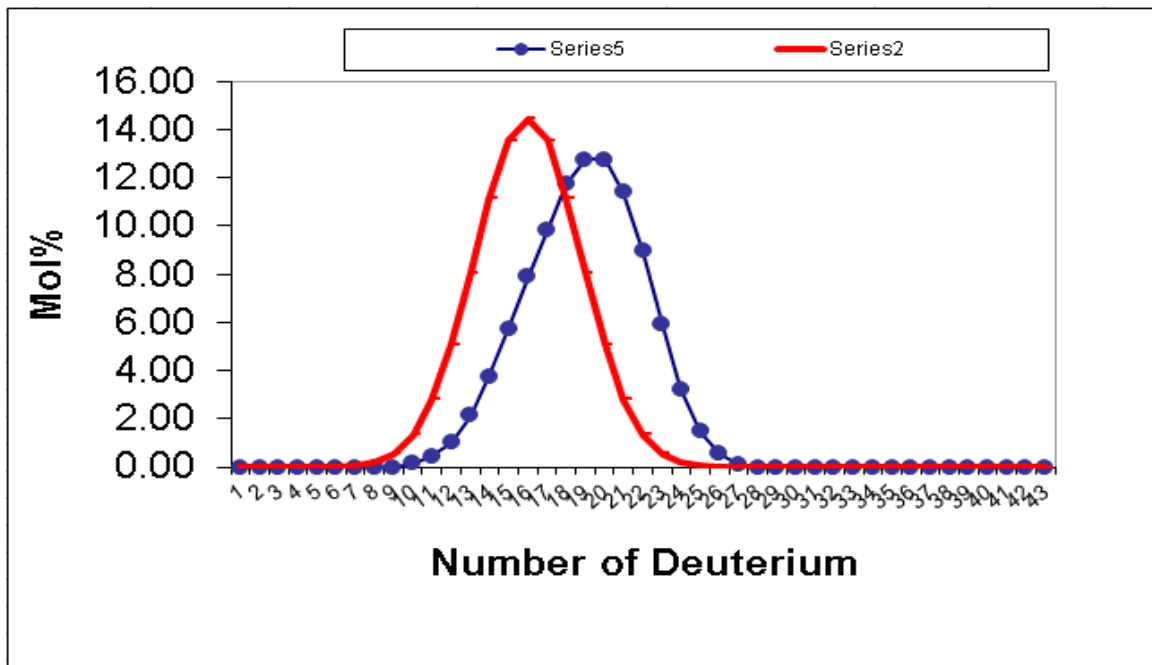


Figure B.7 JN-19: C₁₄ paraffin

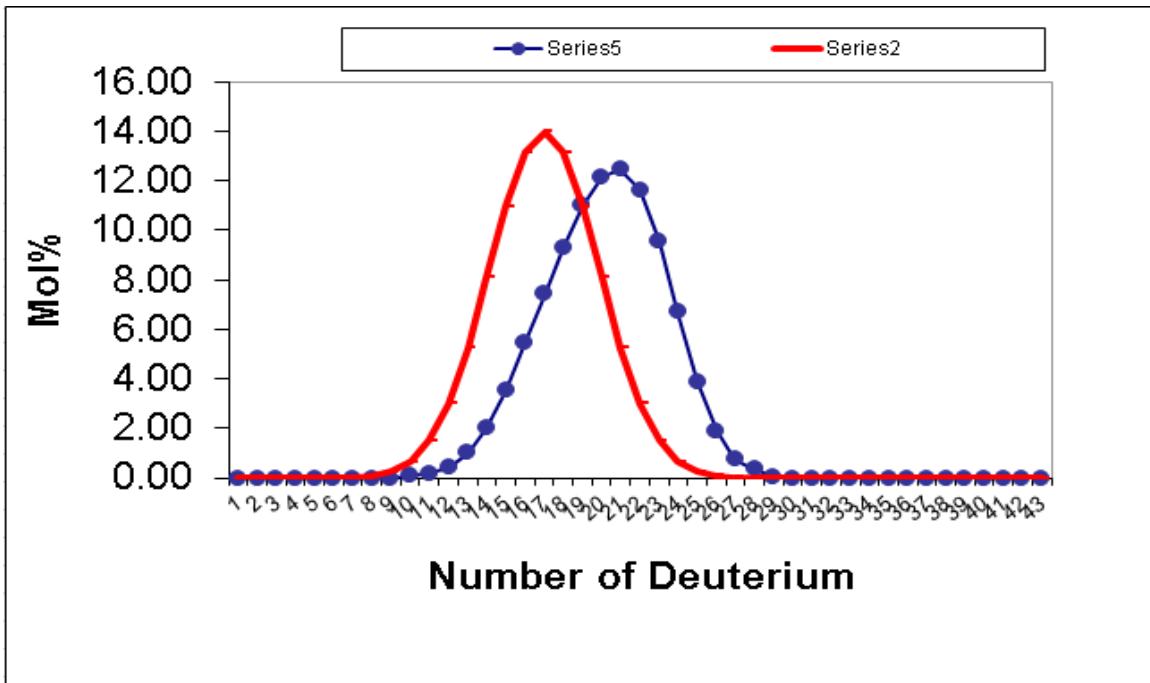


Figure B.8 JN-19: C₁₅ paraffin

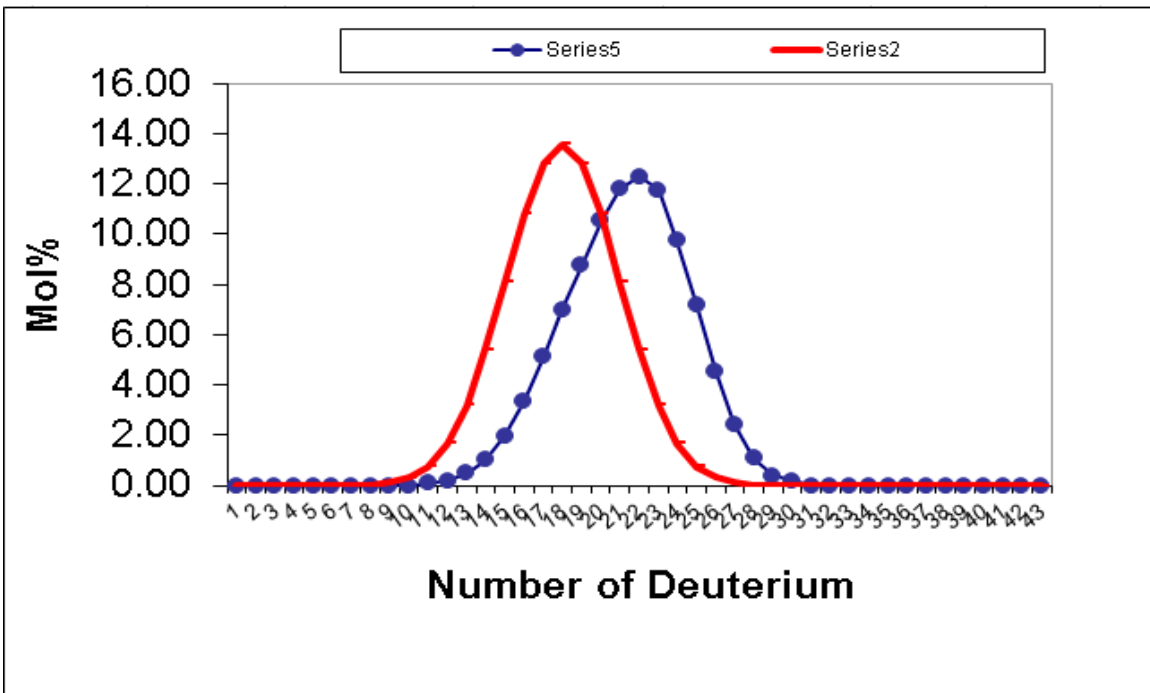


Figure B.9 JN-19: C₁₆ paraffin

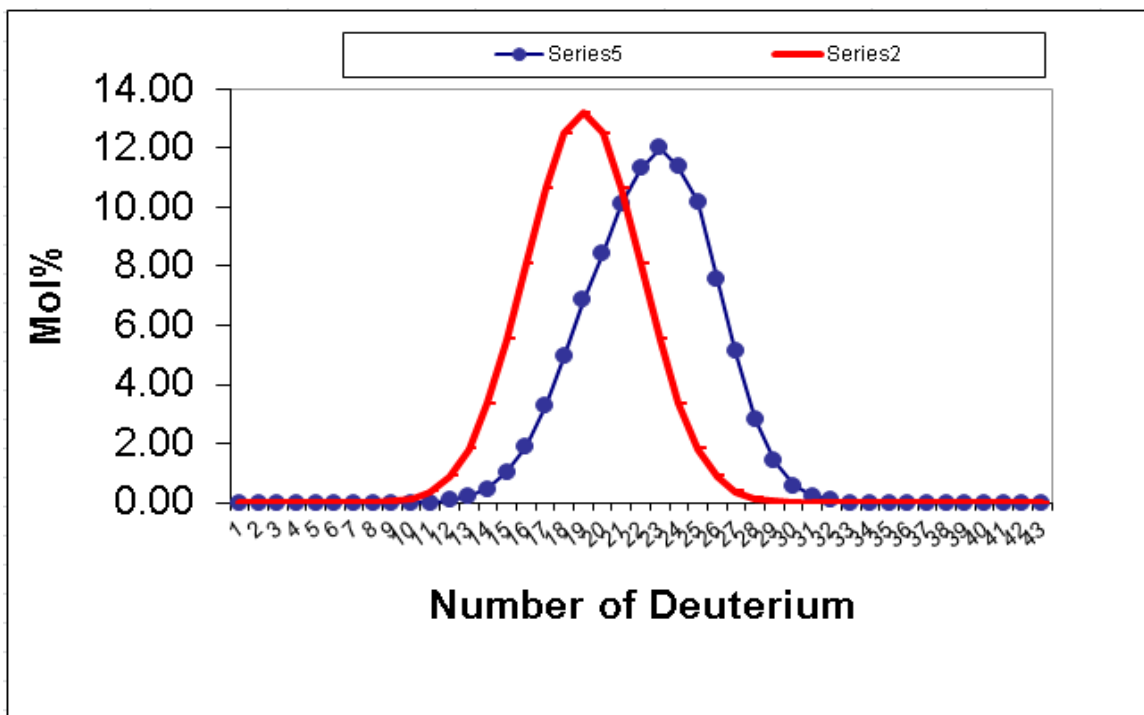


Figure B.10 JN-19: C₁₇ paraffin

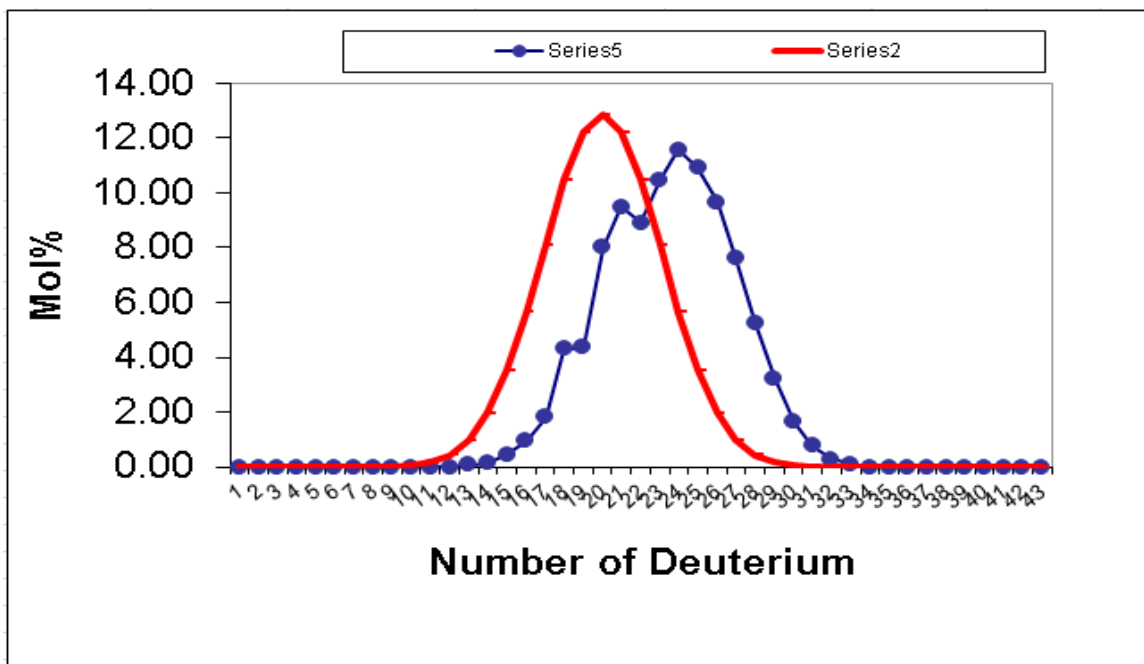


Figure B.11 JN-19: C₁₈ paraffin

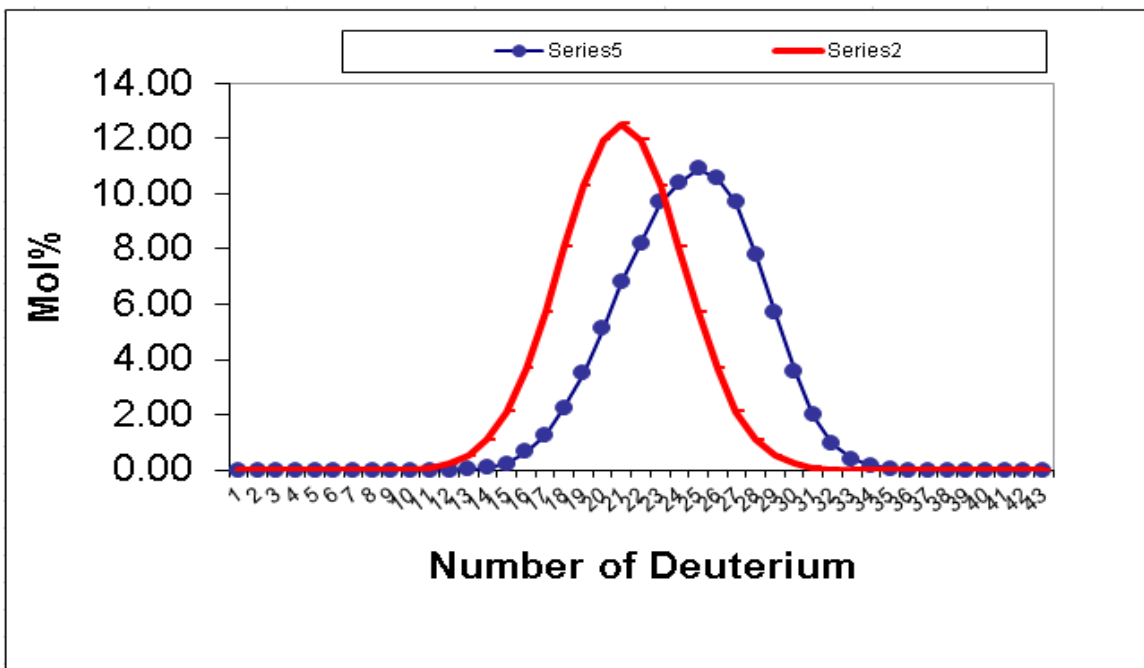


Figure B.12 JN-19: C₁₉ paraffin

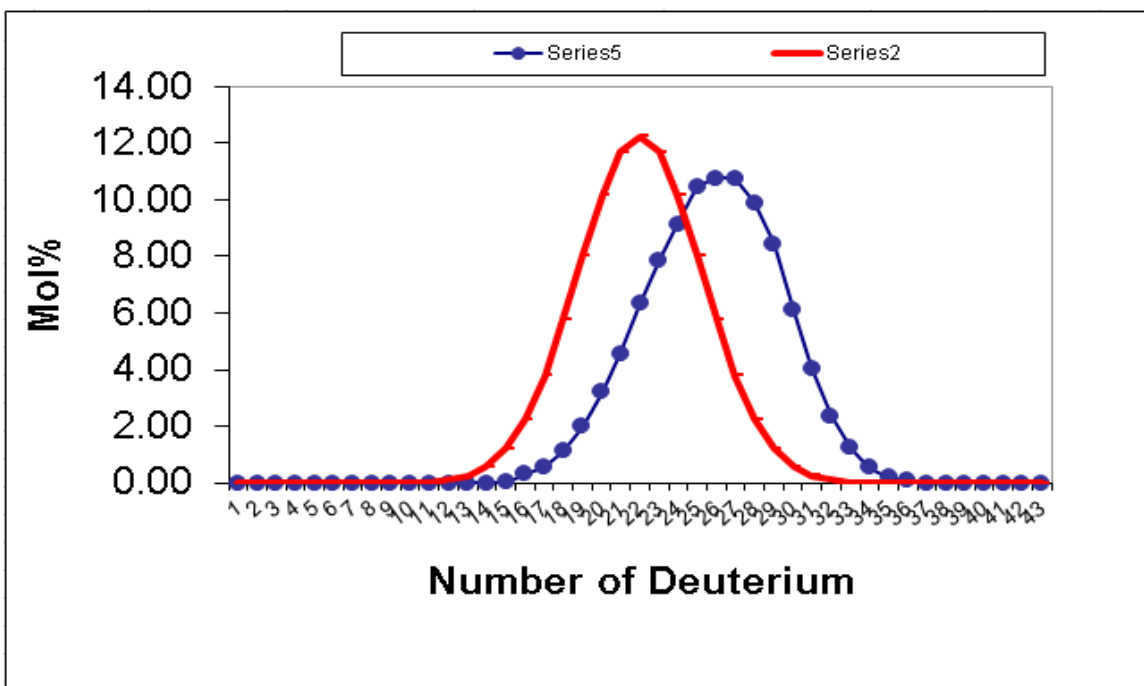


Figure B.13 JN-19: C₂₀ paraffin

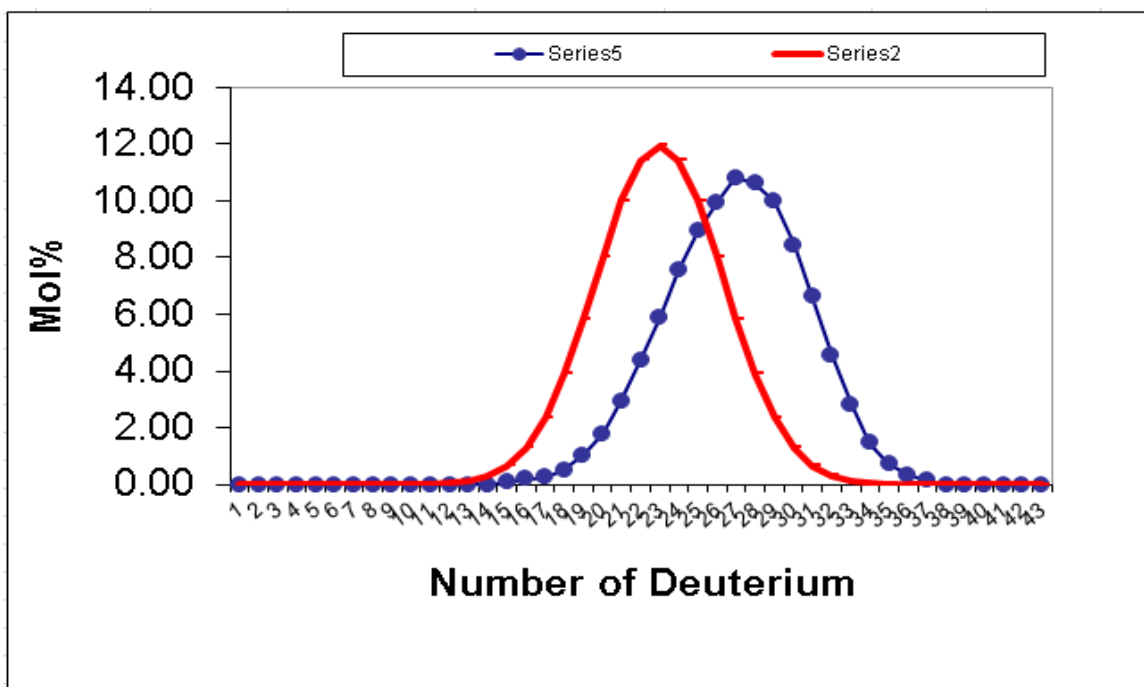


Figure B.14 JN-19: C₂₁ paraffin

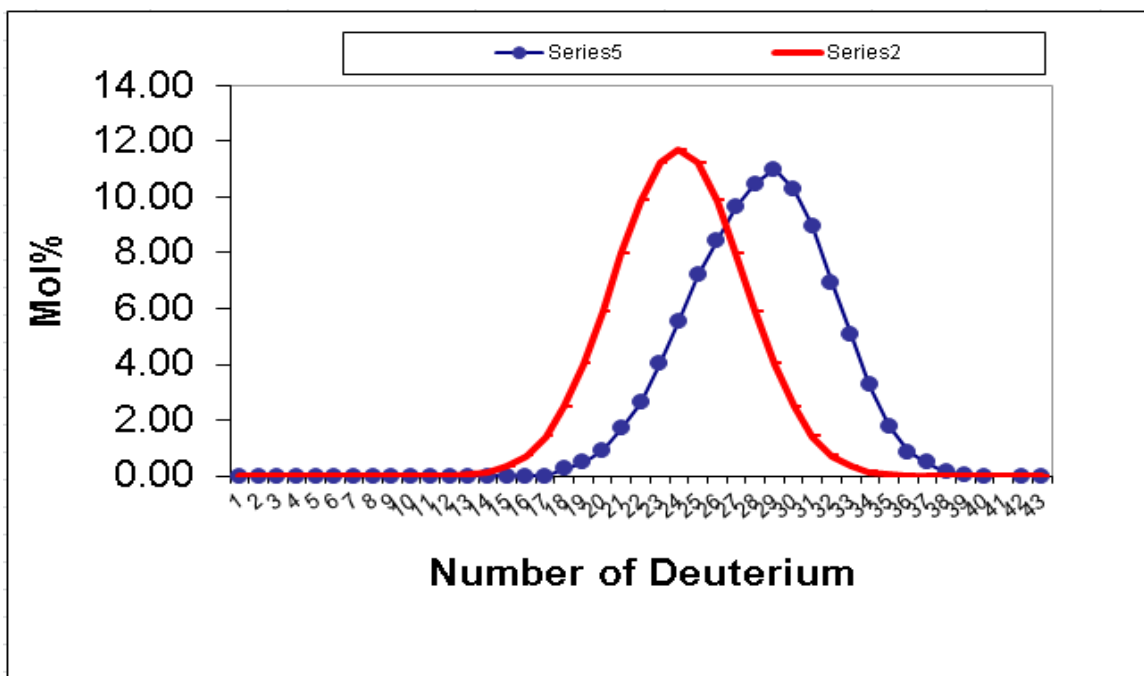


Figure B.15 JN-19: C₂₂ paraffin

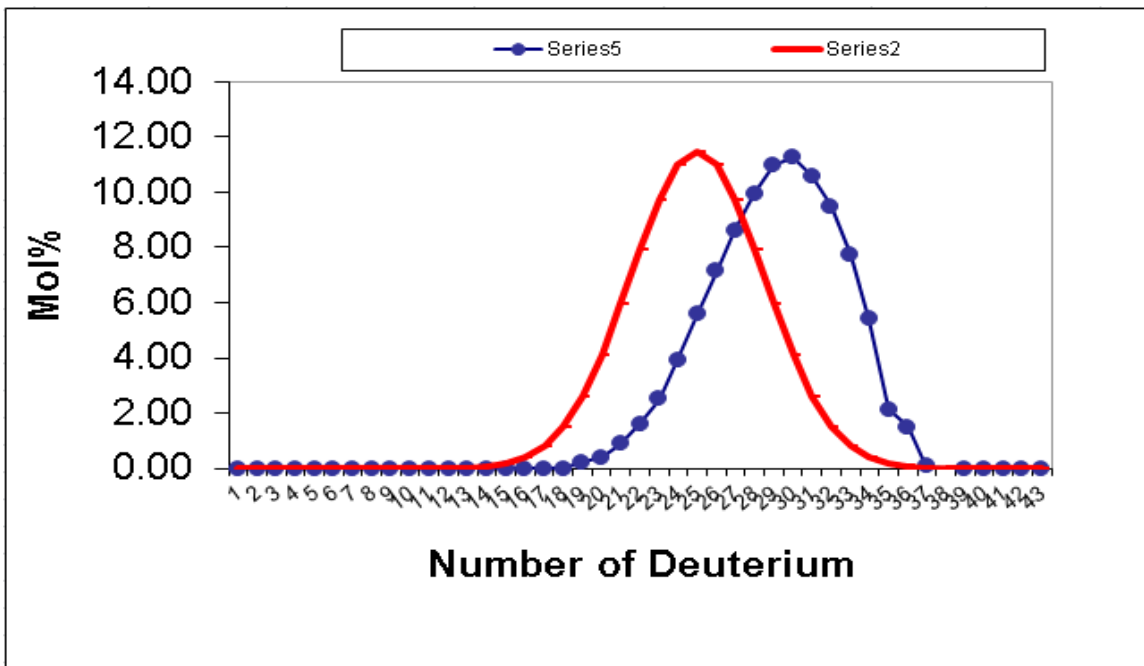


Figure B.16 JN-19: C₂₃ paraffin

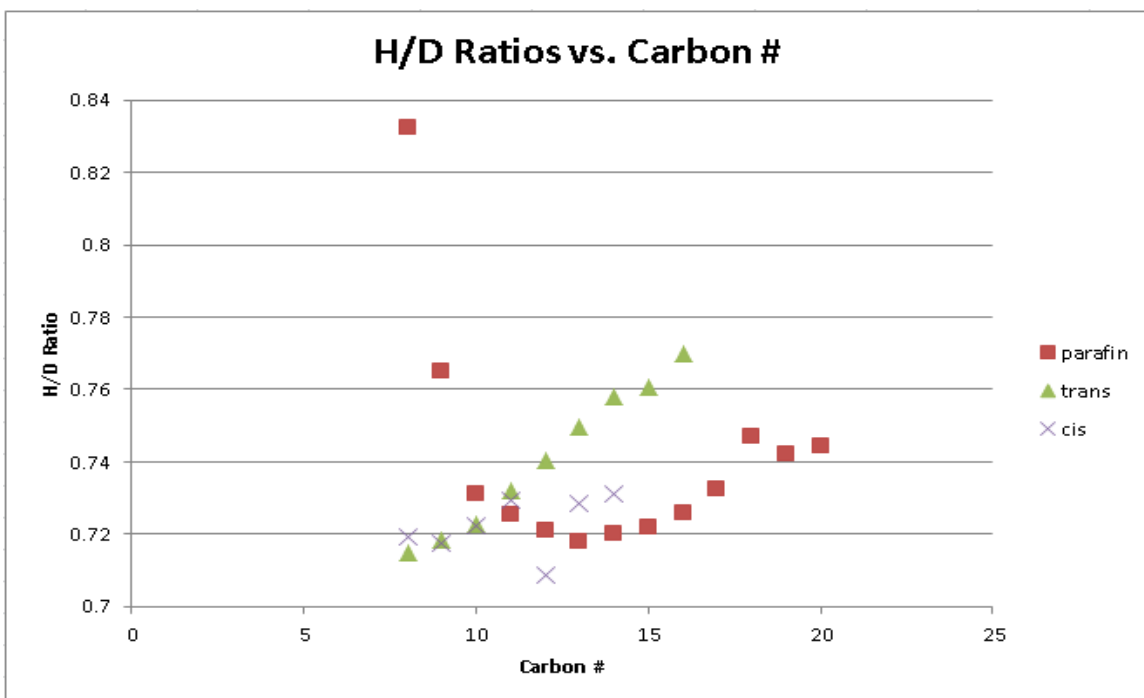


Figure B.17 Ru 1st Run: JN06

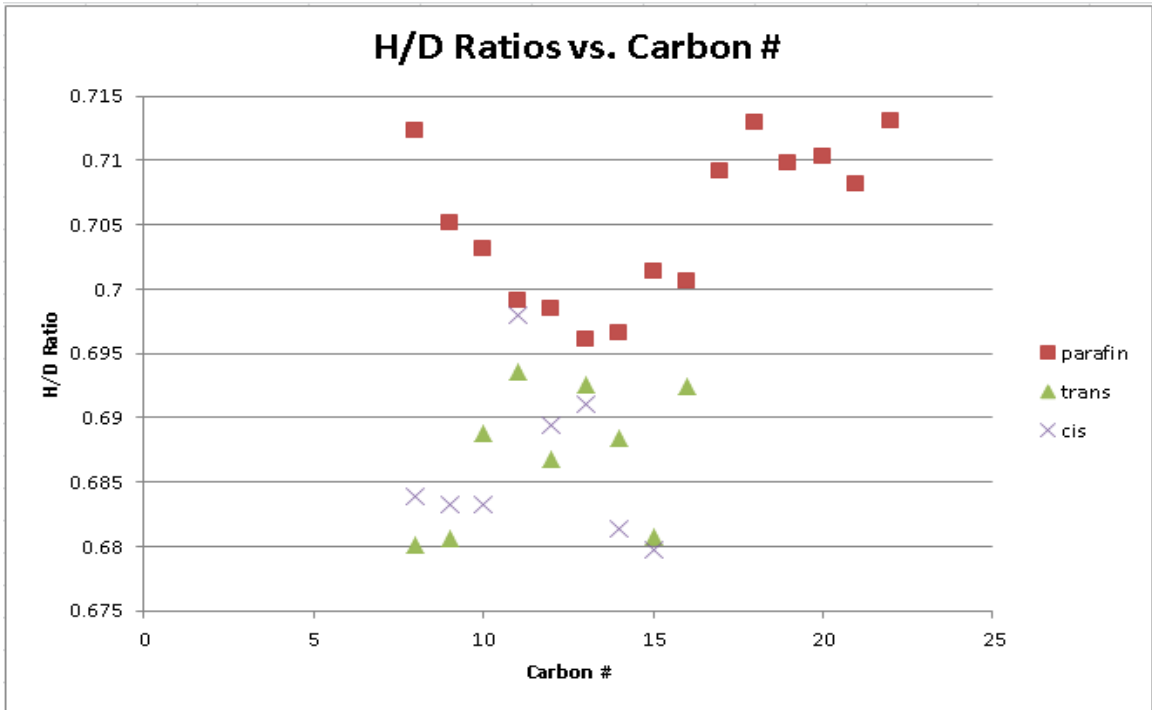


Figure B.18 Ru 1st Run: JN08

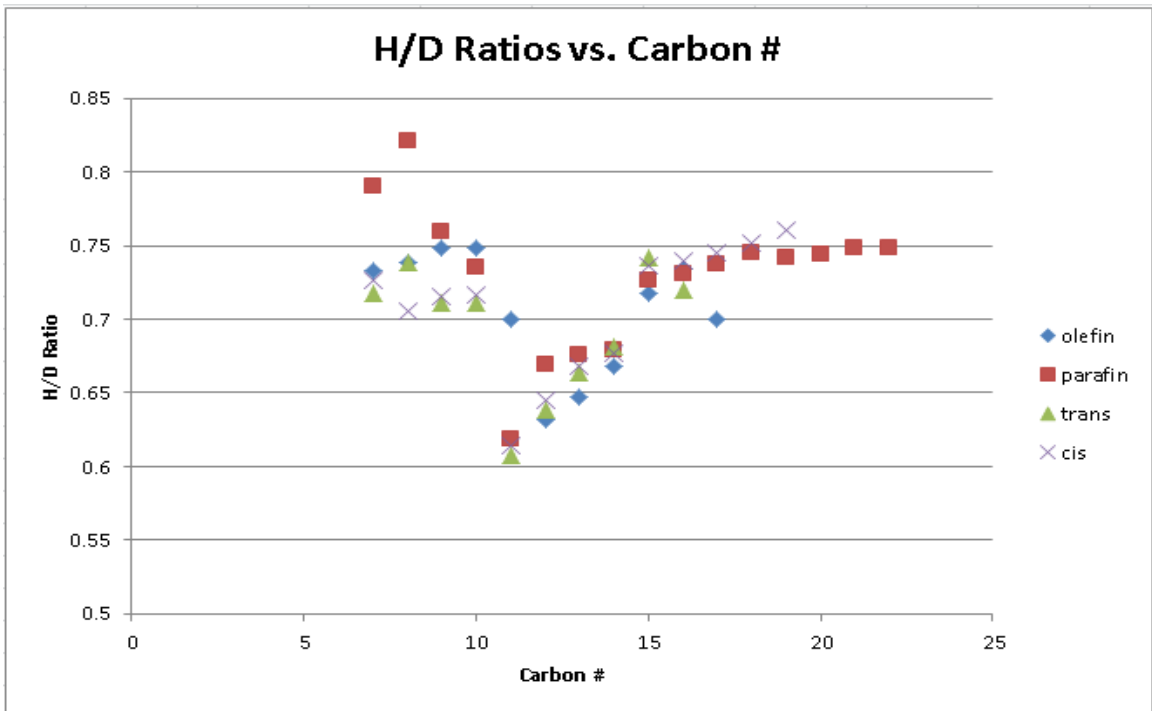


Figure B.19 Ru 2nd Run JN2-1

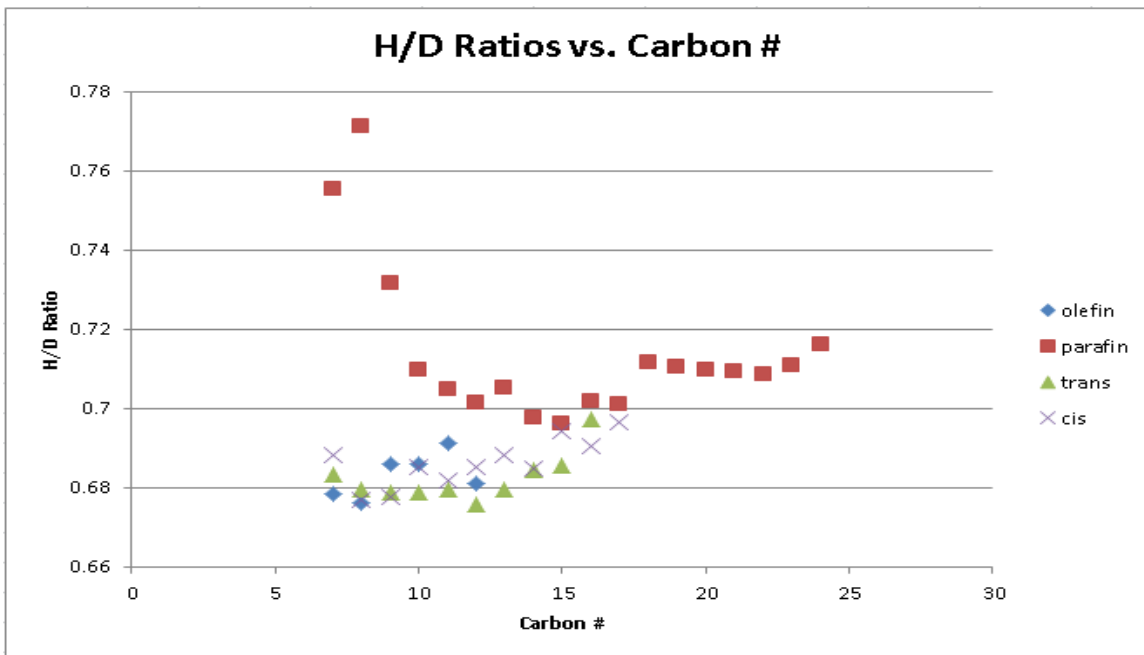


Figure B.20 Ru 2nd Run JN2-2

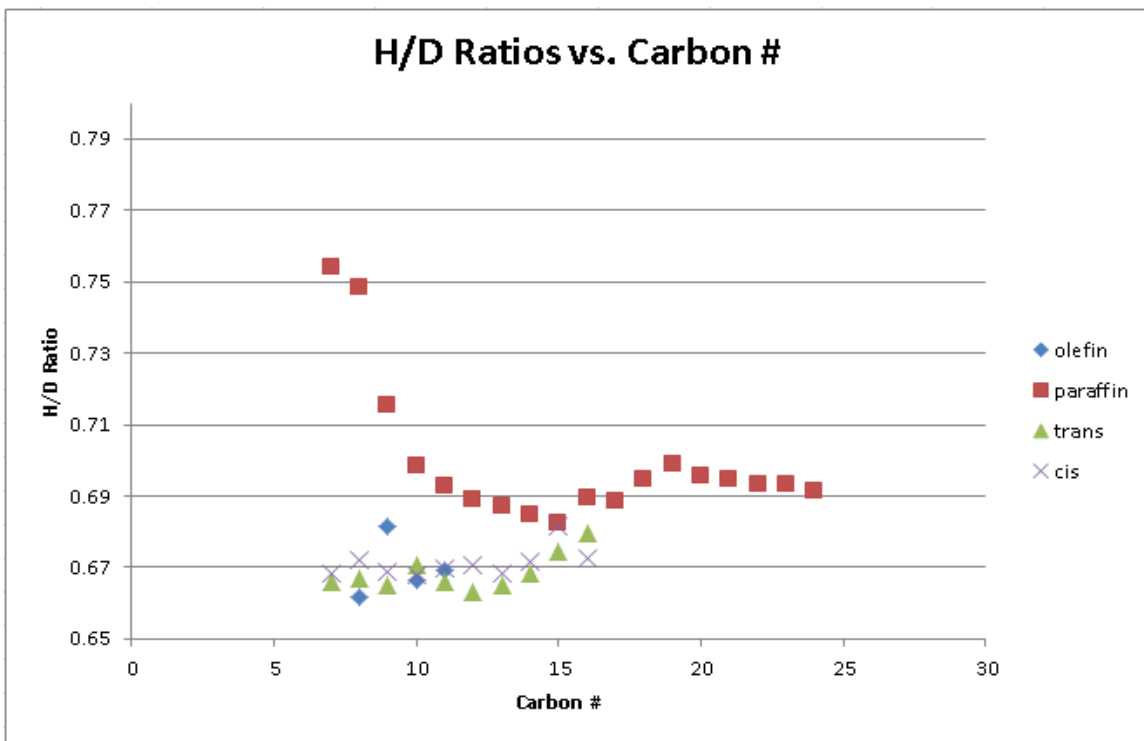


Figure B.21 Ru 2nd Run JN2-3

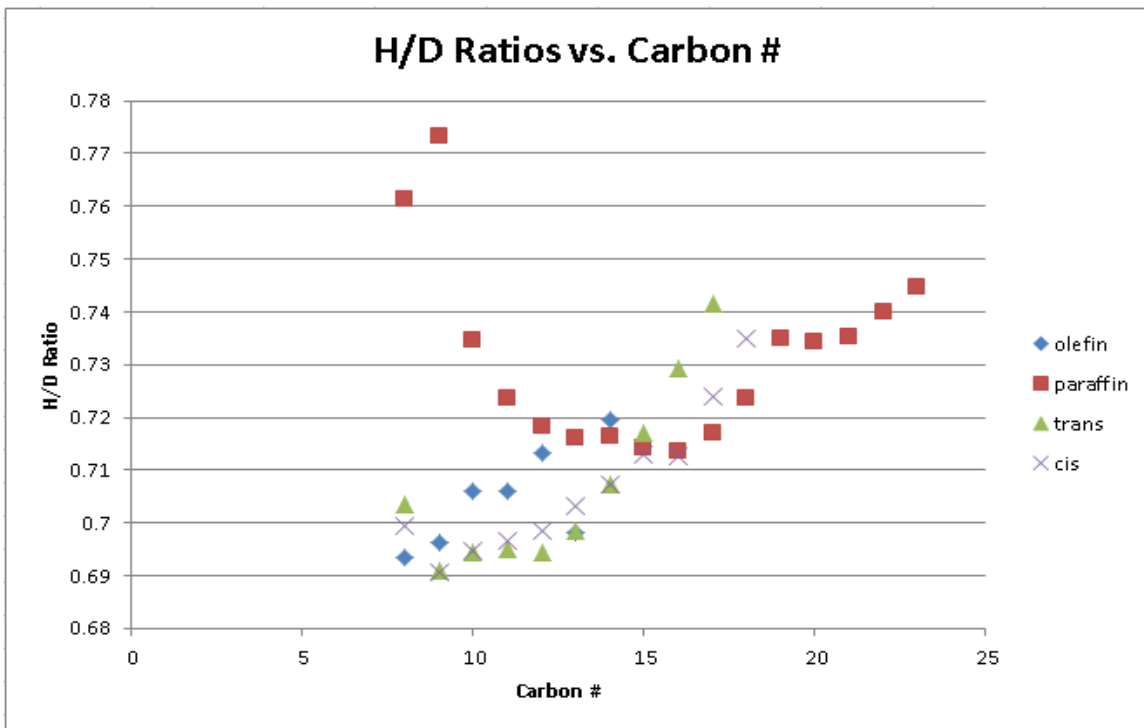


Figure B.22 Ru 3rd Run JN3-1

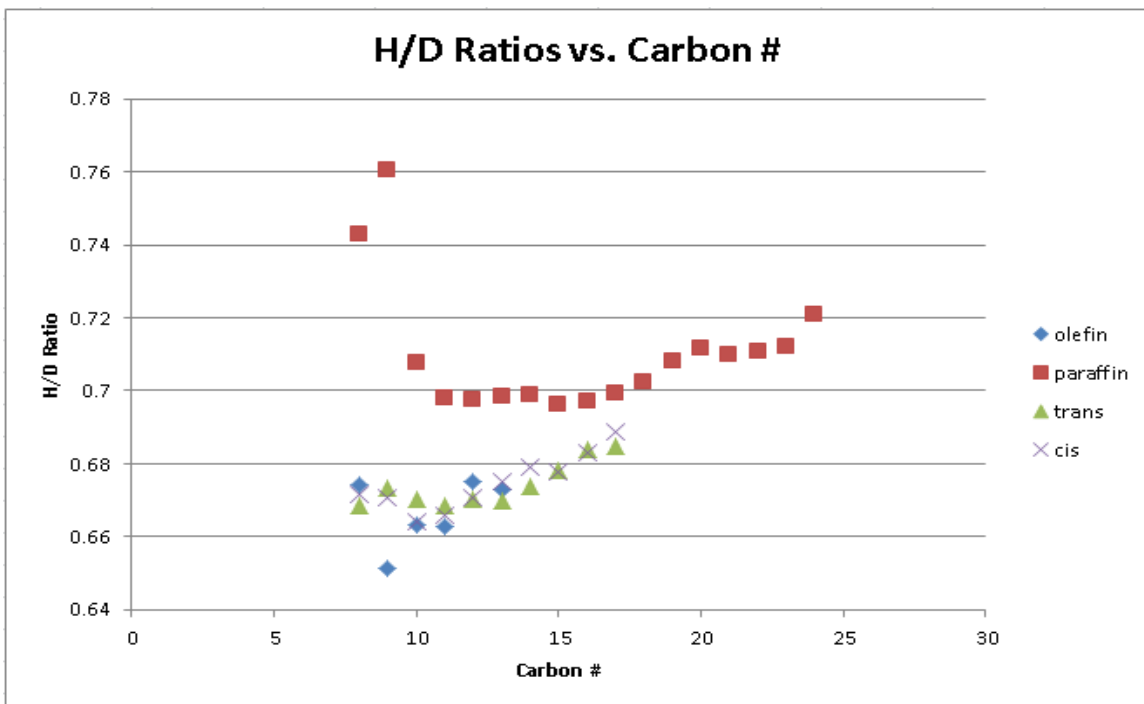


Figure B.23 Ru 3rd Run JN3-2

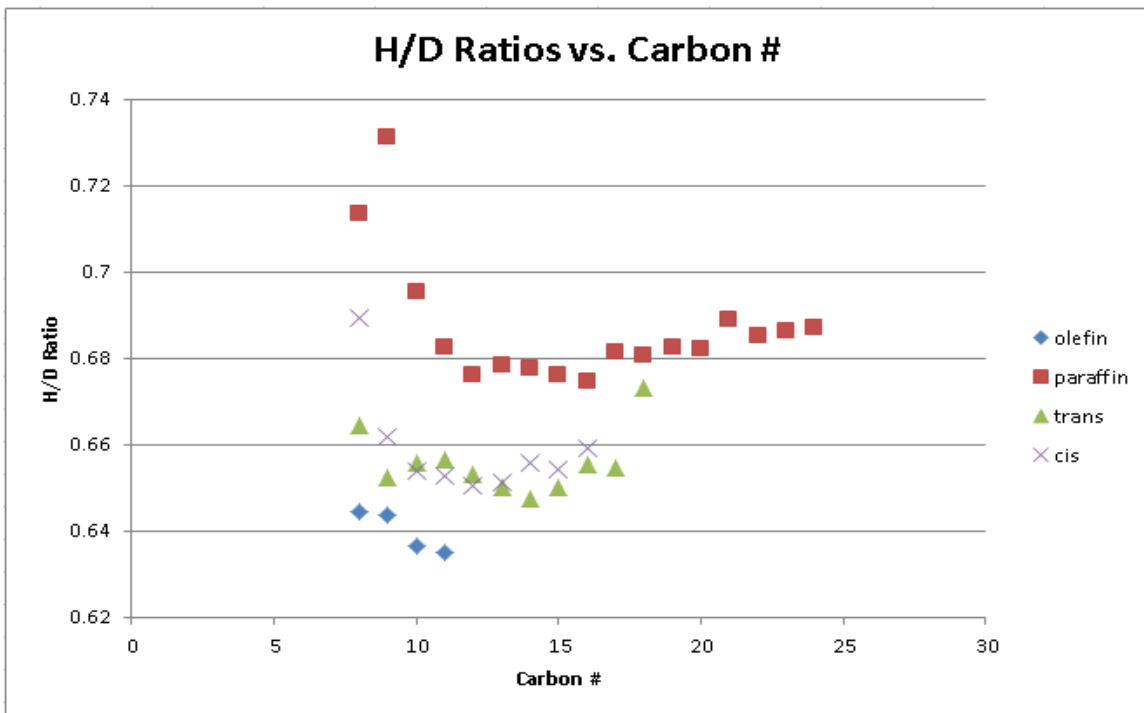


Figure B.24 Ru 3rd Run JN3-3

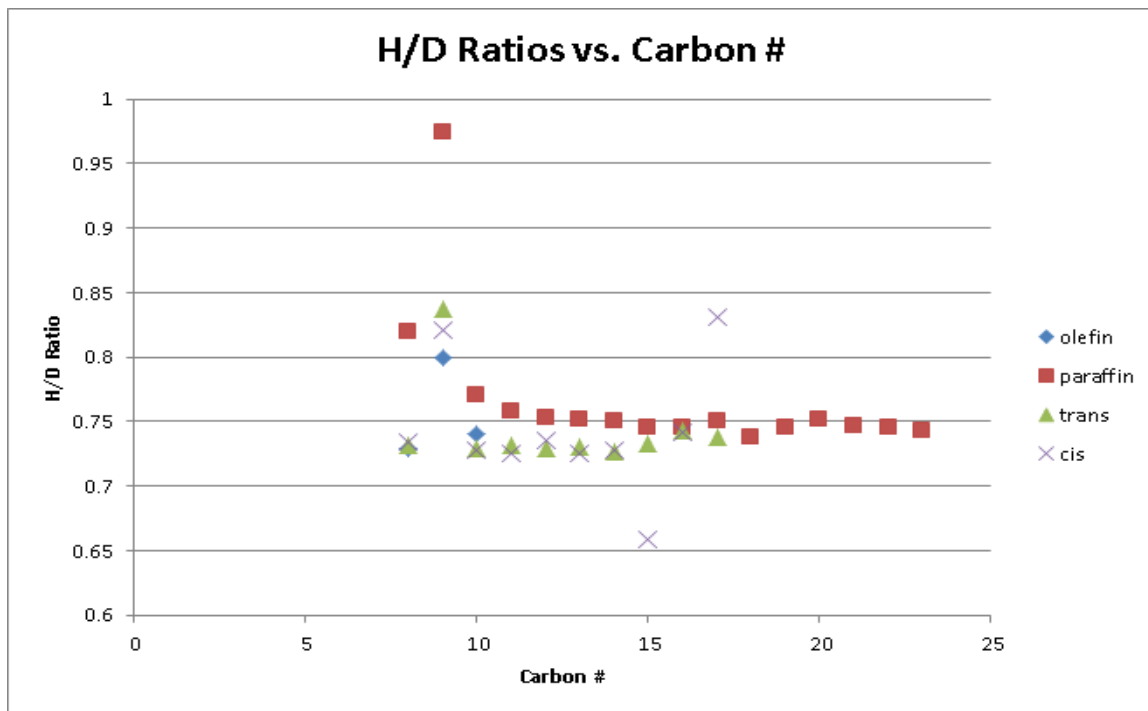


Figure B.25 Ru 6th Run JN6-2